Universitatea
Transilvania
din Brașov

INTERDISCIPLINARY DOCTORAL SCHOOL

Faculty of Mechanical Engineering

Octavian JITARAȘU

Lightweight structures for ballistic protection

SUMMARY

Scientific supervisor

Prof. Dr. Eng. Simona LACHE

BRAȘOV, 2025

CONTENTS

ACKNOWLEDGEMENTS

The PhD thesis entitled **Lightweight structures for ballistic protection** presents the findings of scientific research conducted under the careful supervision of Prof. Dr. Eng. Lache Simona. I am enormously thankful to her for the support and trust she has shown me, for her perseverance in scientific accuracy, and most importantly, for her solid presence and exemplary guidance during the research. I am grateful for the exceptional role model she represents, as a mechanical engineer and professor.

I would like to thank my scientific guiding committee members, Prof.Dr. Eng. Math. Vlase Sorin, and Prof. Dr. Eng. Scutaru Maria Luminița for their constructive remarks regarding my research work.

I would like to extend my gratitude to the Department of Mechanical Engineering at Transilvania University of Brasov for the support provided in the entire research activity, especially to Assoc. Prof. Dr. Eng. Velea Marian Nicolae for his priceless assistance in conducting particular experimental aspects of this research. Additionally, I express my gratitude to him for his continuous encouragement and support since my student years, during which I explored the field of lightweight structures for ballistic protection.

I am thankful to those who provided assistance during the research, particularly Prof. Dr. Eng. Teodorescu Horațiu from Transilvania University of Brasov, as well as Prof. Dr. Eng. Rotariu Adrian and Dr. Eng. Matache Liviu from the Military Technical Academy "Ferdinand I" of Bucharest, for their valuable support in conducting several experimental phases of this research.

I am extremely grateful and would like to express my thanks to the team at the Naval Special Operations Training Center and the 164th Naval Special Operations Division, especially to Mr. Călin Ovidiu-Ioan, Mr. Mogâlă Alexandru, and Mr. Bucur Eugen, for their support and assistance in conducting the ballistic experiments.

Lastly, I wish to express my gratitude to my family and friends for their support and encouragement.

Octavian JITARAȘU

INTRODUCTION

Body armors have been developed to protect wearers from various environmental threats such as chemicals, fire, UV radiation and heat, as well as to defend against ballistic impacts, sharp fragments and stabbing injures. Throughout mankind's evolution, a wide range of body protection solutions have been developed for personal safety. Nowadays, there is an intense effort to develop body armor protection technologies to enhance safety, comfort and reduce weight.

The primary function of body armor is to mitigate the kinetic energy of a projectile upon impact, effectively reducing or preventing the penetration of the bullet into the wearer's body. The secondary functions of protective armor systems are to protect the wearer from a variety of threats while maintaining a high level of comfort. It is obvious that no armor system can provide protection against all possible threats. Therefore, the performance of protective body armor is usually designed to meet specific levels of protection customized for its intended use.

As threats have increased, armor systems have become significantly heavier to provide adequate protection. This increase in weight places a substantial load on warfighters, affecting their mobility and endurance. Over the years, the need for low-density, high-performance and cost-effective materials has increased significantly. This increasing requirement has resulted in intense research over the last decades, focused on the development of lightweight body armor systems. Many of the advances in armor performance have resulted from the introduction of novel or improved materials, demonstrating the essential role of material innovation in this field. Recently, researchers have faced a significant challenge: the development of high-quality armor materials capable of withstanding the high-velocity ballistic impact of modern weapons. This requires innovative solutions and advanced materials to ensure that the resulting armor systems offer effective protection while maintaining the required balance between weight, performance and cost.

To improve body armor systems, two critical challenges must be approached. Firstly, it is essential to develop materials that outperform existing ones. Secondly, it is essential to design armor structures that maximize the potential of both existing and improved materials. This involves designing materials in a way that optimizes their protective properties. Advanced simulation and experimental methods are essential to effectively approach these challenges. The selection of materials, their geometric configuration and assembly methods are essential in armor design. Each material component performs a specific role, not only in dissipating the kinetic energy of projectiles or mitigating blast effects, but also in maintaining the structural integrity of the armor. It is therefore significant to note that the general behavior of an assembled armor system facing a given threat is more complex than the simple sum of the behaviors of its individual components. This highlights the importance of a comprehensive approach in the design and engineering of effective armor systems.

Not long ago, composite materials were used together with various metals to achieve the required ballistic protection. Ceramics have partially replaced heavy metals such as steel and aluminum alloys in personal and structural protection due to superior ballistic performance, including significant advances in specific strength and hardness. Modern armor structures usually contain a combination of two main materials: a ceramic (most often) or metallic face layer, followed by multi-layer laminated

polymer composites, reinforced with fibers or fabrics. This combination utilizes the unique properties of each material to improve the global effectiveness of ballistic protection.

In order to achieve cost-effective and comfortable body armor, it is essential to select the accurate design, materials and manufacturing processes. The optimal body armor design must balance three conflicting characteristics: effective protection, mobility and comfort. This balance ensures that the armor provides adequate defense against threats while allowing ease of movement and comfort for the wearer. With careful consideration of these factors, armor systems can be developed that meet the rigorous demands of modern protection requirements.

Advanced composite armors can be designed from multiple layers, including ceramic, fabric and anti-trauma layers, to enhance ballistic protection. The performance of each layer critically influences the overall effectiveness of the armor system. In some designs, a rubber layer is incorporated to support the ceramic tile layer and improve both the overall performance and comfort of the armor.

The main objective remains the design, development and optimization of novel armor structures achieved through simple and cost-effective manufacturing technologies, while reducing overall weight and maintaining high levels of protection. The aim is to develop armor systems that not only offer superior protection, but also improve wearer mobility and comfort, making them more practical for use in demanding environments.

In this regard, the research conducted within this thesis focuses on **developing a novel solution for the ballistic protection industry. This solution aims to provide a cost-efficient body armor system that ensures a high level of protection. Additionally, the research attempts to identify major challenges and technical gaps in developing the next generation of lightweight protection materials, including rubber-based composites, and to propose a strategic path forward for their improvement**.

Below is presented a brief overview of the research conducted through this doctoral thesis.

Chapter 1 presents a general overview of ballistic protection, highlighting the role of rubber in energy absorption, impact mitigation, and structural reinforcement for advanced armor systems. This is followed by a critical review of the state of the art which leads to the formulation of the research objectives established for the present thesis.

Chapter 2 is dedicated to briefly presenting the research goals and objectives followed throughout the research.

In **Chapter 3**, the design and development of both soft and rigid ballistic protection structures are explored, highlighting the role of rubber in improving impact absorption and structural integrity. Various configurations of UHMWPE-rubber composite panels and rubber-ceramic composite plates are analyzed to optimize energy dissipation, flexibility, and ballistic resistance.

Chapter 4 analyses the mechanical behavior of rubber in ballistic applications, focusing on its hyper-elastic properties, energy absorption capabilities, and impact mitigation potential. Through theoretical modeling, numerical simulations, and experimental testing, the chapter evaluates how rubber materials respond under extreme loading conditions, providing understandings into their role in improving ballistic protection. The findings establish a foundation for optimizing rubber-based composite structures for improved durability and energy dissipation.

In **Chapter 5**, the integration of SBR-65 rubber with UHMWPE UD fabric is explored to evaluate its energy absorption capabilities and impact resistance in soft armor configurations. The chapter examines the ballistic behavior of fabric structures, highlighting wave propagation mechanisms, failure modes, and the role of rubber in improving protective efficiency. Through experimental testing and numerical simulations, different panel configurations are analysed, showing how the placement of the rubber layer influences projectile deceleration, back-face deformation, and overall ballistic performance.

In **Chapter 6**, the integration of PUR-85 and SBR-65 rubber with ceramic and UHMWPE UD fabric is explored, to evaluate its energy absorption capabilities and impact resistance in rigid armor configurations. Various impact models, energy absorption mechanisms, and damage evolution processes are considered for analysis, highlighting the role of rubber in mitigating stress waves and enhancing overall structural integrity. Through experimental testing, the effectiveness of rubber-ceramic hybrid configurations in improving ballistic resistance is demonstrated.

In **Chapter 7** the original contributions and general conclusions of the present doctoral thesis are formulated. In addition, suggestions for future research are introduced and discussed.

1. Critical review of the state of the art on recent advances and perspectives of ballistic materials and equipment

1.1 General considerations

Terminal ballistics begins when a projectile impacts an armored target and ends when the projectile is completely stopped or fully penetrates the armor. This phase involves the interaction between the projectile and the target material, including deformation of the projectile and armor, as well as energy transfer and dissipation mechanisms. An understanding of terminal ballistics is essential for the design of effective armor systems and for optimizing the protective capabilities of materials.

Based on the projectile-target energy transfer phenomenon, energy dissipation and damage mechanisms, the impact event can be classified into three categories: low-velocity impact, high-velocity impact and hypervelocity impact. This classification is due to the significant changes in energy transfer, energy dissipation and target damage mechanisms as the projectile velocity changes. *Low-velocity impact* occurs at velocities below 500 m/s, typical of handgun threats. In this scenario, the bullet deforms into a "mushroom" shape before being stopped. *High-velocity impact* occurs at velocities between 500 and 1000 m/s, common for rifle ammunition. Here, the bullet tends to shatter on impact. *Hypervelocity impact* involves projectiles traveling at velocities exceeding 1000 m/s, such as those from improvised explosive devices (IEDs). At these extreme velocities, the local target materials behave as fluids, leading to complex interaction dynamics [2, 3].

The study of ballistics and the development of advanced armor systems are primarily determined by the need to respond to specific ballistic threats, especially projectiles, which vary widely in terms of velocity, energy, and penetration mechanisms. Understanding the dynamics of projectile impact, energy dissipation, and material behavior provides the basic knowledge needed to design effective protective solutions. However, the effectiveness of any armor system ultimately depends on its ability to address the unique characteristics of different types of ballistic threats, ranging from low-velocity handgun bullets to high-velocity rifle ammunition and hypervelocity projectiles from improvised explosive devices (IEDs). In the next section, the types of ballistic threats will be explored in detail, categorizing them based on their velocity, energy, and penetration capabilities, and examining how these factors influence the design and performance of armor systems.

1.2 Types of ballistic threats

Ballistic threats are characterized by low- and very high-velocity projectiles, including bullets, shrapnel, fragments and similar objects, commonly associated with military operations. These threats constitute significant challenges because of their speed and their potential to cause significant damage. Ballistic threats can be categorized into four main classes [1, 9, 10, 11, 12]:

- *small arms projectiles*, which can have soft cores typically made of lead or hard cores made of steel or tungsten carbide, are shot from handguns, rifles, and machine guns;

- *fragment simulating projectiles (FSP)*, which are made to reproduce the actions and effects of shrapnel fragments resulting from the explosion of munitions, such as bombs, grenades, or artillery shells;

- *long rods*, known for their elongated shape, which are commonly utilized in anti-armor applications;

- *shaped-charge jets and explosively formed projectiles (EFP)*, which are advanced threats that concentrate explosive energy to create high-speed projectiles capable of penetrating armor. These threats exhibit significantly greater penetration capabilities than conventional kinetic energy projectiles.

In general warfare, bullets and fragments are the primary cause of injuries.

1.2.1 Small arms projectiles

Typical bullets are constructed with either round (hemispherical) and flat noses, which are commonly used for handguns, or pointed noses (ogive and conical), which are typically associated with rifle ammunition, as illustrated in Figure 1.3. These nose shapes have a significant impact on the bullet's performance, affecting factors such as flight stability, penetration capability, and the effects on targets upon impact.

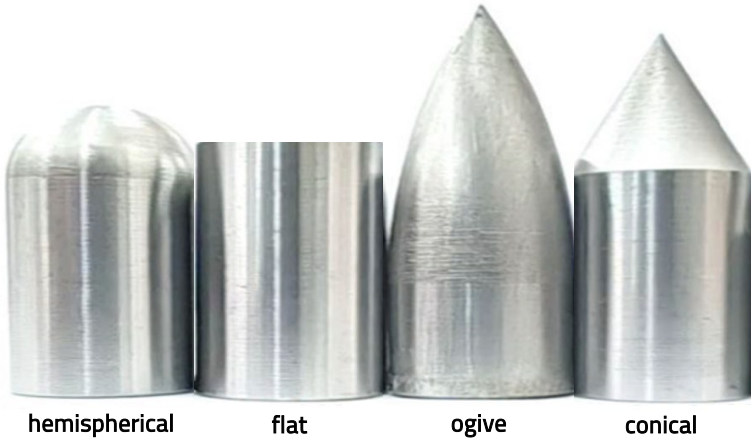

Figure 1.3 Different forms of the projectile nose [18]

In summary, the design and material composition of bullets play a significant role in determining their performance, including flight stability, penetration capability and impact effects. The different types of bullets mentioned above describe specific purposes in military contexts, improving effectiveness in various operational situations. This comprehensive familiarization with the characteristics of bullets contributes to choosing the right ammunition to achieve specific tactical requirements.

1.2.2 Fragments

Fragments can be classified into two categories: natural and preformed. A *natural fragment* refers to a piece of material that breaks off or separates naturally from a larger object without the influence of external shaping or fabrication processes. These fragments can result from various forces such as

impact, stress, or environmental conditions, and are often irregular in shape. Fragments from artillery weapons are usually natural fragments resulting from the shell casing. These fragments are created by the breakup of the casing surrounding the explosive and are dispersed and shattered by the detonation of the explosive filler. *Preformed fragments* are intentionally manufactured parts packed in or around the explosive mixture to increase its fragmentation effect upon detonation. For obtaining statistically significant data on armor performance against fragmentation threats, a significant number of trials are often needed. This process, which can be costly and time-consuming and result in highly variable data, is more efficiently and cost-effectively achieved through the use of fragment simulating projectiles (FSPs) in laboratory testing, Figure 1.5.

Figure 1.5 Fragment simulating projectile (FSP)

As illustrated in Figure 1.5, the flat tip with sharp edges is designed to simulate cutting and penetrating actions. This feature simulates how real fragments would interact with and penetrate various materials.

1.2.3 Projectile deformation and damage

The deformation and damage of a projectile upon impact with the target is influenced by the composition of the core, the rate of deceleration experienced during impact, and the angle of impact. To analyze and understand in detail the different deformation and damage mechanisms of bullets, they are classified into the following common types: bullet mushrooming, bullet jacket stripping, core erosion, bullet fracture and bullet bending [17, 25, 26, 27, 28, 29].

The discussion on ballistic threats, including small arms projectiles, fragments, and their deformation mechanisms, highlights the critical need for effective ballistic protective systems. Understanding the behavior of projectiles upon impact, their penetration capabilities, and the factors influencing their performance provides a basic understanding of the design of body armor and other protective structures. The next section will explore how different armor designs and materials are adapted to mitigate the diverse threats discussed, ensuring optimal protection while balancing factors such as weight, flexibility, and durability.

1.3 Design considerations for ballistic protective systems. Classification and analysis of body armor structures

The weight of body armor is essential to the mobility of its wearer. A common material option for protection applications are metal structures, especially steel. Though, the density of metals is quite high and therefore not practical for the design of lightweight ballistic body armors. Laminated composite materials, which are generally lighter than metals, but having high mechanical properties and offering performance comparable to steel, can be used largely in the structure of ballistic protection equipment. The multilayer hybrid armor system containing several layers of materials from different classes (usually ceramics and high-strength and high-modulus fibers), also known as ceramic composite armor system, offers an advantage over hard monolithic ceramic or steel plates in terms of ballistic performance and ballistic limit per unit mass. This type of armor is an assembly of laminated composite materials containing a hard striking face with high compressive strength and a flexible backing plate with high tensile strength [1, 30, 31]. The basic function of this armor is to defeat an impacting bullet. The main role of the striking plate is to reduce the speed of the bullet and to deform and break it into small fragments. The function of flexible backing plate is to capture the broken fragments, dissipate the remaining kinetic energy of the projectile and keep the integrity of the body armor [32, 33]. Hard materials, such as ceramic tiles (for example: alumina, silicon carbide, boron carbide, or titanium diboride), are used as striking faces. Ceramic is an appropriate candidate material for the striking face due to its hardness at minimum density. Backing plate is normally made of fiber-reinforced composites (for example: aramid, ultra-high-molecular-weight polyethylene, fiberglass and carbon fiber), which are relatively lightweight and flexible. In certain armor designs, the incorporation of a rubber layer allows the impact energy to be redistributed over a larger area. The striking face and backing plate are bonded together using ballistic adhesives [34].

The design of body armor, as discussed in this section, focuses on achieving a balance of protection, comfort, and mobility while addressing specific threats through the use of advanced materials and layered structures. However, the effectiveness of body armor is not only determined by its material composition or design; it also depends on the level of ballistic protection it provides against various threats. In the following section, the standardized classification systems used to define the protective capabilities of body armor will be discussed. These levels, which range from protection against low-velocity handgun bullets to high-velocity rifle projectiles, play a critical role in guiding the selection and design of armor systems to meet specific operational requirements. By understanding these protection levels, it is possible to understand better how body armor is designed to address different threat scenarios, ensuring optimal safety and performance for the wearer in various combat and tactical environments.

1.4 Ballistic protection levels in body armor design

Body armors structures must be subjected to specific tests to ensure that all components meet the minimum performance standards before they can be used. The ballistic resistance test is conducted in accordance with body armor standards established by the United States of America and the European Union. The most usually referenced standards are the NIJ Standard-0101.07, which outlines testing

procedures, in conjunction with NIJ Standard-0123.00, which describes ballistic protection levels, and the Home Office Body Armour Standard (2017) [56, 57, 58]. These standards provide comprehensive guidelines for techniques, apparatus, physical settings, and terminology to evaluate the ballistic impact properties of various body armors.

Having established a comprehensive understanding of the standards and testing procedures for body armor, including the evaluation of ballistic resistance and the categorization of protection levels, materials that play a crucial role in enhancing ballistic protection will be explored. The next section will investigate into ceramics for ballistic protection, examining their properties, advantages, and applications in the development of advanced body armor systems designed to provide superior defense against high-velocity and high-mass projectiles.

1.5 Ceramics for ballistic protection

Typically, ceramic materials used in armor configurations are either monolithic tile or in hybrid composite design (hard-faced ceramic plate placed in front of the projectile and high-performance fiber placed towards the human body). The common ceramic materials are used in armor designs as a monolithic plate, Figure 1.11a. Monolithic plates are generally thought of as a single, rigid, layer of homogenous ceramic material. This kind of structure typically do not incorporate multi-hit capability when they are impacted by projectiles. To improve ballistic protection, reducing tile size is an effective strategy. By minimizing tile size, the area which is vulnerable to impacts is significantly reduced if a single tile is compromised. This design approach is known as 'mosaic armor', Figure 1.11b. These structures have been developed to supply multi-hit resistance. In mosaic armors, numerous ceramic tiles are joined together in a patterned arrangement (hexagonal, rectangular, square, balls and cylindrical shapes) therefore the broken of one tile would produce minimum destruction to the other tiles through restraining the crack propagation.

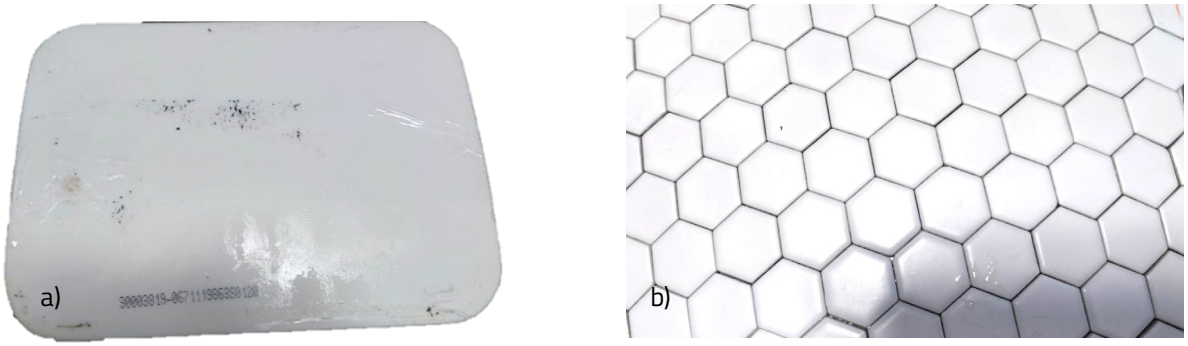

Figure 1.11 The design of ceramic tiles in ballistic armors: a) monolithic; b) hexagonal tiles arranged in a mosaic pattern

Introducing an additional rubber layer in front of the ceramic can significantly influence the ballistic performance of brittle materials. Si et al. [86] conducted ballistic testing on a polyurea-reinforced ceramic/ metal armor, including three types of polyurea elastomer positions (front, middle, and rear). The study concludes that polyurea significantly enhances the ballistic performance of ceramic composite armor, particularly when applied to the front face. Jitarașu and Lache [87] conducted numerical simulations and ballistic testing using various types of projectiles on different configurations

of monolithic ceramic composite armors, including those with and without a rubber layer as a striking coating. Their studies showed that composite amour systems with rubber layers on the front side offer superior energy absorption performance.

The combination of monolithic and mosaic structures, along with the strategic placement of rubber layers and other materials, can optimize ballistic performance, offering high protection against a variety of ballistic threats. The continuous development and refinement of these designs ensure that armor systems can meet evolving protective needs.

Having explored the mechanical properties, design innovations, and fabrication techniques of ceramic materials in ballistic armor, it is essential to consider another critical component of modern protective systems: fibers. The next section will explore into the various types of fibers used in ballistic applications, examining their unique properties, performance characteristics, and the role they play in enhancing the overall effectiveness of armor systems. By understanding the interaction between ceramic materials and high-performance fibers, a comprehensive understanding of how advanced composite armors are designated to provide superior protection against a wide range of ballistic threats.

1.6 Fibers used in ballistic applications

Continuous development in the bulletproof materials field, particularly in soft fabric ballistic vests are leading to advances in this area. In the past two decades, some fibers with advanced mechanical properties have been produced for ballistic impact usage. These fibers are generally lightweight and have higher energy-absorbing abilities. Today, synthetic fibers are the dominant class of materials used in bulletproof vests, especially in industries requiring superior mechanical, thermal and chemical stability. These high-performance fibers (HPF) are technical fibers known for their superior strength and stiffness (modulus), low density and ability to withstand high temperatures, chemicals, abrasion, fatigue, and cuts [34, 89, 90].

Aramid and UHMWPE are the main fibers utilized in the fabrication of ballistic protective equipment. These materials exhibit superior tensile strength and reduced weight compared to alternative materials, making them highly effective for bulletproof applications. These superior mechanical performances are significantly influenced by the manufacturing processes of the fibers. For example, the dry-jet wet spinning method used in the production of aramid fibers ensures optimal molecular alignment, resulting in high tensile strength and modulus. Similarly, the gel spinning process used for UHMWPE fibers enhances their tensile properties by aligning the polymer chains during fiber formation. Understanding and optimizing these manufacturing techniques are crucial for achieving the desired mechanical performance in ballistic protective materials [92, 122, 123].

The materials discussed in this section, from high-performance synthetic fibers to natural fibers, provide the background for technical textiles designed to meet the high requirements of ballistic protection. The next section will look in detail at how these materials are processed into advanced textiles, exploring the integration of their mechanical properties, energy absorption capabilities, and structural designs to create specialized fabrics that enhance protection, flexibility, and functionality in ballistic applications.

1.7 Technical textiles for ballistic protection

Ballistic fabrics are critical in personal and vehicle protection systems, designed to stop the high-velocity projectiles. The effectiveness of these fabrics depends on their ability to absorb and dissipate energy from impacts. This involves a combination of the textile's local energy absorption capabilities and the efficiency with which this absorbed energy is transferred to the crossover points of the yarns, dissipating energy through stretching and breaking. Ballistic fabrics can be categorized into three main types based on their construction: woven, unidirectional laminated (UD), and nonwoven. Additionally, the architecture of these fabrics can be further divided into 2D and 3D structures, with 2D fabrics being planar and 3D fabrics having a more complex three-dimensional form, that can enhance their ability to absorb and dissipate energy.

1.7.1 Important aspects for the performance of ballistic fabrics

The performance of ballistic fabrics is influenced by a wide range of factors, from the structural characteristics of the fabrics to the properties of the projectiles. Some of the influencing factors include fiber type and properties, fabric architecture and the interaction between layers on impact. Inter-yarn friction and fabric-projectile interactions play a crucial role, influenced by factors such as geometry and projectile velocity. In addition, environmental conditions, including temperature and humidity, can have a significant impact on the effectiveness of these structures.

Following the basic understanding of ballistic textiles, the next section discusses high-performance fiber-reinforced composites, which represent a significant development in ballistic protection technologies. While fabrics provide critical energy absorption and impact resistance, composites integrate these advanced fibers with resin matrices to form rigid, lightweight, and highly durable structures. These composites exploit the unique properties of fibers like aramid, UHMWPE, and carbon, combining them with adapted matrix systems to achieve superior ballistic performance. The following section will explore the design, fabrication, and performance optimization of these fiber-reinforced composites, highlighting their role in advanced applications, where enhanced strength, reduced weight, and greater resistance to complex threats are critical.

1.8 High-performance fiber-reinforced composites for ballistic protection

Composites are made by mixing two or more distinct materials to create a structure with new or improved properties. This combination often results in superior performance characteristics compared to traditional materials. For example, fiber-based composite materials, widely used in ballistic applications, use the strength and lightweight of fibers to provide superior impact resistance. These composite materials not only offer improved durability but also significant weight reduction, which is essential for applications requiring high mobility and strength. In addition, composite materials exhibit very good chemical and weather resistance, which makes them suitable for use in various environments. The various types of reinforcements and matrix materials allow the properties of composites to be adaptable. By carefully selecting and aligning fiber reinforcements, composites with directional properties can be considered to satisfy specific structural requirements. This versatility

makes composites ideal for applications requiring distinct properties in different directions. In composite structures, the discontinuous constituent, referred to as the reinforcement, is integrated into the continuous constituent known as the matrix. This integration results in a synergistic material that shows improved performance characteristics.

1.8.1 Important aspects for the performance of ballistic fiber-based composites

During ballistic impacts, various factors contribute to the failure of composite materials. Distinguished among these are matrix cracking, delamination, fiber failure, and frictional energy losses that occur between the composite material and the impacting projectile. The mechanisms of energy absorption during such impacts are primarily influenced by frictional losses. This energy dissipation process involves yarn slippage, interaction between adjacent layers, and the interactions occurring between the projectile and the composite material itself. These frictional responses are particularly pronounced at lower impact velocities. When a composite material is subjected to ballistic impact, its response can be categorized into local and global reactions. At lower velocities, a global reaction, characterized by the propagation of stress waves, is typically observed. As the impact velocity increases, this global response transitions into a local response, showing as shear or plug failure. At lower velocities, there is sufficient time for the transfer and dispersion of the impact energy across a wide area of the composite material. This increased impact duration facilitates the generation and propagation of elastic waves, including shear and flexural waves, to the boundaries of the structure. Consequently, the material's ability to absorb and dissipate energy is improved, reducing the probability of catastrophic failure [178].

The high performance of composite materials has been involved in advancing ballistic protection technologies, providing their ability to combine impact resistance with lightweight properties. However, while the fiber reinforcements and matrix structures of composites are critical for energy absorption and damage mitigation, the adhesive and resin systems used within these structures also play an essential role. These systems influence not only the bonding and integrity of the materials but also their mechanical behavior under high-stress conditions. The subsequent section explores the adhesives and resins used in ballistic protection structures, examining their contributions to energy dissipation, structural cohesion, and the overall enhancement of composite performance in demanding applications.

1.9 Adhesives and resins used in ballistic protection structures

Adhesive interlayers play a significant role in composite ballistic structures, strongly influencing their impact response. Recent studies such as those by Shen et al. [210] and Başer et al. [211] have shown that the thickness of the adhesive layer, especially in ceramic composite armors, can influence the ability of the armor to absorb energy, reduce ceramic spalling and manage shear stress. A thicker adhesive layer improves energy absorption by distributing the stress from the ceramic to the composite backing, while a thinner layer helps prevent bending and spalling of the ceramic tiles. In addition, the

bond strength and failure displacement of the adhesive interlayer are critical to multiple impact performance as they determine the ability to retain and confine the layers of material in the composite.

Resins also play an essential role in ballistic armor systems, acting as binders that hold ballistic fibers in position and orientation to protect against high-velocity projectiles. These resins not only help to distribute the load evenly between fibers after impact, but also prevent the propagation of microcracks and increase the durability of the structure. Although the resins themselves do not have ballistic resistance properties, they are essential for binding and securing the reinforcing fibers, contributing to kinetic energy distribution through mechanisms such as matrix cracking, debonding, fiber shearing, hydrostatic crushing, tensile breaking and frictional sliding. The selection of the resin system can significantly influence the total absorbed energy and damage resulting from ballistic impact.

The next section will focus exclusively on rubber in ballistic applications, exploring its unique material properties, innovations in its integration within armor systems, and its expanding role in meeting the demands of modern warfare and security. As a multi-purpose and high-performing material, rubber holds the potential to redefine the limitations of ballistic protection, offering new solutions to complex challenges while ensuring optimal safety, flexibility, and efficiency.

1.10 Rubber materials in ballistic protection

In the field of ballistic protection, material selection is extremely important to ensure both safety and effectiveness. Among the multitude of materials available, rubber has developed as an important component in various ballistic applications. Its unique combination of flexibility, energy absorption and cost-effectiveness make it an attractive choice in the design of protective solutions. The flexibility of rubber allows it to deform under stress and return to its original shape once the stress is removed. This characteristic is essential in ballistic applications as it allows the material to absorb and dissipate the energy from impact, reducing the potential for penetration and back-face deformations. The viscoelastic nature of rubber allows it to convert a significant portion of the impact energy into heat, reducing the force transmitted through the material [227]. Another characteristic of rubber is its ability to absorb kinetic energy. On impact, the rubber deforms, and this deformation process absorbs energy, reducing the force transmitted through the material. The rubber's ability to deform on impact helps absorb the kinetic energy of projectiles, increasing the effectiveness of the protective system. Rubber's relatively low density contributes to its attraction in ballistic applications where weight is a critical factor. The use of rubber allows lightweight protective systems to be designed without compromising performance. This advantage is particularly important in personal protective equipment where overweight can restrict mobility and efficiency. In addition to its mechanical properties, rubber is also a cost-effective material. Its high availability and ease of manufacture contribute to its affordability. Moreover, the durability of the rubber ensures a long service life, reducing the need for frequent replacements and therefore long-term costs. Rubber has very good resistance to various environmental factors including temperature fluctuations, humidity and UV radiation. This combination of low initial costs and durability makes rubber an economically attractive option for ballistic applications.

The strategic use of rubber in military applications highlights its strength and effectiveness in enhancing ballistic protection. Whether used in armor systems, defensive structures, firing ranges or projectile catching systems, rubber materials contribute significantly to mitigating impact forces, absorbing shock waves and improving safety in combat and training environments. Due to continuing advances in elastomer engineering and composite materials technology, the role of rubber in next-generation ballistic applications is expected to expand even further.

1.10.1 Mechanisms of ballistic energy absorption in rubber materials

Upon ballistic impact, rubber undergoes significant compression and deformation, which are primary mechanisms for energy absorption. The viscoelastic nature of rubber allows it to deform under the high strain rates typical of ballistic events, thus dissipating kinetic energy and reducing the force transmitted through the material. This deformation process involves both elastic and plastic responses, making the material to absorb energy efficiently. Rubber layers can act as shock absorbers, absorbing and dissipating energy upon impact over a larger area, thus improving the ballistic resistance of armor structures. During deformation, a portion of the kinetic energy from the projectile is converted into heat within the rubber material. This heat dissipation contributes to the overall energy absorption capacity of the rubber. Additionally, the inherent resilience of rubber leads to a rebound effect, where the material tends to return to its original shape after deformation. This elastic recovery can further dissipate energy and reduce the probability of material failure under repeated impacts.

Rubber layers show notable multi-hit capabilities due to their elasticity, energy absorption properties, and self-recovering behavior after impact. When hit by high-velocity projectiles, rubber materials experience localized deformation, absorbing kinetic energy through elastic deformations. Unlike brittle materials, which experience permanent cracking and fragmentation upon impact, rubber layers tend to distribute stress over a larger area and gradually recover their shape, making them effective for repeated impacts. The material's ability to withstand multiple impacts without significant structural damage is improved by its high tensile strength and elongation at break, which prevent catastrophic failure even when pierced.

1.11 Conclusions

Ballistic protection systems represent the crossroad of advanced materials science, engineering innovation and strategic design to protect personnel against complex and evolving threats. The evolution from traditional heavy metal armor to advanced composites, ceramics and hybrid structures highlights continuous research to improve protection, mobility and efficiency.

The advancement of modern ballistic protection systems is primarily driven by the development of innovative materials. Composites, high-performance fibers, ceramics, adhesives and resins have been essential in developing protective capabilities. Ceramics such as alumina (Al_2O_3), silicon carbide (SiC), and boron carbide (B_4C) provide very high hardness, enabling them to shatter and erode projectiles upon impact. Their integration into hybrid designs, such as mosaic armor, enhances multi-hit performance and damage limitation. Backing plates combined with ceramic striking faces further improve energy

absorption by capturing debris and redistributing impact forces. Fibers, including aramid (e.g., Kevlar) and ultra-high-molecular-weight polyethylene (UHMWPE), offer tensile strength and lightweight properties. They are involved in reinforcing composites and enabling flexibility while maintaining high energy absorption. Adhesives and resins play a vital role in maintaining structural integrity, distributing interfacial stresses, and optimizing multi-layered systems for improved performance under high-stress impacts.

Among these advancements, rubber has proven to be a revolutionary material in the design and performance of ballistic protection systems. Its distinct properties such as elasticity, energy absorption, and resistance to crack propagation, effectively address critical challenges in the design of modern armor systems. Rubber's ability to absorb and redistribute impact energy significantly improves the performance of composite and ceramic-based systems. Rubber's critical applications in ballistic systems include:

a) *energy absorption and distribution*: rubber layers, particularly in honeycomb configurations, improve the dissipation of kinetic energy, minimizing blunt trauma and back-face deformation. This is critical for reducing injury to personnel.

b) *improving multi-hit resistance*: mosaic armor designs, where rubber is used to bond ceramic tiles, limit the spread of damage and ensure that a single impact does not compromise adjacent tiles. This capability is vital in scenarios involving multiple projectile strikes.

c) *crack propagation prevention*: the presence of rubber between ceramic tiles prevents cracks from spreading across the entire armor surface, thereby maintaining structural integrity even after high-energy impacts.

d) *dynamic performance improvement*: studies have shown that rubber coatings or interlayers significantly improve the resistance of armor to dynamic stresses, including the shock waves generated by high-velocity impacts.

Additionally, the flexibility of rubber contributes to the comfort and wearability of personal protective equipment, ensuring that ballistic vests and helmets maintain operational efficiency. Its use in vehicular armor systems also improves adaptability by providing lightweight solutions that do not compromise structural integrity.

This comprehensive overview of ballistic protection systems sets the premise for the role that rubber can potentially have in the advancement of this field. By addressing challenges such as energy absorption, damage limitation, multi-hit resistance and cost-effectiveness, rubber has established itself as a fundamental component in the design of modern armor systems. Beyond its current applications, continuing research into advanced rubber composites, elastomeric coatings, and novel bonding techniques promises to further improve the durability and effectiveness of protective systems.

Taking into account the critical review of the state of the art in ballistic protection systems and the conclusions formulated on its basis, this doctoral thesis aims to develop an innovative armor solution to improve ballistic performance of personal protective equipment using lightweight and cost-effective materials. As presented in detail in Chapter 2, the research focuses on integrating advanced materials, particularly rubber, to optimize impact resistance, energy absorption, and multi-hit performance conforming to established protection standards.

2. Research goals and objectives

The main goal of this doctoral thesis is to develop an innovative armor solution to improve the ballistic performance of personal protective equipment using lightweight and cost-effective materials. The conducted research in this regard aims to propose a solution that addresses current limitations in armor manufacturing for advanced lightweight materials used in ballistic protection, specifically focusing on reducing the weight and manufacturing costs of protective systems and components. An essential aspect is the integration of materials with superior energy absorption properties, such as rubber, while ensuring high-impact resistance and conforming to established ballistic protection standards. The novel structures proposed and analyzed in this research must achieve balance between several critical factors, including impact resistance, maintaining structural integrity after impact, multi-hit resistance, and effective energy dissipation to minimize ballistic trauma and back-face deformation. This approach will contribute to the advancement of next-generation body armor technologies, leading to improved safety, better performance, and greater acceptance in both military and civilian applications.

To achieve the main goal of the doctoral thesis, the following objectives have been set:

1. Critical review of the state-of-the-art in the field of lightweight structures for ballistic protection;
2. Design and development of novel ballistic protection structures for soft and rigid body armors, in accordance with body armor standards established by state agencies;
3. Theoretical and experimental analysis of hyper-elastic behavior of rubber materials used in novel ballistic structures;
4. Theoretical and experimental analysis of the novel soft ballistic structures at low-velocity impact;
5. Theoretical and experimental analysis of the novel rigid ballistic structures at high-velocity impact.

3. Design and development of novel ballistic structures for soft and rigid body armors

The continuous advancement in ballistic protection materials has led to the exploration of innovative composite structures that combine flexibility and strength. Traditional armor systems use rigid materials to stop projectiles, but novel designs incorporating hyper-elastic components, such as rubber, offer improved energy absorption and impact mitigation. This chapter presents the design and development of both soft and rigid ballistic protection structures, focusing on material selection, layering strategies, and structural optimization.

3.1 Design and development of soft ballistic protection structures

Soft armor ballistic structures, known as UHMWPE-rubber composite panels, consist of two different material layers: ultra-high molecular weight polyethylene unidirectional fabric (UHMWPE UD – Dyneema HB26) at a density of 970 kg/m^3, and styrene-butadiene rubber with a hardness of 65 Shore and a density of 1530 kg/m^3 (SBR-65).

Three different configurations of UHMWPE-rubber composite panels have been used in this research, taking into account the rubber layer's relative position. The first configuration (PE-RCP-S) consists of an SBR-65 rubber layer which is sandwiched between two plies of UHMWPE UD sheets. The thickness of the rubber layer is 5 mm and for the two plies of UHMWPE UD sheets there are 9 stacked layers, each of them of 0.2 mm thickness, for each individual ply. The following two configurations consist of a SBR-65 rubber layer and a ply of UHMWPE UD sheets. The thickness of the rubber layer is the same as in the first configuration and for the ply of UHMWPE UD sheets there are 18 stacked layers, each of them of 0.2 mm thickness. The only difference between the two configurations is the placement of the rubber layer. In the second configuration (PE-RCP-F), the rubber layer is located in the striking face, while in the third configuration (PE-RCP-B), the rubber layer is located at the back face of the ballistic panel.

3.2 Design and development of rigid ballistic protection structures

The methodology for preparing rigid ballistic structures for testing is illustrated in Figure 3.3 and involves several important steps. First, the rubber honeycomb structures were manually cut to precise dimensions Figure 3.3b, followed by the assembly of a hexagonal mosaic ceramic tile pattern, where mosaic ceramic tiles were inserted into the honeycomb structure, Figure 3.3c. Once all components were prepared, the stacking of material layers was performed, Figure 3.3d. To improve structural integrity and reduce stress concentrations at material interfaces, two layers of self-reinforced polyethylene terephthalate (SrPET) fabric were incorporated at each interface between different materials (e.g. rubber-ceramic, ceramic-ceramic etc.), Figure 3.3e, improving tensile strength and adhesion. The assembled structure was then secured using a stretching film, enclosed within a vacuum

bagging film, and sealed with tacky tape at both ends, Figure 3.3f to ensure hermetic conditions for the subsequent curing process. The specimens, Figure 3.3g, experienced vacuum-assisted curing in an oven, where controlled heat and pressure facilitated proper material bonding and void elimination, Figure 3.3h. At the end of the curing cycle, the hardened ballistic composite structure was removed from the vacuum bag, resulting in a fully consolidated, impact-resistant configuration suitable for ballistic testing, Figure 3.3i.

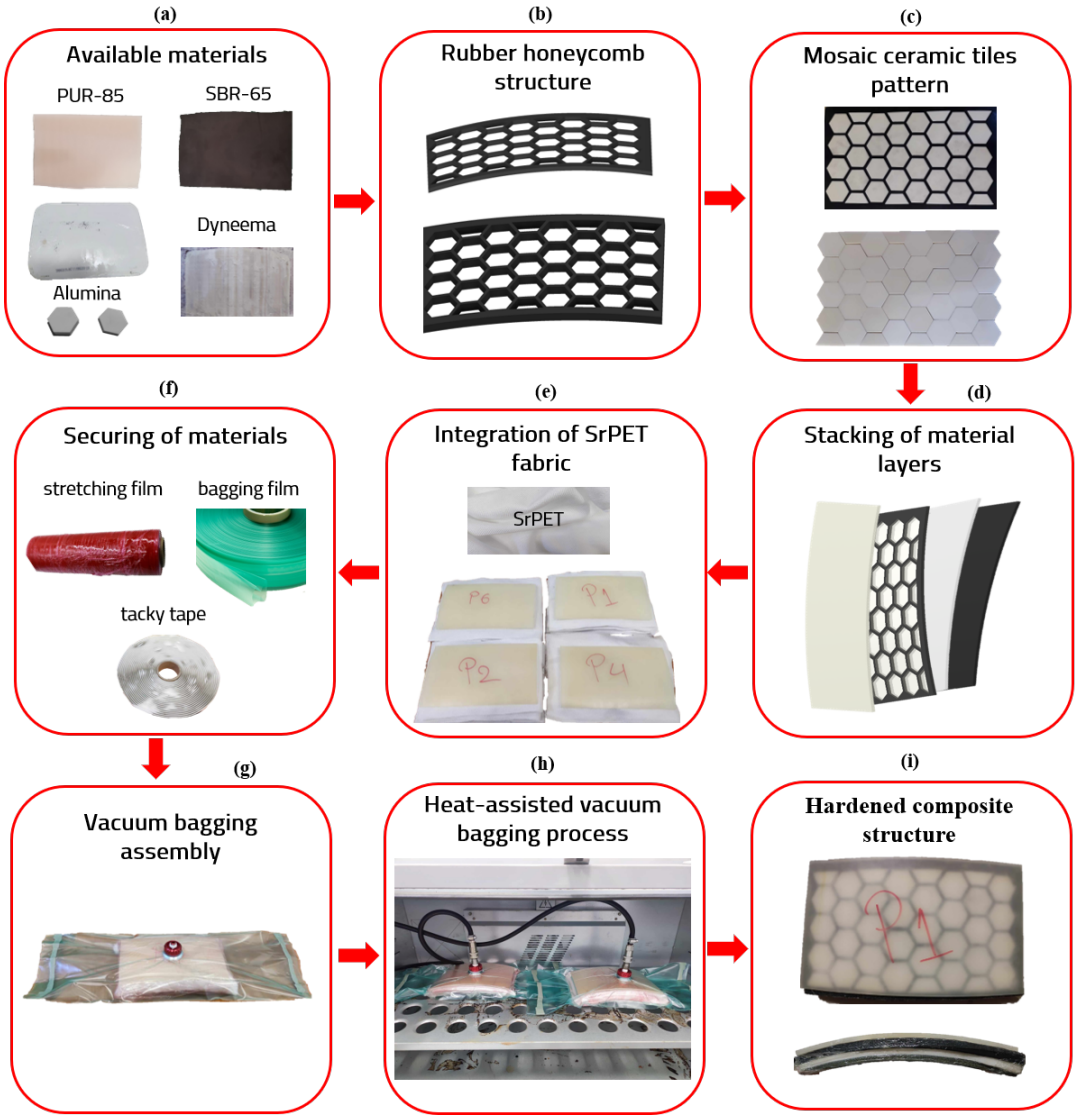

Figure 3.3 Schematic diagram for preparing rigid ballistic structures for testing

In this research, seven different configurations of rubber-ceramic composite plates have been used, considering two aspects: the arrangement of the ceramic tiles and the presence of the honeycomb rubber layer inside the structure. The first configuration (P1) consists of a striking layer of PUR-85 rubber, followed by two layers of Al_2O_3 hexagonal ceramic mosaic tiles arranged in a staggered pattern. Adjacent ceramic tiles are separated by elastic webs at the interface, where a honeycomb structure of SBR-65 rubber holds the ceramic tiles. This is followed by a ply of Dyneema HB26 sheets and a backing layer made of SBR-65 rubber. The ceramic and rubber layers, including the honeycomb structure, have a thickness of 5 mm. The UHMWPE UD sheet consists of 30 stacked layers, each with a thickness of 0.2 mm. The second configuration (P2) follows the same design as the first but differs in the stacking

of the two mosaic tile layers, which are placed directly together without the attachment of rubber honeycomb structures. The arrangement patterns remain the same as in the first configuration, along with the layer thickness. The 3rd configuration (P3) includes a striking layer of PUR-85 rubber, followed by an Al_2O_3 ceramic monolithic tile, a ply of Dyneema HB26 sheets, and a backing layer of SBR-65 rubber. The layer thickness remains consistent with the first two configurations, except for the monolithic ceramic tile, which has a thickness of 10 mm. The 4th configuration (P4) has the same design as the first configuration, but the two layers of mosaic ceramic tiles are stacked together in an aligned arrangement. The 5th configuration (P5) has the same design as the 2nd configuration, but the two layers of mosaic ceramic tiles are stacked together in an aligned arrangement. The 6th configuration (P6) includes a striking layer of PUR-85 rubber, followed by an Al_2O_3 ceramic mosaic tiles layer, a ply of Dyneema HB26 sheets, and a backing layer of SBR-65 rubber. Adjacent ceramic tiles are separated by elastic webs at the interface, where a honeycomb structure of SBR-65 rubber holds the ceramic tiles. The layer thickness remains consistent with other configurations, except for the mosaic ceramic tiles layer and honeycomb rubber structure, which has a thickness of 10 mm. The last configuration (P7) follows the same pattern as the 6th but differs in that the mosaic tiles layer is stacked without including of rubber honeycomb structures.

3.3 Weight and cost considerations of soft and rigid ballistic structures

The weight of ballistic protection systems is a crucial factor influencing mobility and operational effectiveness. Soft armor configurations, typically composed of high-performance fiber fabrics such as aramid or UHMWPE, offer superior flexibility and low weight, often less than 3-5 kg for a full vest system. In contrast, rigid armor structures that incorporate ceramic strike faces and composite backings provide higher levels of protection but can weigh between 6-12 kg, depending on the configuration. Traditional metal armor systems, such as steel or aluminum plates, although offering good protection, tend to significantly increase the total load, often exceeding 15-20 kg.

Table 3.1 Weight and cost estimation of soft ballistic panel structures

Configuration	Material composition	Approx. weight (kg)	Estimated cost (€)
PE-RCP-S	UHMWPE UD/ SBR-65 rubber/ UHMWPE UD	0.270	25.80
PE-RCP-F	SBR-65 rubber/ UHMWPE UD	0.270	25.80
PE-RCP-B	UHMWPE UD/ SBR-65 rubber	0.270	25.80
PE	UHMWPE UD	0.196	52.77
PE-R	UHMWPE UD/ Epoxy	0.226	53.70
K-U-R	Kevlar UD/ Epoxy	0.282	71.53
K-F-R	Kevlar fabric/ Epoxy	0.331	32.79

Table 3.1 and Table 3.2 present comparative overviews of the soft and rigid ballistic configurations analyzed in this study, detailing their material composition, approximate weight, and estimated production cost. In the case of soft armors (Table 3.1), the first three configurations (PE-RCP-S, PE-RCP-F, and PE-RCP-B) represent the proposed designs developed in this work, which incorporate

UHMWPE UD and SBR-65 rubber to achieve improved flexibility, energy absorption, and reduced cost. The remaining soft armor configurations are based on commonly used solutions involving Kevlar or UHMWPE with epoxy matrices. For rigid ballistic plates (Table 3.2), P1-P7 configurations correspond to the proposed multilayer structures developed in this research, combining alumina ceramics (monolithic or mosaic), rubber layers, UHMWPE UD, and SrPET. The remaining configurations (C_{mos}-K, C_{mos}-PE, C_{mono}-K, and C_{mono}-PE) reflect existing structural solutions typically composed of ceramic composites combined with Kevlar or UHMWPE backing layers.

The proposed configurations (PE-RCP-S, PE-RCP-F, and PE-RCP-B), which integrate UHMWPE UD layers with SBR-65 rubber, demonstrate competitive advantages in terms of lower weight and reduced cost compared to existing soft armor solutions at the same thickness. These designs are lighter and more economical, offering a cost-effective alternative to conventional panels. In contrast, configurations based only on UHMWPE UD with epoxy or Kevlar-based composites tend to be heavier and more expensive to produce. While Kevlar-based designs may offer reliable ballistic protection, they generally increase the overall mass of the system and require higher material investment. The use of SBR-65 rubber in the proposed structures improves flexibility and energy absorption without significantly adding to the weight, making them suitable candidates for applications where mobility, comfort, and cost-effectiveness are essential.

Table 3.2 Weight and cost estimation of rigid ballistic plate structures

Configuration	Material composition	Approx. weight (kg)	Estimated cost (€)
P1	PUR-85 rubber/ 2x Al_2O_3 Mos. + SBR-65 rubber HC/ UHMWPE UD/ SBR-65 rubber/ SrPET	1.867	79.16
P2	PUR-85 rubber/ 2x Al_2O_3 Mos./ UHMWPE UD/ SBR-65 rubber/ SrPET	1.845	82.53
P3	PUR-85 rubber/ Al_2O_3 Mono./ UHMWPE UD/ SBR-65 rubber/ SrPET	2.131	83.75
P4	PUR-85 rubber/ 2x Al_2O_3 Mos. + SBR-65 rubber HC/ UHMWPE UD/ SBR-65 rubber/ SrPET	1.867	79.16
P5	PUR-85 rubber/ 2x Al_2O_3 Mos./ UHMWPE UD/ SBR-65 rubber/ SrPET	1.845	82.53
P6	PUR-85 rubber/ Al_2O_3 Mos. + SBR-65 rubber HC / UHMWPE UD/ SBR-65 rubber/ SrPET	1.867	79.16
P7	PUR-85 rubber/ Al_2O_3 Mos./ UHMWPE UD/ SBR-65 rubber/ SrPET	1.845	82.53
C_{mos}-K	Al_2O_3 Mos./ Kevlar fabric/ Epoxy	1.828	84.33
C_{mos}-PE	Al_2O_3 Mos./ UHMWPE UD/ Epoxy	1.650	152.17
C_{mono}-K	Al_2O_3 Mono./ Kevlar fabric/ Epoxy	2.035	87.57
C_{mono}-PE	Al_2O_3 Mono./ UHMWPE UD/ Epoxy	1.857	155.41

The proposed rigid plate configurations (P1–P7), integrating layered alumina ceramics with SBR-65 rubber, PUR-85 rubber, UHMWPE UD, and SrPET, achieve an optimal balance of weight, protection, and cost. These designs show comparable or lower weights relative to existing ceramic composite plates while maintaining a more accessible production cost. In contrast, conventional configurations that integrate alumina ceramics with Kevlar or UHMWPE, bonded using epoxy (C_{mos} and C_{mono} configurations)

generally show higher material costs, particularly those using UHMWPE with epoxy as a backing. While these traditional systems provide strong ballistic resistance, the epoxy matrix increases fabrication complexity and cost. The integration of rubber components in the proposed configurations not only contributes to improved energy dissipation and multi-hit performance but also reduces back-face deformation without compromising lightweight properties. This makes them suitable for modern armor systems, providing strong protection while maintaining mobility and cost-efficiency.

3.4 Conclusions

The design and development of soft and rigid ballistic protection structures has focused on the use of UHMWPE-rubber composite panels and rubber-ceramic composite plates. The investigation involved the evaluation of multiple material configurations, stacking arrangements, and preparation techniques to improve the mechanical performance and ballistic resistance of the final structures.

The soft armor ballistic structures were based on UHMWPE UD fabric and SBR-65 rubber, with three different configurations, to evaluate the impact of rubber placement on energy dissipation and flexibility. The rigid ballistic structures, on the other hand, incorporated additional ceramic layers, PUR-85 rubber, and a honeycomb rubber structure, significantly improving the ballistic impact resistance. The use of staggered and aligned ceramic tile arrangements was applied to influence impact dispersion and energy absorption efficiency. The SrPET reinforcement was used to optimize structural integrity, reducing delamination risks. The final rigid structures showed a slight curvature, which improves mobility, ergonomic fit, and impact distribution. The vacuum-assisted curing process ensured material consolidation, improving flexibility and durability for the rigid armor ballistic structures.

The soft and rigid ballistic structures developed provide a solid basis for further research and optimization, particularly concerning the placement of rubber layer configurations, the optimization of ceramic plate arrangements and the advancement of hybrid reinforcement strategies. These improvements are essential for the development of the next generation of protective materials, to improve ballistic performance, energy dissipation and structural strength under high impact conditions.

In addition to mechanical performance, a comparative analysis of weight and cost was conducted for both soft and rigid ballistic configurations. The proposed soft armor designs, which incorporate UHMWPE UD and SBR-65 rubber in various stacking sequences, proved to be more cost-effective and lighter than conventional soft armors based on Kevlar or UHMWPE bonded using epoxy. Similarly, the proposed rigid plate configurations (P1–P7) demonstrated a well-balanced combination of reduced weight and lower production cost compared to traditional ceramic composite structures. These results show that the configurations developed within this thesis are practical and effective, making them suitable for conditions where mobility, low cost, and high ballistic protection are all important.

Rubber, as a critical component in energy absorption and impact mitigation, plays an essential role in improving the performance and effectiveness of these ballistic structures. In the following chapter, both theoretical and experimental analyses are conducted to investigate the hyper-elastic behavior of rubber materials used in soft and rigid ballistic structures, since this is essential for understanding their mechanical response under dynamic and ballistic loading conditions.

4. Theoretical and experimental analysis of hyper-elastic behavior of rubber materials used in novel ballistic structures

The increasing requirement for lightweight and flexible ballistic protection materials has led to extensive research into rubber-based composites and structures. Due to their hyper-elastic behavior, rubber materials show significant strain energy absorption, making them ideal candidates for impact mitigation applications. Unlike traditional rigid armor materials, rubber can undergo large deformations while maintaining structural integrity, which enhances its ability to disperse and absorb impact forces. This chapter explores both theoretical and experimental approaches to understanding the mechanical behavior of rubber under extreme loading conditions. By analyzing the strain energy potential, wave propagation mechanisms, and failure modes, a comprehensive assessment of rubber's performance in novel ballistic structures is provided. The following section focuses on the analytical modeling of ballistic impacts, numerical simulations, and experimental investigations to evaluate and improve the protective efficiency of hyper-elastic rubber materials.

4.1. Analytical approach of ballistic impacts on rubber materials

Hyper-elastic models describe materials in terms of strain energy potential, which depends on strain invariants. At high strain rates, as in the case of ballistic impact, the rubber behaves as an incompressible hyper-elastic material.

Rubber is known for being highly rate-dependent, meaning its mechanical properties change when subjected to extremely fast deformations. At high strain rates, rubber behaves in a stiffer manner, reducing its ability to stretch and recover, as shown by Khodadadi et al. [235] and Jitarașu and Lache [87]. This makes it susceptible to brittle failure in the event of a rapid ballistic impact. In slower deformations, rubber can dissipate energy through viscoelastic behavior, absorbing tensile stresses effectively. However, under high-speed impacts, the material does not have enough time to deform elastically, and instead, localized failure occurs at the rear face due to insufficient stress relaxation.

4.2. Experimental approach

The flow-chart depicting the research methodology applied to this chapter is presented in Figure 4. Two rubber materials, SBR-65 rubber, and PUR-85 rubber, have been considered, Figure 4.1a. The hardness of the rubber materials has been determined through testing with a Shore Durometer, Figure 4.1b. Several specimens have then been prepared, Figure 4.1c, and subjected to a series of quasi-static compression and tensile tests, Figure 4.1d, to establish the stress-strain curves for the two materials, Figure 4.1d1. Consequently, a series of dynamic compression tests have been performed using a single-stage gas gun, Figure 4.1e, resulting in the acquisition of force-acceleration vs time signals, Figure 4.1e1. Furthermore, ballistic tests have been conducted, Figure 4.1f to evaluate the impact resistance of the rubber materials under projectile impact, providing critical insights into their protective performance. Additionally, the muzzle velocity of the projectile has been measured using a

chronograph, Figure 4.1f1, ensuring accurate calculation of impact conditions and kinetic energy transfer. Subsequently, using the recorded Photron images and Tracker software, Figure 4.1g, the specimen's displacement under dynamic loading conditions has been obtained, Figure 4.1h, to establish the force-displacement curves for the two materials, Figure 4.1i. By connecting the specimen displacement data and the force time history, the stress-strain curve has been determined, Figure 4.1j. At the same time, a numerical model has been developed to predict the behavior of the two rubber materials. Data from both uniaxial quasi-static tensile tests and dynamic compression testing have been combined to generate a comprehensive curve, Figure 4.1k, which has been then integrated into the numerical software Abaqus/ CAE to calibrate the coefficients for the hyper-elastic constitutive model, Figure 4.1l. The calibrated coefficients were incorporated into the LS-DYNA software to simulate and analyze the response of the two rubber materials under dynamic and ballistic loading conditions, Figure 4.1m.

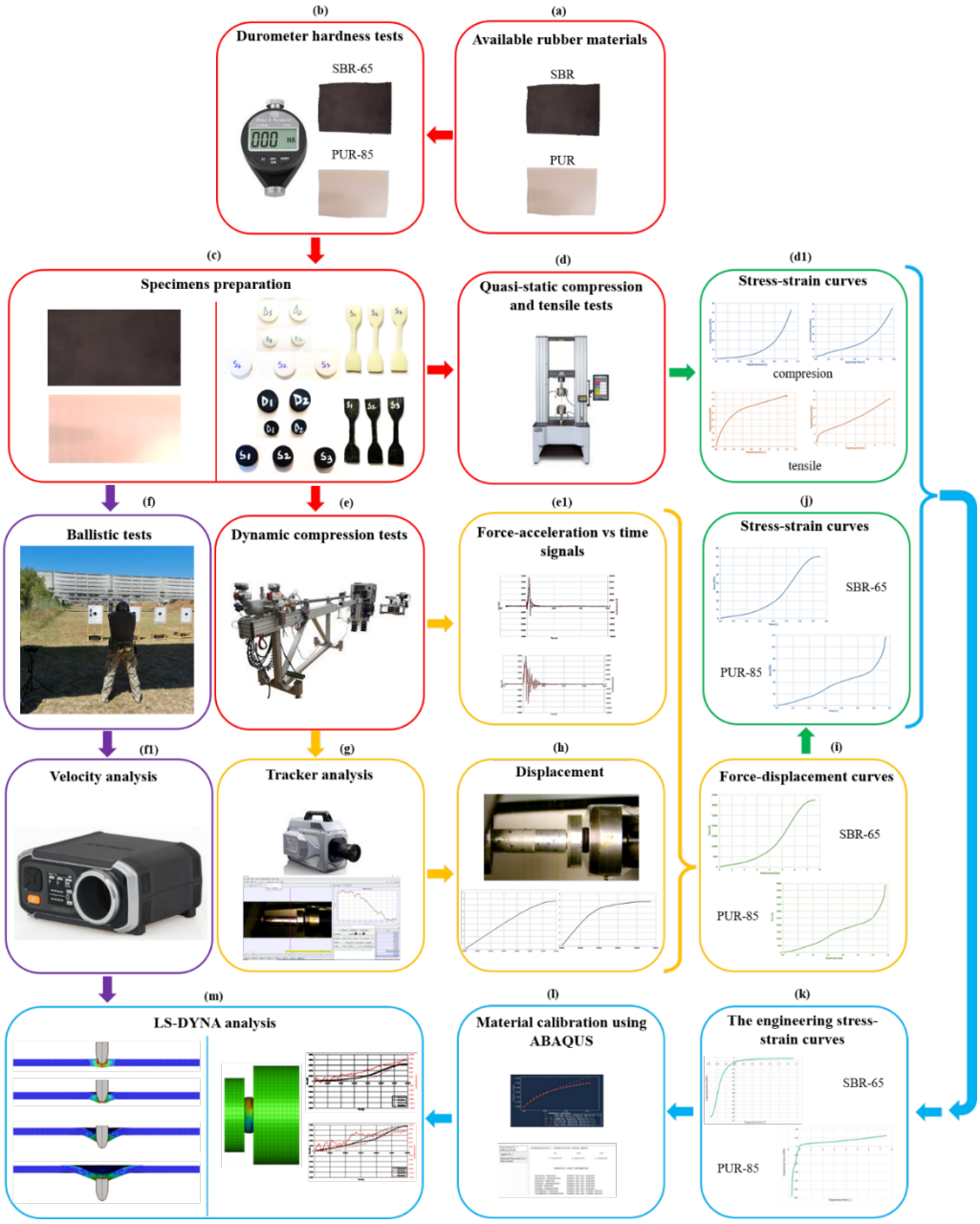

Figure 4.1 Flow-chart of the research methodology

4.2.1. Quasi-static compression testing

In the first step, a series of quasi-static compression tests have been conducted to determine the mechanical behavior of the two rubber materials under static loading conditions. The size of quasi-static compression specimens has been determined according to ISO 815-1:2019(E) standards [266]. The SBR-65 specimens have been cut from a 10 mm thick plate, in cylinders, with a diameter of 30 mm, The PUR-85 specimens have been cut from a 5 mm thin plate - cylinders of 30 mm diameter.

4.2.2. Quasi-static tensile testing

In a further step, tensile tests have been performed according to the ASTM D 412 and ISO 37:2017(E) standards [267, 268]. The specimens consist of SBR-65 and PUR-85 rubber, with 5 mm thickness.

4.2.3. Dynamic compression testing

A single-stage gas gun has been used for the dynamic testing of hyper-elastic rubber materials at various impact velocities. In this experiment specimens of SBR-65 and PUR-85 have been used, with cylindrical shape and diameters of 30 mm and 20 mm respectively. The specimen thickness has been kept the same as in the previous tests: 10 mm for SBR-65 and 5 mm for PUR-85, The different heights of the specimens (10 mm for SBR-65 rubber and 5 mm for PUR-85 rubber) have been selected based on the specific material properties and testing requirements. SBR-65 rubber, being less stiff and softer, required a thicker specimen to ensure accurate measurement of its compression behavior under quasi-static and dynamic conditions. In contrast, PUR-85 rubber, which is stiffer and harder, allowed consistent testing with thinner specimens while ensuring accurate results.

By using a 0.655 kg aluminum flat-end projectile, an even loading of the specimens has been assured. Dynamic tests have been recorded using a high-speed Photron camera set to 60,000 frames per second. Two sets of dynamic tests have been performed for each specimen diameter of hyper-elastic materials. All quasi-static tests and dynamic tests have been conducted under constant room temperature (25° C).

4.2.4. Ballistic testing

The ballistic tests have been performed on the two rubber materials in a shooting range in Mangalia, Romania, belonging to the Ministry of National Defense. The rubber samples tested had a thickness of 10 mm, allowing the evaluation of ballistic resistance and energy absorption capabilities under impact conditions.

A 9 mm pistol (GLOCK 17) with a full metal jacket round nose (FMJ RN) bullet with a mass of 8 g and a diameter of 9 mm has been used. The 9 mm bullet consists of a lead core and a brass jacket.

The rubber samples have been positioned 5 meters away from the test barrel's muzzle. An AC6000 BT chronograph has been used to measure the muzzle velocity of the projectile and has been determined to be 361 m/s. A ballistic calculator has been utilized to determine the projectile's impact velocity, considering shooting factors like ballistic coefficient of the bullet, muzzle velocity of the bullet, bullet

weight and atmospheric conditions such as altitude, temperature, and wind speed. The projectile's impact velocity has been found to be 356 m/s.

4.3. Experimental results and discussion

4.3.1. Quasi-static compression stress-strain curve of hyper-elastic materials

The stress-strain diagrams obtained as a result of the quasi-static compression testing of the two hyper-elastic materials are presented in Figure 4.12. Figure 4.12a and Figure 4.12b show the stress-strain curves for the three specimens of SBR-65 rubber and PUR-85 rubber tested, respectively, each plotted with their average curves, showing the mechanical response of each material to the applied stress.

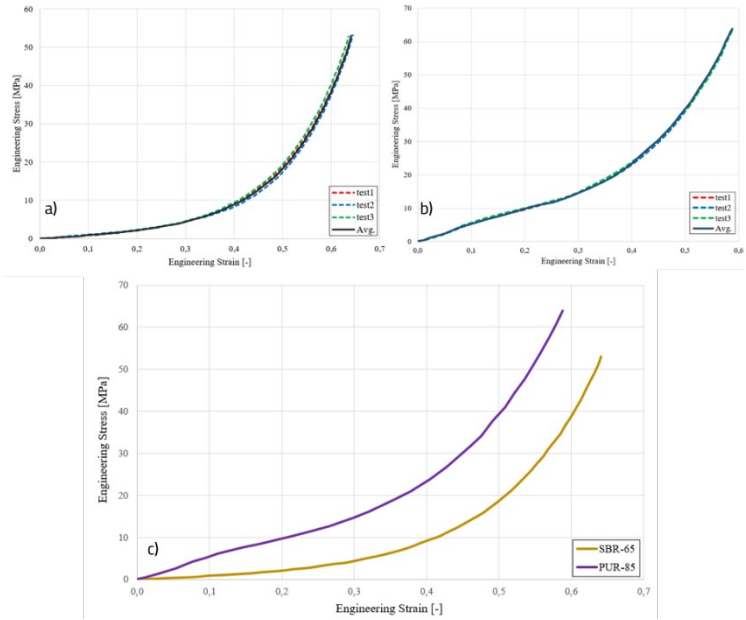

Figure 4.12 Strain-stress curves based on quasi-static compression tests: a) the average curve fo r the three SBR-65 mechanical testing curves; b) the average curve for the three PUR-85 mechan ical testing curves; c) average stress-strain curves for the two rubber materials

Figure 4.12c plots the average stress-strain curves for SBR-65 and PUR-85 rubbers. This highlights the differences in mechanical properties between the two rubber materials, providing a clear visual representation of their respective behaviors under identical testing conditions.

4.3.2. Quasi-static tensile stress-strain curve analysis of hyper-elastic materials

The stress-strain curves of the two hyper-elastic materials are shown in Figure 4.13. Like in the section above, the stress-strain curves for the three specimens of SBR-65 rubber and PUR-85 rubber tested have been plotted, respectively, each with their average curves, Figure 4.13a and Figure 4.13b.

Figure 4.12c and Figure 4.13c clearly show that an increase in the Shore hardness of the rubber corresponds to an increase in the stress of the material. It can be noticed that changes in Shore hardness directly affect the mechanical performance of rubber materials at the same strain values in quasi-static tests.

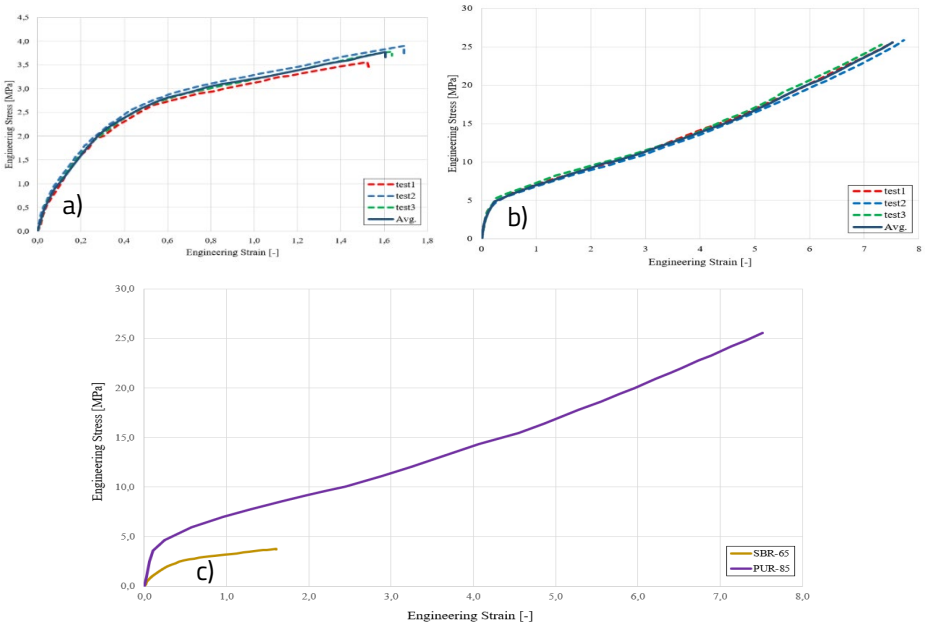

Figure 4.13 Strain-stress curves based on quasi-static tensile tests: a) the average curve for the t hree SBR-65 mechanical testing curves; b) the average curve for the three PUR-85 mechanical te sting curves; c) average stress-strain curves for the two rubber materials

4.3.3. Dynamic compression stress-strain curve of hyper-elastic materials

Experimental data on the dynamic compression of hyper-elastic materials with different Shore hardness have been processed to obtain stress-strain curves at high strain rates. The images recorded during the tests, along with the data acquisition time histories of the force, acceleration, and post-test specimen measurements, have been used to analyze the stress-strain curve.

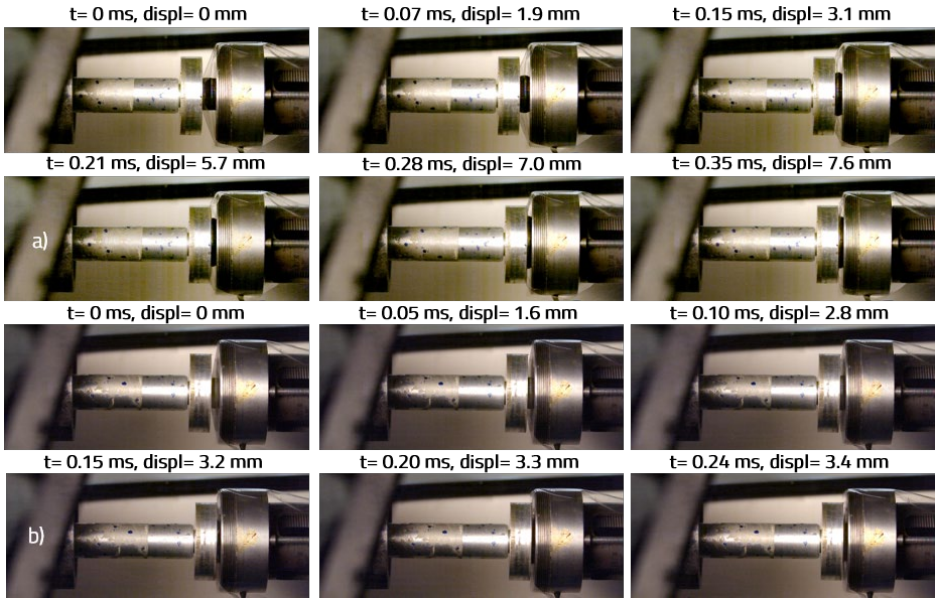

Figure 4.15 Dynamic compression of hyper-elastic specimens:
a) SBR-65 rubber; b) PUR-85 rubber

Using the recorded Photron images and Tracker software, the projectile impact velocity and specimen displacement have been investigated. The impact velocity of the projectile ranges between 12 to 16 m/s. The dynamic compression events recorded with the high-speed camera are shown in Figure 4.15.

By connecting the specimen displacement data and the force time history, the stress-strain curve has been determined, as shown in Figure 4.16.

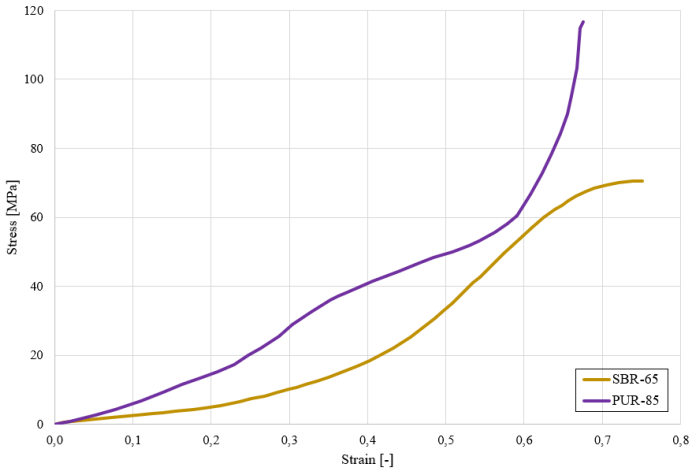

Figure 4.16 Stress-strain curves based on dynamic compression tests

It can be concluded that the dynamic behavior of the two tested rubber materials is different at high strain rates, and their mechanical properties are clearly time dependent. Also, similar to the quasi-static tests, an increase in the Shore hardness of the rubber corresponds to an increase in the material stress.

4.3.4. Ballistic test results and observations

The Figure 4.17 illustrates the bullet penetration and damage characteristics on the SBR-65 rubber sample subjected to ballistic impact. The figure provides a detailed view of both the striking face (entry hole), Figure 4.17a, and the backing face (exit hole) of the rubber specimen, Figure 4.17b, supported by macroscopic and microscopic (60X magnification) analyses.

Figure 4.17a displays the entry hole created by the projectile upon initial contact with the rubber surface. The macroscopic image shows a clean, circular perforation with a diameter much smaller than the diameter of the projectile (d_{s_SBR} = 1.5 mm), indicating localized material compression and shear failure at the point of impact.

Figure 4.17b shows the exit hole formed by the projectile upon impact with the SBR-65 rubber. The macroscopic image shows a slightly irregular and partially closed perforation, suggesting that the rubber attempted elastic recovery post-impact. However, the microscopic image shows more extensive material damage (d_{r_SBR} = 2.5 mm), with visible tearing and radial fracture pattern, indicating localized tensile failure due to extreme stress concentration at the rear surface. The outward expansion of fractured edges suggests that the projectile fully perforated the rubber layer, but with significant energy dissipation.

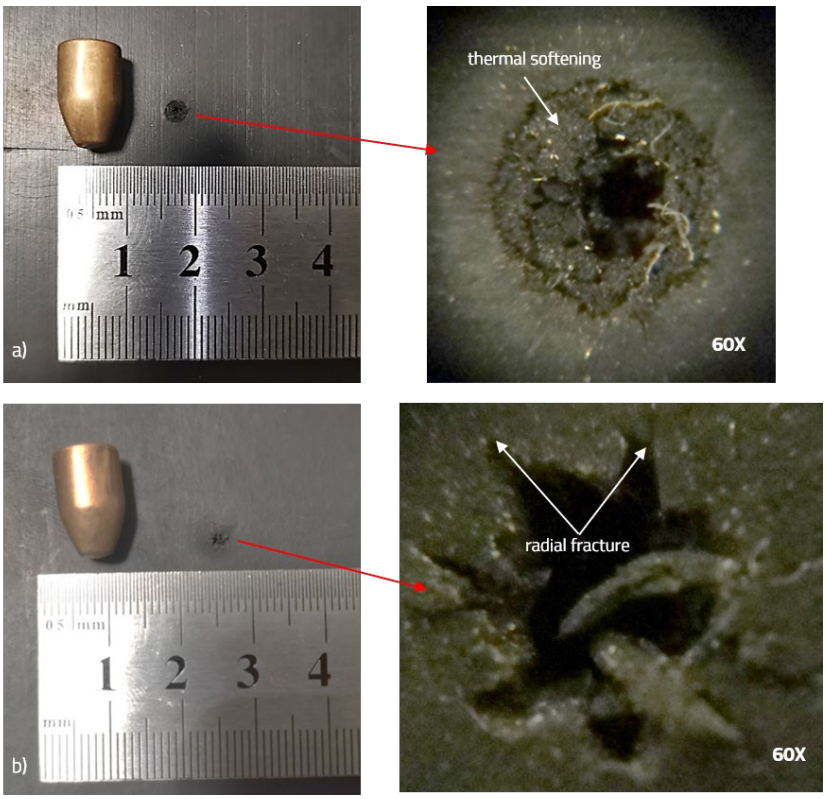

Figure 4.17 Bullet penetration hole in SBR-65 rubber:
a) striking face; b) backing face

Figure 4.18 illustrate the bullet penetration behavior in PUR-85 rubber under ballistic impact.

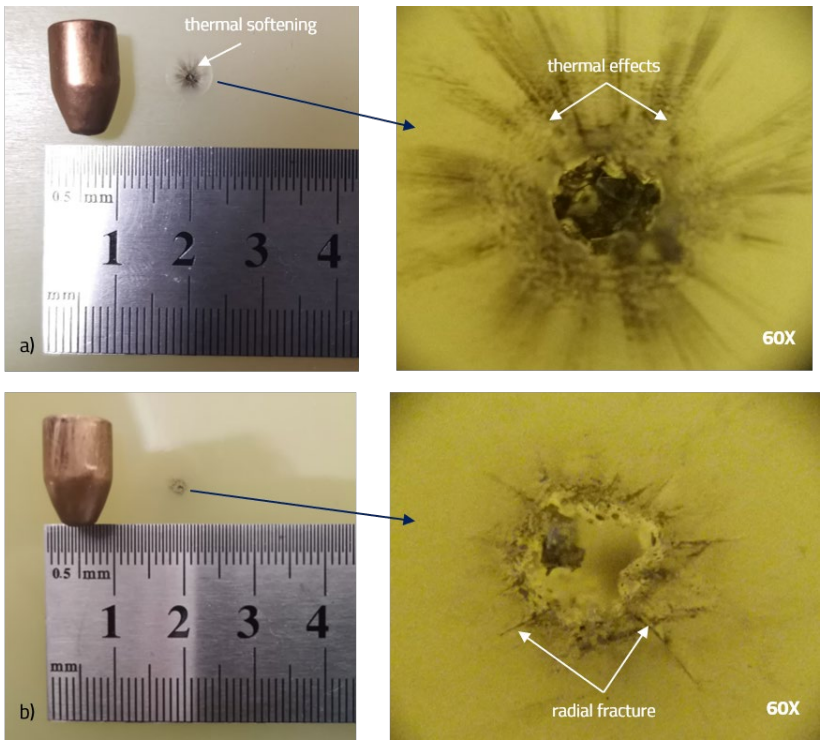

Figure 4.18 Bullet penetration hole in PUR-85 rubber:
a) striking face; b) backing face

The macroscopic image of the striking face, Figure 4.18a, displays a small, well-defined entry hole (d_{s_PUR} = 1 mm) with minimal surface damage, suggesting that the bullet perforated the material with minimal lateral deformation. Compared to SBR-65 rubber, PUR-85 displays a cleaner penetration profile, indicating a more localized response to impact due to its higher stiffness. The microscopic image of the backing face, Figure 4.18b, highlights clear radial fracture pattern around the exit hole. The fracture lines extending radially outward suggest tensile rupture due to stress propagation.

4.4. Numerical modelling

4.4.1. Dynamic constitutive model for the investigated rubber materials

To describe the behavior of the two rubber materials and their hyper-elastic characteristics, a numerical analysis has been performed, by using the Mooney-Rivlin constitutive model.

The stress-strain curve has been derived from uniaxial quasi-static compression and tensile tests, along with dynamic compression testing, which provided the input data for the *MAT_MOONEY_RIVLIN_RUBBER model. To create an accurate numerical model of the hyper-elastic materials under dynamic loading conditions, the stress-strain curves used should include both the compression (negative values) and tensile (positive values) domains. By combining data from both uniaxial quasi-static tensile tests and dynamic compression testing, a comprehensive curve was generated, as presented in Figure 4.20.

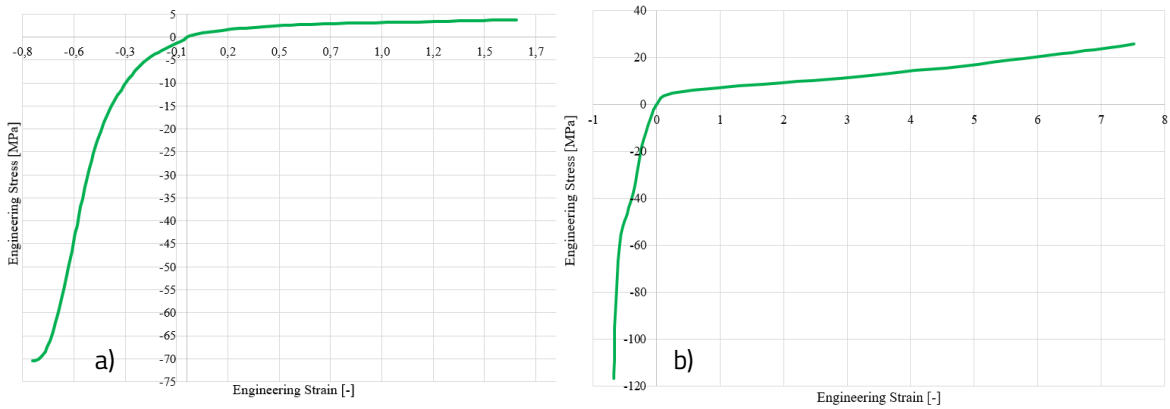

Figure 4.20 The engineering stress-strain curve used for the Mooney-Rivlin model:
a) SBR-65 rubber; b) PUR-85 rubber

The C_{10} and C_{01} coefficients for the Mooney-Rivlin constitutive model have been calibrated using Abaqus/ CAE.

The criterion used for rubber failure is the maximum principal strain. While quasi-static tensile tests suggest that the elongation at break of SBR-65 rubber is approximately 160% and of PUR-85 rubber exceeds 750%, findings from a comprehensive set of simulations indicate that the elongation at break for hyper-elastic materials is estimated to be 140% for SBR-65 rubber and 760% for PUR-85 rubber under dynamic loading conditions.

4.4.2. Constitutive modelling for ballistic impact on rubber materials

To model and analyze the ballistic impact between the 9 mm bullet and the two different rubber materials, a numerical model has been developed using LS-DYNA software. The impact has been assumed to be perfectly normal, and double symmetry has been taken into account, meaning only a quarter of the parts has been modeled, as shown in Figure 4.21. This approach is often used in ballistic impact simulations to reduce computational costs. Solid elements have been used for analysis.

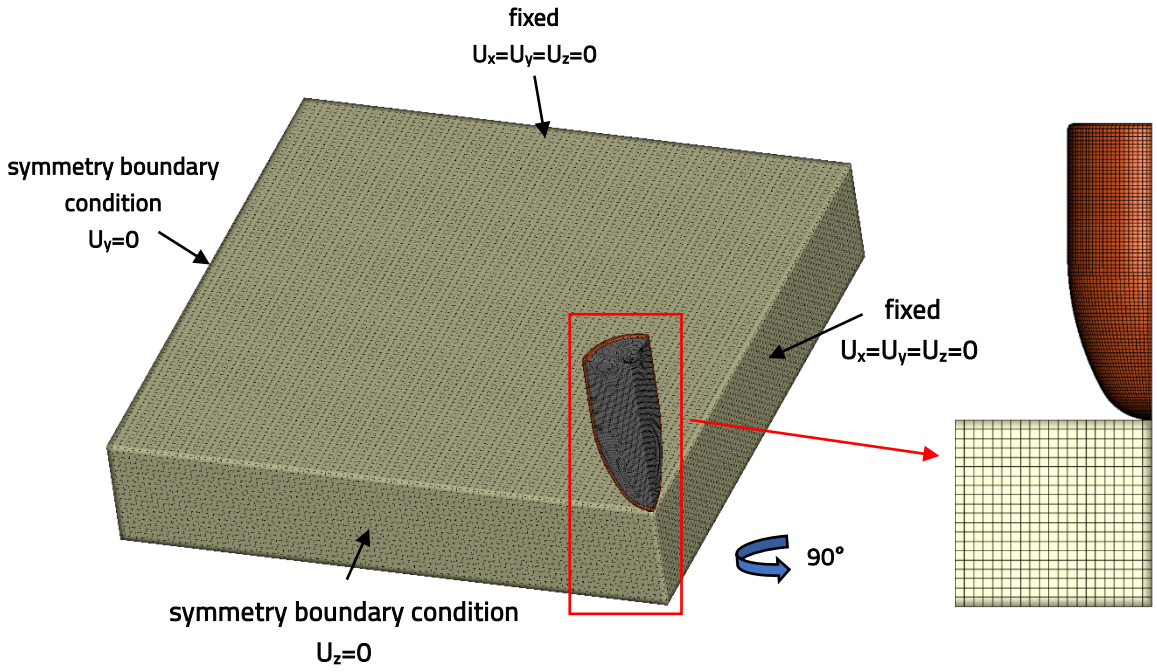

Figure 4.21 Finite element model and boundary conditions for ballistic impact on rubber materials

Since the deformation of the projectile is neglectable and not relevant for the numerical analysis, for computational time reasons, the *MAT_RIGID model has been assigned to both parts (lead core and brass jacket).

The interaction between the bullet and rubber layer has been modeled with CONTACT_ERODING_SURFACE_TO_SURFACE and the contact between parts of the same body has been realized using the CONTACT_ERODING_SINGLE_SURFACE algorithm.

The mesh sensitivity has been analyzed by considering an element size of 0.5 mm for the rubber layer and of 0.2 mm for the projectile, Figure 4.21.

4.5. Validation of the numerical models. Comparison of numerical and experimental results

4.5.1. Validation of dynamic behavior

The force-acceleration versus time curves derived from the dynamic compression simulations have been compared with the corresponding data from tests, for SBR-65 and PUR-85 rubber materials, Figure 4.22.

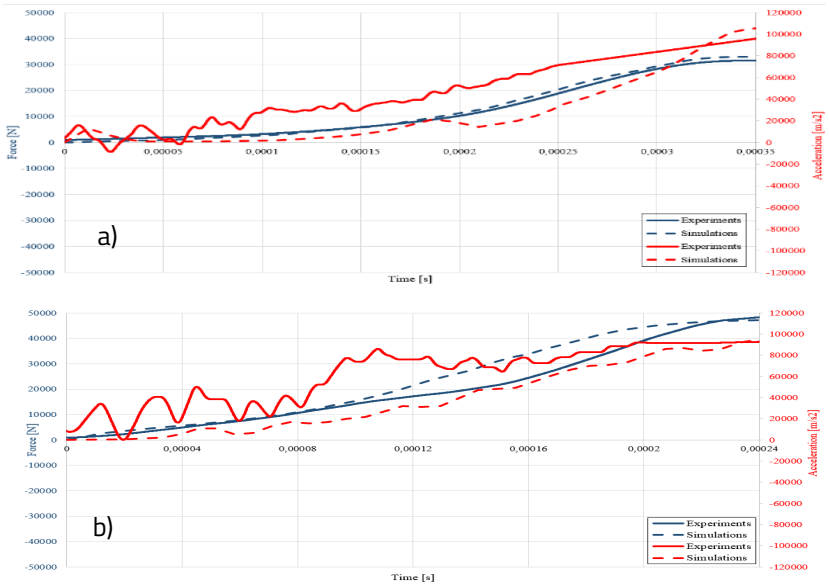

Figure 4.22 Experimental and numerical force-acceleration versus time curves obtained d uring the dynamic compression of specimens: a) SBR-65 rubber; b) PUR-85 rubber

Both graphs depict a close correlation between numerical and experimental results. There is an obvious agreement between the force-acceleration versus time curves obtained experimentally and numerically. prediction of rubber materials behavior by the constitutive model agrees very well with the experimental results investigated in the present work.

Last but not least, the results of dynamic compression simulation conducted on the two hyper-elastic materials are presented in Figure 4.23, by specimen displacement at various stages of the compression process.

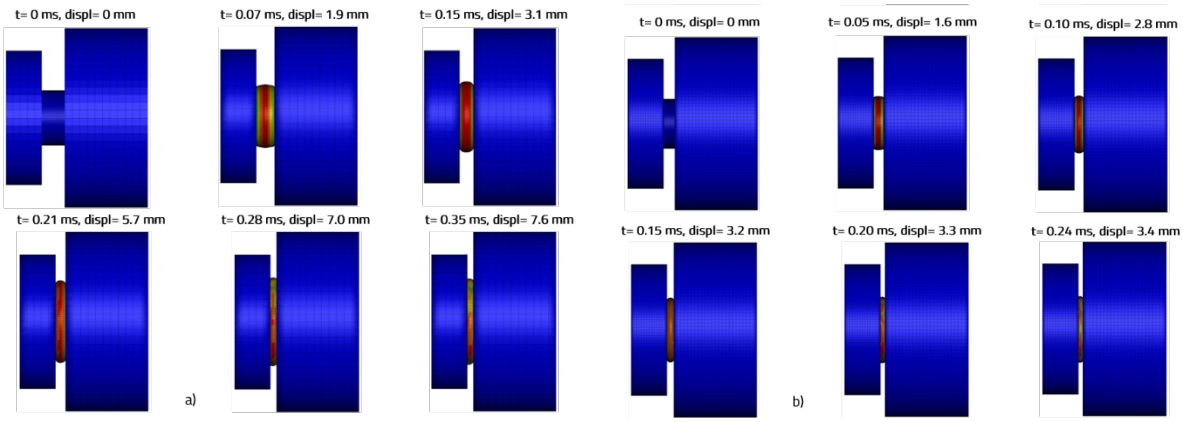

Figure 4.23 Numerical simulation on dynamic compression of hyper-elastic specimens: a) SBR-65 rubber; b) PUR-85 rubber

Figure 4.15 and Figure 4.23 show a close agreement between numerical and experimental results in terms of specimen deformation for the two hyper-elastic materials subjected to dynamic compression.

4.5.2. Ballistic impact validation

To simulate the impact behavior between the 9 mm FMJ bullet and the two rubber materials, the ballistic event has been assumed to be perfectly normal, the penetration process being simulated at 356 m/s striking velocity.

The comparison between numerical simulations and experimental results for SBR-65 and PUR-85 rubbers under ballistic impact conditions demonstrates a strong correlation, confirming the computational models' accuracy in predicting material behavior. Despite some variations in exit hole expansion and material recovery, the fundamental impact response observed experimentally was well-represented numerically, confirming the usefulness of these models for predicting rubber behavior under high-velocity impacts and optimizing ballistic protection designs.

4.6. Conclusions

The study of SBR-65 and PUR-85 rubber materials under both numerical and experimental conditions has provided valuable insights into their mechanical behavior and ballistic performance. The combination of quasi-static, dynamic, and ballistic tests has allowed for a comprehensive understanding of how these materials respond under different strain rates and impact conditions. The numerical models developed using LS-DYNA finite element simulations demonstrated a high degree of agreement with experimental findings, accurately capturing shockwave propagation, penetration mechanics, and material failure patterns.

Both SBR-65 and PUR-85 rubbers show distinct advantages when used as protective materials, with their performance varying significantly under different loading conditions. SBR-65 rubber, with its high elasticity, superior energy absorption, and deformation capacity, has proven to be highly effective at distributing impact forces and reducing kinetic energy transmission. Its adiabatic softening effect allows for improved impact mitigation, making it an ideal backing layer in ballistic plates, where it can absorb and dissipate energy efficiently, thereby reducing blunt force trauma and stress concentration. In contrast, PUR-85 rubber, with its higher toughness and greater resistance to impact, demonstrated a stiffer response with localized deformation and brittle-like failure under high-strain-rate conditions. Its ability to withstand multiple impacts without significant damage makes it a suitable material for the striking layer in a ballistic plate system, particularly when used in combination with ceramic tiles. Positioned on top of the ceramic layer, PUR-85 can contribute to projectile fragmentation and capture, preventing ricochet and secondary damage while maintaining the integrity of the protective structure. This dual-layer approach influences the strengths of each material to create a more efficient ballistic structure capable of withstanding high-velocity impacts while minimizing structural failure and energy transmission.

Starting from these findings, the next chapter explores the theoretical and experimental analysis of novel soft ballistic structures under low-velocity impact, where SBR-65 rubber will be integrated with UHMWPE UD fabric to further evaluate its energy absorption capabilities and effectiveness in improving the protective performance of soft armor configurations.

5. Theoretical and experimental analysis of the novel soft ballistic structures at low-velocity impact

In the previous chapter, the analytical approach to ballistic impacts on rubber materials was discussed, along with an in-depth analysis of the mechanical behavior of SBR-65 and PUR-85 rubbers under quasi-static, dynamic, and ballistic conditions. Based on these findings, the current chapter focuses on the integration of SBR-65 rubber with UHMWPE UD fabric to further evaluate its energy absorption capabilities and effectiveness in enhancing the protective performance of soft armor configurations. To achieve a comprehensive understanding of the protective potential of these hybrid structures, it is essential to first examine the behavior of fabrics under ballistic impact. This chapter begins with an analytical approach, highlighting the fundamental principles of single yarn impact theory and extending to an analytical model for ballistic impact on fabric structures. Following this, the failure mechanisms and damage evolution of woven fabrics under high-velocity impact are analyzed, providing critical insights into their structural response, energy dissipation mechanisms, and interaction with rubber-based layers in ballistic protection applications.

5.1. Analytical approach

5.1.1. Single yarn impact theory

The ballistic response of multi-layer fabric panels is first studied by observing the reaction of a single yarn to ballistic impact. An analytical model of a single yarn helps in understanding the ballistic impact mechanisms for these multi-layered fabrics, incorporating various internal and external factors. When a single yarn is subjected to a ballistic impact, it undergoes both longitudinal and transverse deformations. Upon impact, longitudinal and transverse strain waves propagate outward from the impact point at different velocities. The experimental observations indicate a triangular-shaped transverse deflection that increases with time until the yarn failure. The longitudinal wave, moving at the speed of sound in the material (c_0), induces tensile stress (σ_0) and strain (ε_0). The transverse wave, traveling with a velocity of c_1 behind the longitudinal wave, changes the motion of the material to align with that of the projectile. Behind the transverse wave front, all particle velocities correspond to the projectile velocity (V). As the impact continues, the yarn's strain reaches its breaking point, leading to failure. The behavior and propagation velocities of these waves are influenced by the yarn's tensile modulus, density, and pre-tension [1, 128].

5.1.2. Analytical model for ballistic impact on fabric structures

When the bullet nose strikes the yarns in the warp and weft directions, the fibers are subjected to intense stress. This induces a longitudinal strain wave that propagates away from the contact zone, coupled with a transverse strain wave. The propagation of longitudinal strain waves moves through the yarns at the speed of sound within the material. Higher transverse wave velocity is essential for rapid dissipation of impact energy. In high-velocity impacts, not all yarns are impacted simultaneously,

leading to early breakage of some yarns. This phenomenon suggests that the initial energy absorbed by the fabric may be relatively low, highlighting the importance of obtaining a higher transverse wave velocity to improve the overall impact resistance. Both longitudinal and transverse waves propagate through the yarns continuously until the strain reaches the breaking point.

Following the basic understanding of ballistic textiles, the next section discusses high-performance fiber-reinforced composites, which represent a significant development in ballistic protection technologies. While fabrics provide critical energy absorption and impact resistance, composites integrate these advanced fibers with resin matrices to form rigid, lightweight, and highly durable structures. These composites exploit the unique properties of fibers like aramid, UHMWPE, and carbon, combining them with adapted matrix systems to achieve superior ballistic performance. The following section will explore the design, fabrication, and performance optimization of these fiber-reinforced composites, highlighting their role in advanced applications, where enhanced strength, reduced weight, and greater resistance to complex threats are critical.

5.2. Failure mechanism and damage evolution of woven fabrics under ballistic impact

The behavior of a fabric under ballistic impact exhibits similarities to that of a single yarn. When a projectile impacts a fabric, both transverse and longitudinal waves are generated, like to the responses observed in single yarn impacts. Stress waves form at the point of impact, traveling along the yarns to the fabric's edges and reflecting back. These waves are partially transmitted and further reflected at the warp-weft crossover points. The speed of stress wave propagation along the yarns is influenced by their density and stiffness, impacting the energy dissipation of the fabric. The kinetic energy of the projectile is dissipated through fiber deformation and inter-fiber friction caused by slipping or sliding. The microstructure and frictional properties of the fibers significantly influence the fabric's energy absorption capacity. In multilayer fabrics, the energy is absorbed by successive layers until the projectile is arrested. The physical contact (bonding) between the layers facilitates both planar and perpendicular energy transfer, resulting in higher energy absorption in multilayer textile structures [31].

5.3. Experimental approach

5.3.1. Ballistic testing

Protective armor structures must be produced under international standards established by the United States of America and the European Union, as discussed in first chapter. The main objective of ballistic armor is to stop bullets from penetrating. The Home Office Body Armour Standard (H01 protection level) has been used to test the UHMWPE-rubber composite panels, which means that the ballistic panels can provide resistance against a 9 mm full metal jacket round nose (FMJ RN) bullet, with a specified mass of 8 g and a velocity of 365 m/s ± 10 m/s [35]. In order to protect the internal organs against non-penetrating wounds, the back face deformation (BFD) indentation must measure less than 44 mm, in accordance with this standard.

The ballistic tests have been performed on the three configurations previously presented in a shooting range in Mangalia, Romania, belonging to the Ministry of National Defense. The same ballistic testing methodology was applied as for the two types of rubber materials, utilizing a GLOCK 17 pistol with a 9 mm FMJ RN bullet, where the muzzle velocity (361 m/s) was measured using an AC6000 BT chronograph, and the impact velocity (356 m/s) was determined using a ballistic calculator. A caliper has been used to determine the depth of penetration of the armor panels. After the ballistic examination, UHMWPE-rubber composite panels have been cut and a cross-section has been taken to identify the types of damage and determine the damage mechanisms.

5.3.2. Experimental results and discussion

Figure 5.9 illustrates the projectile impact damage and failure mechanisms in the PE-RCP-B configuration.

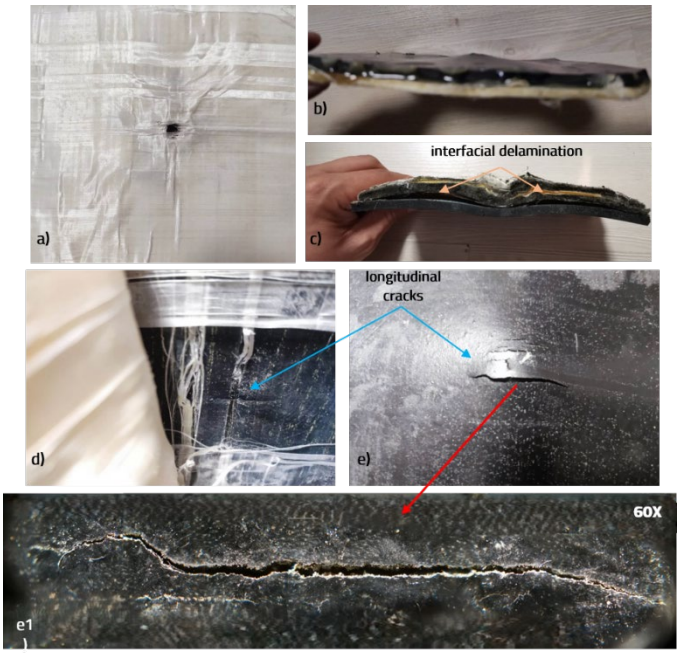

Figure 5.9 Projectile impact damage in the PE-RCP-B configuration: a) bullet penetration hole; b) back face deformation of the armor panel; c) cross-section of the armor panel; d) cracks in the rubber layer – striking face; e) cracks in the rubber layer – back face

The PE-RCP-B configuration highlights the effectiveness of using UHMWPE UD with a rubber backing layer in ballistic protection, as the panel successfully stopped the projectile while minimizing deformation and secondary damage.

Figure 5.10 illustrates the deformation of the 9 mm full metal jacket (FMJ) bullet after impacting the three configurations mentioned above. In Figure 5.10c (PE-RCP-B configuration), the projectile has experienced extreme plastic deformation, forming a bowl-shaped or petal-like structure with complete jacket rupture. The extensive radial splitting suggests that the projectile experienced significantly high resistance upon impact. The rubber backing layer in this configuration contributed to additional stress on the projectile upon deceleration, leading to fragmentation and severe jacket separation. This extreme deformation indicates that the projectile lost its structural integrity before perforation could occur.

Figure 5.10 Projectile deformation after impact: a) PE-RCP-S configuration; b) PE-RCP-F configuration; c) PE-RCP-B configuration

These findings confirm that the rubber-UHMWPE UD hybrid armor configurations significantly affect projectile behavior, with different energy absorption and failure mechanisms influencing projectile deformation and integrity.

5.4. Numerical modelling

5.4.1. Finite element modeling

To model and analyze the ballistic impact between the 9 mm bullet and the three configurations of UHMWPE-rubber composite panels investigated, a numerical model has been developed using LS-DYNA software. The impact has been assumed to be perfectly normal and double symmetry has been taken into account, meaning only a quarter of the armor panel has been modeled. Solid elements have been used for analysis.

The interaction between the bullet and different armor panel layers (UHMWPE and rubber) has been modeled with CONTACT_ERODING_SURFACE_TO_SURFACE. The contact between parts of the same body has been realized using the CONTACT_ERODING_SINGLE_SURFACE algorithm. To simulate the separation effect between each UHMWPE sheet and the debonding of the rubber layer from the UHMWPE plies, TIEBREAK_SURFACE_TO_SURFACE contact algorithm has been applied.

5.4.2. Constitutive modelling

The MAT_JOHNSON_COOK model has been used for the metallic parts of the 9 mm bullet. The EOS_GRUNEISEN equation has been utilized to establish a strain rate threshold during projectile compression.

The material model for UHMWPE layers has been defined as MAT_COMPOSITE_FAILURE_SOLID_MODEL, which is based on the Chang-Chang failure criterion.

In order to maintain the numerical stability and ensure accurate time steps, additional failure control measures have been integrated into the simulations. The tensile fracture strength has been set to 0.4 and has been introduced through the MAT_ADD_EROSION keyword to identify and eliminate highly distorted elements [277].

5.4.3. Simulation of penetration

To simulate the impact behavior between the 9 mm FMJ bullet and the three configurations of soft UHMWPE-rubber panels, the ballistic event has been assumed to be perfectly normal, the penetration process being simulated at 356 m/s striking velocity.

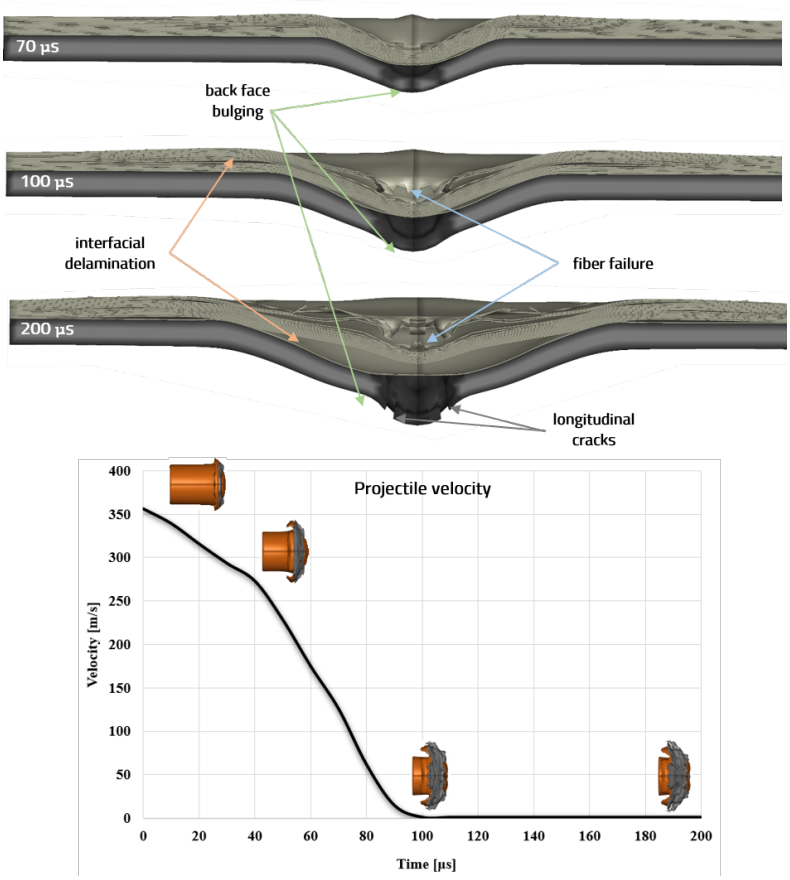

Figure 5.16 Damage status of PE-RCP-B configuration

Figure 5.16 presents a numerical simulation of the impact response of the PE-RCP-B configuration. The graph at the bottom of Figure 5.16 illustrates the decrease in projectile velocity over time, showing the progressive dissipation of energy during penetration. The projectile velocity continuously

decreases, with a significant deceleration occurring between 60 and 100 μs, corresponding to the moment when the stress waves meet the rubber backing layer. Overall, Figure 5.16 captures the dynamic response of the PE-RCP-B configuration, demonstrating how the UHMWPE UD layers absorb the initial impact energy, while the rubber backing layer helps dissipate residual stresses and prevent perforation. The observed failure mechanisms, including fiber fracture, interfacial delamination, back face bulging, and rubber cracking, validate the composite armor's effectiveness in stopping high-velocity projectiles through progressive energy absorption and material interaction.

Figure 5.18 illustrates the plastic deformation of the 9 mm FMJ projectile after impact in the three different composite panel configurations.

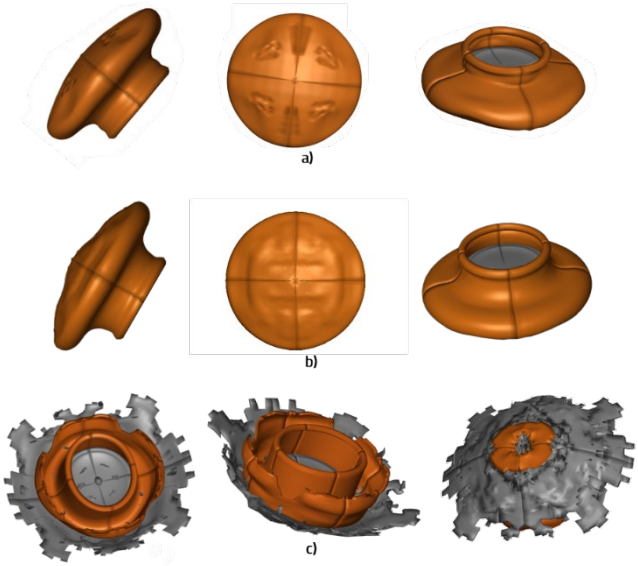

Figure 5.18 Projectile deformation after impact: a) PE-RCP-S configuration; b) PE-RCP-F configuration; c) PE-RCP-B configuration

Overall, Figure 5.18 provides insight into the projectile's response to impact in different configurations, confirming that the rubber and UHMWPE UD layers play a crucial role in energy dissipation and deformation control. The mushrooming effect observed in PE-RCP-S and PE-RCP-F highlights progressive plastic deformation, whereas the extensive fragmentation in PE-RCP-B suggests a more abrupt and forceful stopping mechanism. This numerical simulation confirms that the impact performance of these armor configurations varies significantly depending on the position of the rubber layer within the composite structure.

5.5. Validation of the numerical models. Comparison of numerical and experimental results

The ballistic testing experiments and fracture appearance of the ballistic panels suggest that the damage to soft armors occurs in two distinct failure modes. The first mode is shear plugging, which occurs when penetration takes place if the induced shear stress exceeds the critical shear strength of the material. On the striking face of the PE-RCP-S and PE-RCP-B configurations, a well-defined perforated hole is present with the same diameter as the projectile. For the striking ply of UHMWPE UD, shear plugging is the dominant failure mechanism. Several layers of UHMWPE UD fail through shear plugging, but the projectile possess significant residual energy. The remaining intact UHMWPE

layers absorb the residual kinetic energy of the projectile through tensile deformation mechanisms. At this stage, the projectile moves forward, along with the moving layers of UHMWPE UD and stretching the rubber layer in the PE-RCP-B configuration, while piercing through it in the PE-RCP-S configuration. The rubber layer ultimately fails when tensile fracture occurs. In the PE-RCP-B configuration, despite not being perforated, the rubber layer exhibits considerable damage on its back face. Longitudinal cracks are visible in the rubber layer within the impact zone. Figure 5.9e shows the development of secondary cracks branching from the main longitudinal crack, indicating progressive damage accumulation in the impacted area. These longitudinal cracks in the rubber layer at the impact point contribute to the material's ultimate tensile failure. When a high-velocity projectile strikes the surface of the ballistic panels, it exerts a substantial force in an extremely short period. This sudden and intense loading induces rapid deformation and stress within the rubber and UHMWPE UD layers. As the projectile penetrates the first UHMWPE UD layers and is halted by the composite panel, a rapid energy transfer occurs, generating high-stress levels in the materials, particularly within the rubber layer. If the rubber does not have adequate time to stretch or deform progressively, localized stress concentrations can exceed its tensile strength, leading to crack formation as a way of dissipating accumulated energy.

The second failure mode is bulging, which is associated with delamination. In the PE-RCP-S configuration, where the rubber layer is sandwiched between two UHMWPE UD plies, three layers of UHMWPE UD are penetrated, and the back-face deformation measures approximately 10.5 mm. In the PE-RCP-F configuration, where the rubber layer is positioned as the striking face, only two UHMWPE UD layers are penetrated, but the back-face deformation increases to approximately 11 mm. On the other hand, in the PE-RCP-B configuration, where the rubber layer is positioned as the backing face, three UHMWPE UD layers are penetrated, but the back-face deformation is slightly lower at approximately 8.5 mm. These results indicate that the placement of the rubber layer significantly influences the back-face deformation of the armor panels.

Following ballistic testing, the captured projectiles were examined, as showed in Figure 5.10 and Figure 5.18. The projectiles retained their original weight after impact, indicating that plastic deformation was the dominant effect and erosion was negligible. The bullets experienced significant circumferential expansion and reduction in length, as detailed in Table 5.4.

Table 5.4 Diameter and length deformation of the bullets before and after impact

Configuration	Before deformation (mm)		After deformation (mm)			
			Numerical		Experimental	
	Diameter	Lenght	Diameter	Lenght	Diameter	Lenght
PE-RCP-S	9	15	14.31	9.08	14.1	9.2
PE-RCP-F			17.08	8.58	16.4	8.9
PE-RCP-B			24.10	9.06	23.3	9.6

5.6. Conclusions

This chapter investigated the ballistic performance of a novel soft protective armor structure composed of ultra-high molecular weight polyethylene unidirectional (UHMWPE UD - Dyneema HB26) and

styrene-butadiene rubber (SBR-65). Three different configurations of armor panels were developed, differing in the placement of the rubber layer as a striking face, an intermediate layer, or a backing layer. Experimental tests have been conducted to evaluate the ballistic performance of the three different armor panel configurations. The experimental tests were conducted according to the Home Office Body Armour Standard against H01-level threats. At the same time, a numerical model of the same three configurations has been developed and validated by experimental results. Both simulations and experimental results confirmed that all three configurations successfully prevented projectile perforation. The numerical simulations further demonstrated that the placement of the rubber layer significantly influences the deceleration of the projectile, with the backing face configuration achieving the most rapid deceleration. Additionally, back face deformation measurements indicated that the PE-RCP-B configuration resulted in the lowest deformation, suggesting improved ballistic efficiency when the rubber layer is positioned as a backing layer.

The analysis of the damaged projectiles post-impact revealed that the bullets experienced significant plastic deformation but maintained their original weight, indicating that erosion did not play a role in their deformation process. The deformation of the projectiles varied depending on the placement of the rubber layer. In the PE-RCP-S and PE-RCP-F configurations, the projectiles exhibited a distinct mushroom shape, while in the PE-RCP-B configuration, the bullets displayed severe deformation, forming a bowl-like shape with complete separation of the copper jacket from the lead core. This suggests that the PE-RCP-B configuration induced the highest stress concentration on the projectile, resulting in extreme plastic deformation and structural failure.

Two primary failure mechanisms have been identified in the soft armor panels: shear plugging and bulging. Shear plugging was dominant in the UHMWPE UD layers, where the projectile penetrated multiple layers before being arrested. In the PE-RCP-S and PE-RCP-B configurations, the rubber layer exhibited longitudinal cracks along the impact zone, indicating tensile failure due to stress wave propagation. The hyper-elastic behavior of the rubber layer was shown in the PE-RCP-F configuration, where the perforation hole was significantly smaller than the projectile caliber, demonstrating the material's capacity for elastic recovery. Bulging failure occurred due to delamination and back face deformation. The PE-RCP-B configuration had the lowest back face deformation (approximately 8.5 mm), highlighting its superior impact resistance. This suggests that the placement of the rubber layer plays a crucial role in controlling stress wave dispersion and energy dissipation.

Overall, this research contributes to the development of lightweight, cost-effective soft protective armor solutions. The combination of UHMWPE UD and rubber layers improves ballistic performance by providing energy absorption, stress redistribution, and hyper-elastic deformation. The findings suggest that positioning the rubber layer as a backing face optimizes the protective performance by minimizing back face deformation and maximizing projectile energy dissipation. These insights can be applied to the design of advanced soft armor solutions, offering improved protective capabilities without increasing material thickness or weight.

Based on these findings, the next chapter explores the theoretical and experimental analysis of novel rigid ballistic structures under high-velocity impact. This investigation focuses on configurations where the SBR-65 rubber layer is positioned as a backing layer and integrated as a honeycomb structure with incorporated ceramic tiles, while a PUR-85 rubber layer is used as the striking face placed on the ceramic tiles.

6. Theoretical and experimental analysis of the novel rigid ballistic structures at high-velocity impact

In the previous chapter, the theoretical and experimental analysis focused on novel soft ballistic structures subjected to low-velocity impact, highlighting the role of UHMWPE UD and SBR-65 rubber in improving energy absorption and ballistic resistance. Based on these insights, this chapter changes the focus to high-velocity ballistic impacts on rigid armor configurations, where ceramic plates, SBR-65 rubber, and PUR-85 rubber are integrated into composite structures. The objective is to evaluate the energy absorption capabilities and protective effectiveness of these materials in improving the ballistic performance of rigid armors. To achieve this, it is crucial to understand the behavior of ceramic and fiber-based composites under ballistic impact, including their failure mechanisms and damage evolution. Through a combination of analytical modeling, experimental testing, and numerical simulations, this chapter provides a comprehensive evaluation of how these materials interact under extreme impact conditions, offering valuable insights for optimizing the design of next-generation ballistic protection systems.

6.1. Analytical approach

6.1.1. Analytical model for ballistic impacts on ceramic plates

Modeling these ballistic impact events of ceramic tiles is a complex challenge that requires both numerical and analytical approaches to address aspects such as fracture and crack propagation. Various models, such as simplified ones like Florence's [278] and more detailed ones like those by Walker and Anderson [279], as well as Zaera and Sanchez-Galvez [280], are available, each offering different levels of complexity and suitability for specific applications.

Having explored the analytical modeling of ballistic impacts on ceramic armor, it is equally important to consider the role of fiber-based composites in modern protective structures. The next section explores into the analytical models for ballistic impacts on fiber-based composites, examining their unique energy absorption mechanisms, failure modes, and structural responses under high-velocity impact conditions. Understanding these models is essential for optimizing hybrid armor designs that combine ceramics with fiber-reinforced composites to achieve enhanced ballistic resistance.

6.1.2. Analytical model for ballistic impacts on fiber-based composite

When a projectile impacts a composite material, it generates instantaneous stresses that propagate through the material in the form of waves at velocities dependent on the material properties. These stress waves travel in all directions, causing deformations that are analyzed using 1D, 2D or 3D approaches. Simplified 1D and 2D analysis for thin plates assumes uniform deformation throughout the thickness. However, thicker plates show varying strain and stress distribution through the thickness, requiring a more complex 3D analysis to account for wave propagation. The main purpose of the analytical formulation is to estimate the energy absorbed by different mechanisms, the contact

force, as well as the projectile velocity and displacement over time. In addition, it attempts to determine the ballistic limit velocity and contact duration for different laminate thicknesses. This comprehensive analysis helps to understand impact dynamics and to optimize the design of laminate structures for improved ballistic performance. Many researchers such as Daniel and Liber [283], Sierakowski and Chaturvedi [284], Xue et al. [285], Naik et al. [286, 287], Paradela, Sanchez-Galvez et al. [288, 289], Bresciani et al. [290], Langston [291], and Jintao and Moubin [277] have typically used two strategies to study high-speed projectile penetration of composite targets: stress wave propagation and energy balance. Developing an analytical model that accurately simulates penetration dynamics is a significant challenge because of the complexity involved.

After establishing the analytical models for ballistic impacts on ceramics and fiber-based composites and understanding their role in energy absorption and structural response, it is crucial to examine the failure mechanisms and damage evolution in ceramic tiles under ballistic impact. The following section focuses on the mechanical response of ceramic plates when subjected to high-velocity projectiles, analyzing the impact-induced fracture processes, stress wave propagation, and penetration mechanics that govern their ballistic performance.

6.2. Failure mechanism and damage evolution of ceramic tiles under ballistic impact

6.2.1. Analysis of mechanical impact on ceramic tiles

When a projectile impacts a ceramic plate, energy transfer occurs in three distinct modes [69, 87]:

a) the projectile penetrates the striking face of the ceramic plate, piercing it and exiting through the rear face with residual energy, indicating that the projectile's impact energy exceeds the dissipation capacity of the ceramic plate.

b) the projectile partially penetrates the ceramic plate, with the ceramic material fully absorbing the impact energy of the projectile.

c) the projectile fully penetrates the ceramic plate, reaching the rear face with zero residual energy. The speed at which this complete penetration occurs is defined as the ballistic limit.

6.2.2. Penetration mechanics of ceramic plates

Under ballistic impact, ceramic tiles exhibit behavior distinct from other materials, influenced by radial confinement and the presence of a backing plate. When a backing plate is attached, the ceramic tile shows high penetration resistance due to its high compressive strength, causing significant deformation at the projectile's nose. If the projectile's impact velocity is insufficient, it will either shatter or ricochet, a phenomenon known as interface defeat or infinite dwell. If the projectile withstands the initial impact, the ceramic begins to crack, initiating tensile fractures that form circular rings around the impact area. These cracks propagate through the ceramic to the backing face, uniting into a conical fracture. Without a backing plate, a plug would be ejected, piercing the ceramic. When a backing plate is present, the stress is redistributed circumferentially, generating radial cracks alongside the conical fracture. Lateral cracks in the plane of the striking surface are subsequently initiated. The backing plate

captures residual projectile fragments and comminuted ceramic particles, leading to the formation of micro-cracks and micro-voids, which pulverize the ceramic tile and erode the projectile. In the case of multiple impacts on a single ceramic tile, the first impact will perform as previously described, but subsequent impacts will penetrate through, without significant resistance, reducing the ceramic's effectiveness. To mitigate this, armors are designed with multiple ceramic tiles (ceramic mosaic armors) to limit the propagation of fractures and maintain protective integrity [2, 55, 87].

Having analyzed the failure mechanisms and damage evolution in ceramic tiles under ballistic impact, it is equally important to investigate the response of fiber-based composites under similar conditions. The next section explores the failure mechanisms, energy dissipation processes, and structural degradation in fiber-based composites, highlighting their role in enhancing ballistic protection through mechanisms such as delamination, fiber rupture, and shear failure. Understanding these behaviors is essential for optimizing hybrid armor designs that integrate both ceramic and composite materials for superior impact resistance.

6.3. Failure mechanism and damage evolution of fiber-based composites under ballistic impact

When a composite structure is subjected to projectile impact, it undergoes various forms of deformation and damage. The initiation and extent of this deformation are influenced by factors such as projectile velocity and geometry, fiber properties, matrix characteristics, and interfacial adhesion. Upon ballistic impact, a compression wave is generated at the impact zone. This wave travels through the material's thickness and, upon reaching the rear surface, is reflected back as a tensile wave, which can cause delamination. Weak fiber-to-matrix adhesion in the composite is particularly significant during projectile impacts, as it contributes to delamination of the composite. This delamination process allows the fibers to elongate until they break. Despite this, a certain degree of structural stiffness is still necessary. Higher fiber-to-matrix adhesion can be used depending on the threat level to improve overall material performance. Composite structures typically exhibit high resistance to ballistic impacts by effectively dissipating the energy involved. This dissipation occurs through various damage modes, including matrix cracking, fiber failure, and delamination. However, the initial delamination substantially reduces the load-bearing capacity of fiber-based composites. This delamination aids in energy dissipation by forcing fibers to elongate and absorb energy, although it also contributes to the overall degradation of the material's mechanical properties. The fracture behavior of composites often involves a combination of fiber shear and tensile failure. One of the weaknesses in fiber-based composites is the actual failure of the fibers due to delamination within the matrix. The pointed projectiles can induce shear stress, leading to fiber shear breakage, while the flexural strength causes fiber failure due to stretching.

6.4. Experimental approach

6.4.1. Ballistic testing

The Home Office Body Armour Standard (Special protection level - L17A1 bullet) has been used to test the rubber-ceramic composite plates, which means that the ballistic panels can provide resistance against a 5.56 mm M855 bullet, with a specified mass of 4.01 g and a velocity of 920 m/s ± 15 m/s [35]. In order to protect the internal organs against non-penetrating wounds, the back face deformation (BFD) indentation must measure less than 30 mm, in accordance with this standard.

The ballistic tests have been performed on the rigid ballistic plate configurations previously presented in a shooting range in Mangalia, Romania, belonging to the Ministry of National Defense. A 5.56 assault rifle (M4 carabine) with a 5.56x45 mm NATO bullet (M855) has been used. The M855 bullet consists of a front steel penetrator, a lead core and a copper jacket.

The rigid samples have been positioned 15 meters away from the test barrel's muzzle. According to the tactical and technical characteristics of both the assault weapon and the bullet, the initial velocity of the projectile has been determined to be 922 m/s. A ballistic calculator has been utilized to determine the projectile's impact velocity, considering shooting factors like ballistic coefficient of the bullet, muzzle velocity of the bullet, bullet weight and atmospheric conditions such as altitude, temperature, and wind speed. The projectile's impact velocity has been found to be 902 m/s. In order to evaluate the penetration depth of the projectile in ballistic tests, Koh-I-Noor Plastilina (clay whiteness) has been used. A caliper has been used to determine the depth of penetration of the armor panels.

6.4.2. Experimental results and discussion

Figure 6.14 illustrates the bullet penetration hole in the PUR-85 rubber layer (P1 configuration) after being impacted by an M855 projectile at 902 m/s. Figure 6.14a represents the striking face of the PUR-85 rubber layer, which acts as the first energy-absorbing component in the P1 configuration. The entry hole (d_{s_P1} = 1 mm) in the PUR-85 rubber layer presents a localized rupture zone, where the projectile's impact caused material displacement and radial crack propagation. High resolution image on the right highlights a rough and irregular perforation profile, indicating high strain rates and stress concentration at the moment of impact. The darkened edges around the perforation suggest localized heating and friction-induced degradation of the rubber material, which occurs due to the high-velocity impact of the projectile. The radial damage pattern surrounding the penetration site indicates shock wave propagation through the rubber material, leading to localized tearing and crack formation. The nature of this perforation suggests a combined failure mechanism of localized shearing, tensile fracture, and compression failure. Figure 6.14b provides a view of the backing face of the PUR-85 rubber layer, capturing the bullet exit hole (d_{r_P1} = 1.5 mm). High resolution image on the right side provides a detailed view of the penetration hole in the rubber layer, where tensile failure and tearing mechanisms are evident. The irregular edges and sharp contours of the hole suggest a combination of ductile and brittle failure modes, influenced by the stress wave interactions between the ceramic and rubber interfaces. The pulverized ceramic suggests that localized stress concentration and shock wave propagation caused micro-tearing and interfacial delamination at the point of impact. The external dispersed

damage area indicates the presence of high strain rates and the reflection of stress waves at the rubber-ceramic interface, which contributes to energy dissipation and increases the ballistic resistance of the ballistic panel.

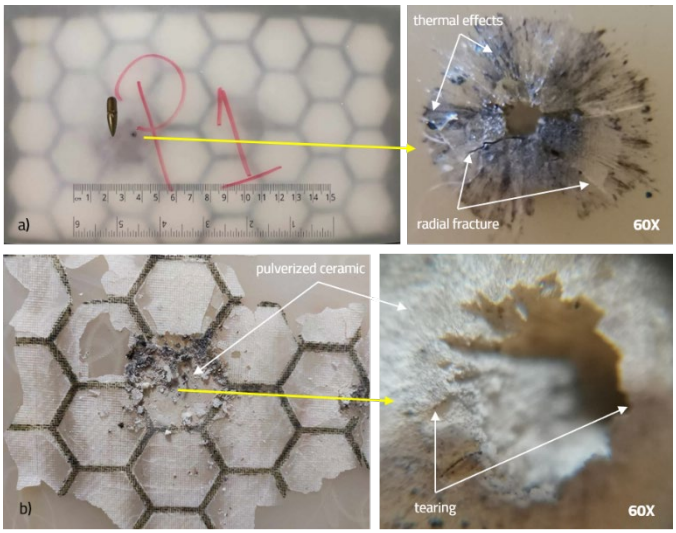

Figure 6.14 Bullet penetration hole in the PUR-85 rubber layer (P1 configuration):
a) striking face; b) backing face

The UHMWPE UD layers play a crucial role in energy dissipation and projectile arrest in the P1 composite armor structure. Figure 6.16a provide detailed insights into the penetration effects, failure mechanisms, and structural response of the UHMWPE layers after the ballistic impact. In Figure 6.16a, the location of the impact is evident, indicating localized material damage in the UHMWPE layers as a result of the projectile penetrating through the previous ceramic layers. The damage model suggests that the projectile carried significant residual kinetic energy after perforating the ceramic layers, resulting in fiber shearing.

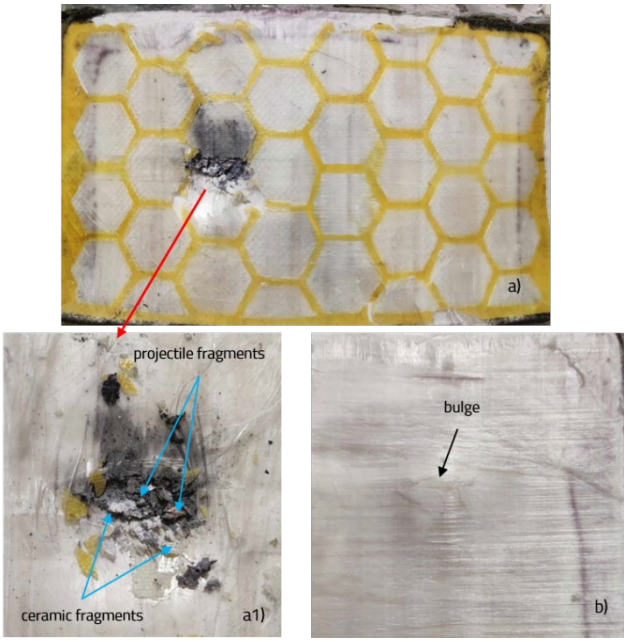

Figure 6.16 Bullet penetration hole in the UHMWPE layers (P1 configuration):
a) striking face; b) backing face

The rear surface of the UHMWPE layers, shown in Figure 6.16b, shows a well-defined bulge, indicating a high-energy absorption and progressive failure mechanisms in the structure. This bulging effect results from the localized out-of-plane deformation of the composite layers, a common characteristic in fiber-based ballistic materials where tensile failure dominates rather than immediate perforation.

Figure 6.29 presents the observed damage in the SBR-65 rubber backing layer from the P4 configuration. Figure 6.29a, the striking face of the SBR-65 rubber layer, presents a localized stress concentration area, highlighted by a white deformation pattern at the SrPET fabric interface. This stress concentration zone is surrounded by fine concentric cracks, indicating the way the impact-generated stress waves propagated through the armor structure. The presence of these concentric cracks suggests a significant energy transfer from the projectile through the upper armor layers. Figure 6.29b, the backing face of the SBR-65 rubber layer, shows a visible longitudinal crack, extending along the impact direction. The longitudinal crack developed as a result of the extreme stretching of the rubber layer under high-velocity impact conditions. As the projectile was progressively decelerated within the UHMWPE layers, the force transmission to the SBR-65 backing layer induced a tensile response. However, due to the localized stress concentration and asymmetric load distribution (caused by edge impact effects in the ceramic tiles), the rubber material could not fully recover from the deformation, leading to failure in the form of a longitudinal split.

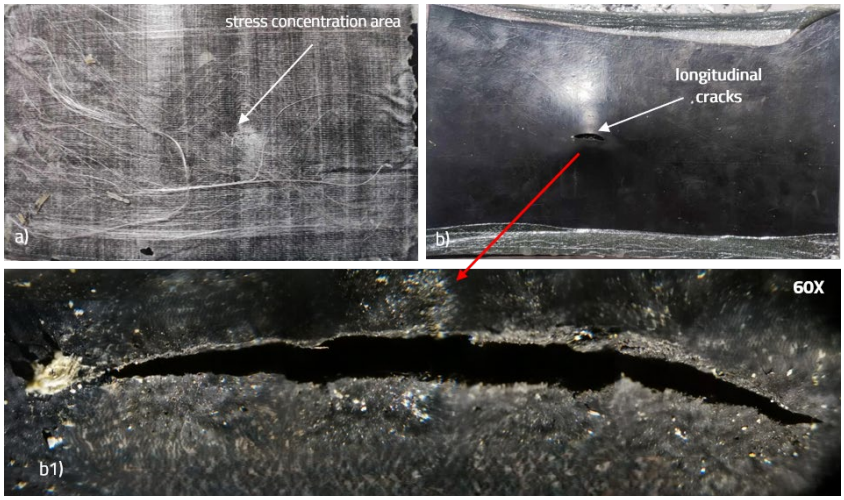

Figure 6.29 Back face damage (P4 configuration): a) striking face of the SBR-65 rubber;
b) cracks in the rubber layer – backing face

Figure 6.35 illustrates the bullet penetration hole in the ceramic layer from the P6 configuration after ballistic impact. In Figure 6.35a, the striking face of the ceramic layer shows a localized impact at the center of a hexagonal tile, leading to extensive fragmentation. The surrounding ceramic remains intact, indicating that the honeycomb rubber structure successfully restricted crack propagation to adjacent tiles. Figure 6.35a1, captured after removal of part of the ceramic fragments, shows the center of the impact zone, displaying radial cracks propagating outward from the penetration site, consistent with brittle fracture mechanics under high velocity impact conditions. In Figure 6.35b, the backing face of the ceramic layer is displayed, showing a distinct perforation in the corresponding hexagonal tile. Notably, the elastic web around the tile edges remains intact, suggesting that the honeycomb rubber structure effectively limited the fracture in the impacted tile. The P6 configuration demonstrates

improved damage localization due to the elastic honeycomb web, which reduces crack propagation beyond the impacted tile.

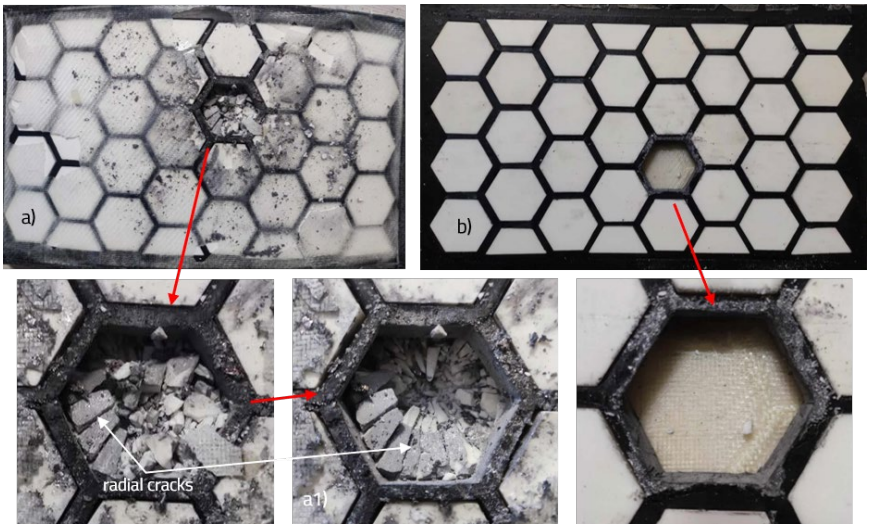

Figure 6.35 Bullet penetration hole in the ceramic layer (P6 configuration):
a) striking face; b) backing face

6.5. Numerical modelling

6.5.1. Finite element modeling

To model and analyze the ballistic impact between the M855 bullet and the rigid ballistic plate configurations investigated, a numerical model has been developed using LS-DYNA software. The impact has been assumed to be perfectly normal, and double symmetry has been taken into account, meaning only a quarter of the armor panel has been modeled, as shown in Figure 6.43. *Solid* elements have been used for ceramic tiles, rubber layers and projectile, and *shell* elements for the UHMWPE UD layers. For the UHMWPE UD fibers, shell elements were selected for the numerical model primarily due to their computational efficiency and suitability for simulating thin-layered materials. In most configurations, except for P1 and P4 configuration, the Dyneema HB26 layers were not penetrated, indicating that the fibers primarily acted as energy-absorbing layers rather than experiencing complete perforation. Considering this behavior, the use of shell elements was found to be optimal choice for several reasons. First, shell elements significantly reduce the computational cost and simulation time while still capturing the essential mechanical response of the UHMWPE layers. This reduction in modeling effort is particularly beneficial in multi-layered armor systems, where complex interactions occur between different parts. Second, consistency across configurations was a key consideration. Maintaining a uniform element type across all simulations ensures comparability of results, preventing inconsistencies that could arise from using different element formulations in different configurations. Finally, while the primary focus of the study was on the role of rubber layers in restricting crack propagation, the UHMWPE layers' deformation and failure mechanisms were still critical for understanding energy dissipation.

The present study adopts a simplified numerical modeling approach, where the projectile is simulated without the copper jacket, as shown in Figure 6.43, ensuring computational efficiency while maintaining accuracy in penetration predictions.

The interaction between the bullet and different armor panel layers (UHMWPE, rubber and ceramic) has been modeled with CONTACT_ERODING_SURFACE_TO_SURFACE. Contact between parts of the same body has been realized using the CONTACT_ERODING_SINGLE_SURFACE algorithm. To simulate the debonding behavior of the SrPET fabric layers, which serve as the interfacial bonding material between different layers, the TIEBREAK_SURFACE_TO_SURFACE contact algorithm was applied. In this case, the values of the NFLS and SFLS coefficients have been set to 85 MPa and 25 MPa, respectively [301, 302].

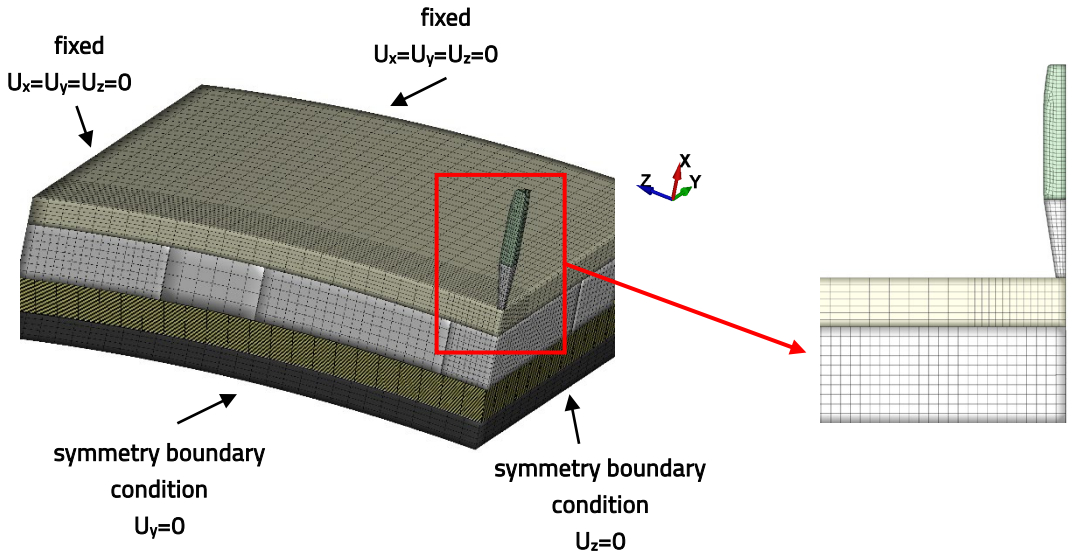

Figure 6.43 Finite element model and boundary conditions

6.5.2. Constitutive modelling

The MAT_JOHNSON_COOK model has been used for the steel penetrator. The EOS_LINEAR_POLYNOMIAL equation of state was implemented to accurately model the relationship between pressure, density, and internal energy in the steel penetrator under high strain-rate and high-pressure conditions. For this formulation, the bulk modulus was set to 164 GPa, ensuring a realistic representation of the material's compressibility and resistance to volumetric deformation during ballistic impact [305].

The MAT_PLASTIC_KINEMATIC material model has been used for the lead slug. This material model is used for isotropic and kinematic hardening plasticity with the option of including rate effect in accordance with Cowper-Symonds strain rate model.

In the case of ceramics, the MAT_JOHNSON_HOLMQUIST_CERAMICS model has been used to predict the behavior of brittle material under large strain. In this model it is supposed that the tensile strength of the ceramic is much lower than its compressive strength and that, when the ceramic is fractured, the material completely loses its tensile strength.

6.5.3. Simulation of penetration

To simulate the impact behavior between the M855 bullet and the rubber-ceramic composite plates, the ballistic event has been assumed to be perfectly normal, the penetration process being simulated at 902 m/s striking velocity.

Simulation results highlight how material interfaces, honeycomb structures and ceramic stacking influence stress distribution and energy absorption in ballistic armor. The main findings reveal compromises between localized stress concentration for impact resistance and wider stress dispersion to reduce damage. The following remarks summarize these main findings, highlighting the fundamental mechanical behaviors observed in different armor configurations.

When a rubber honeycomb structure is integrated behind the ceramic tiles, the PUR-85 rubber front layer experiences very high local stress during impact. In fact, the simulation indicates peak stress values in the PUR-85 rubber on the order of 70–80 MPa in configurations where a honeycomb structure supports the ceramics. For example, in one configuration with direct vertical stacking of two ceramic layers and a honeycomb interface (P4 configuration), the PUR-85 rubber layer reached a peak of 79.8 MPa during the projectile's impact. These are significantly higher stresses than seen in configurations without the honeycomb. The reason is that the honeycomb and segmented ceramic tiles localize the impact force into a smaller area; the elastic honeycomb constrains lateral motion and reflects stress waves back into the rubber and ceramic along the impact axis. In effect, the presence of the honeycomb prevents the impact energy from dispersing quickly to adjacent areas, making the PUR-85 rubber withstand a very intense load, concentrated directly above the projectile. The stress waves in the rubber are highly concentrated, and symmetrical wave patterns have been observed propagating from the impact point, indicating that the energy is being captured and absorbed in a localized region. In summary, when a honeycomb rubber structure is attached, the rubber in front is subjected to extremely high stresses (exceeding 70 MPa) because the structure directs the shock straight back (especially if the ceramic layers are perfectly aligned). This has implications for the ceramics behind – the intense stress wave can promote severe cracking in the ceramic directly under the impact, while adjacent ceramic tiles experience less stress (due to the honeycomb structure). Thus, the honeycomb design produces a compromise: it achieves very high local stress (and energy absorption) in the rubber and ceramics but isolates the impact on a very small surface.

The simulations also examined cases where the projectile strikes at the intersection of adjacent ceramic tiles. This scenario produces a different stress profile in the PUR-85 rubber and the support structure. When the impact is centered on a tile, a single ceramic piece carries the entire load; but at a tile intersection, two or more tiles distribute the impact and initially the structure shows a slightly higher elasticity. As a result, the PUR-85 rubber layer is subjected to a slightly lower peak stress in the case of an intersection impact compared to a direct center impact. For instance, in the case of P5_INT configuration, the maximum stress in PUR-85 rubber was about 52 MPa, lower than the 65–80 MPa seen for centered strikes. This reduction occurs because the impact force is distributed into multiple ceramic tiles and into the gap.

The propagation of stress waves through the armor structure is evidently influenced when the honeycomb layer is removed. In configurations like P2 (no rubber spacer between ceramic tiles), the stress wave travels through a more continuous, homogeneous medium (ceramic-to-ceramic contact),

which means less damping at interfaces. The simulation results indicate that without the honeycomb rubber structure, more of the impact energy is transmitted further but also more uniformly. This had two notable effects: First, the PUR-85 front layer absorbs a fast, direct stress wave (as discussed above) because nothing slows down the stress wave between the two ceramic layers, and second, beyond the first ceramic layer, the stress is less localized - the second ceramic layer and the backing absorb the stress wave over a wider area. In fact, the SBR-65 rubber backing in P2 displayed less bulge compared to P1, implying that the stress was not concentrated in a narrow column by a honeycomb, but rather dispersed.

The ceramic tiles in the armor experience widely varying stress levels depending on the configuration (mosaic vs. monolithic, presence of rubber layer, tile alignment, etc.). In general, the highest stress in ceramic was recorded in the monolithic ceramic scenario, whereas mosaic ceramic tiles had lower peak stresses per tile but more controlled damage. Specifically, in the monolithic single tile case (P3 configuration), the simulation noted an initial impact stress of about 5.5 GPa at the point of projectile contact. This very high stress is because the entire thickness of a single large tile resists the projectile at once, and there are no free edges or segment boundaries to reduce the stress – the ceramic must absorb the full shock until it fails. By contrast, in configurations with mosaic hexagonal tiles (P1, P2, etc.), the initial impact stress in the struck tile was on the order of 3–4 GPa. The smaller tile can fracture at a lower force threshold, and cracks form that effectively evacuate some of the stress (the tile breaks, thus limiting the amount of stress that can be accumulated). Moreover, the presence of the rubber honeycomb structure around the mosaic tiles further limits stress growth in the individual tiles by quickly absorbing some load or deflecting it to adjacent materials. Another factor is the stacking alignment of two ceramic layers: when the second layer tile lies directly behind the first (aligned stacking), the stress wave from the first tile's impact is distributed straight into the second tile, creating a high concentrated stress in that second layer. For example, the P4 configuration showed very strong direct propagation of stress waves. In contrast, if the ceramic tiles are staggered (as in P1 configuration), the projectile impact on a first-layer tile does not immediately strike a plate in the second layer directly, so the stress that reaches the second layer is somewhat distributed (it has to travel through the rubber and into multiple second-layer tiles or across tile interfaces). This staggered arrangement led to a more dispersed fracture pattern in the second layer and generally lower peak stress in any single second-layer tile, though the first-layer tile still withstands a hard strike. Additionally, with a honeycomb interlayer, the stress into the ceramic is partially absorbed. The simulations showed that with an elastic layer attached, the second ceramic layer experiences a more distributed, lower-magnitude stress wave compared to the case without honeycomb structure.

The simulation's findings allow a comparison between using a single thick ceramic tile versus two thinner ceramic tiles (stacked one on top of the other) of equivalent total thickness. The simulation suggests that the single monolithic ceramic tile (of thickness equal to two layered tiles) is more efficient at handling the impact stress in many aspects. First, the monolithic tile provides better load distribution across its area. Because it is one continuous plate, when the projectile hits, the stress can spread out within the tile in a continuous radial pattern. The stress wave isn't immediately stopped by an interface at half-thickness, so it disperses outward, not just backward. This resulted in the monolithic tile absorbing a lot of the energy internally – evidenced by the fact that the back-face deformation of the armor was smaller in the P3 configuration. The backing SBR-65 rubber in P3 showed only a small bulge

with no ruptures or severe stretching, indicating that much of the projectile's energy was expended in shattering the ceramic and did not transmit as suddenly to the back. In other words, the single thick tile retained the stress localized within itself, protecting the later layers. By contrast, in a two-layer ceramic design, the projectile penetrates the first layer and then still has energy to strikes the second – this sequential failure can sometimes concentrate stress into the second layer and into the back. Another aspect is stress concentration at interfaces: a pair of stacked tiles has an interface where stress waves reflect. That reflection can amplify stresses in the front layer or send secondary stresses into the second layer, whereas a single tile has no internal interface to cause secondary shock reflections. The monolithic tile, therefore, reduces the number of shock interfaces in the target, which is beneficial for preventing stress concentrations. Furthermore, similar to P6 and P7 configurations, the continuous tile effectively incorporates a greater volume of material to halt the projectile. On the other hand, the two-layer system concentrates damage at the interfacial region between the layers, potentially allowing the projectile to achieve deeper penetration before dissipating its energy. This is supported by the observation that the single-layer ceramic configurations (such as P3, P6, and P7 configurations) exhibited reduced bulge in the SBR-65 backing layer.

From a mechanical perspective, the simulated penetration of the rubber-ceramic composite armor reveals how the design and material choices control the propagation of stress and energy during a high-velocity impact. The PUR-85 rubber front layer demonstrates a high capacity to absorb energy through large deformations, forming bulges and indentations that indicate effective stress-wave attenuation at the cost of local material damage. The inclusion of a honeycomb rubber interlayer between ceramic tiles significantly alters the stress distribution: it tends to localize and intensify stresses along the projectile's path, while protecting adjacent regions and limiting crack spread. Removing that interlayer has the opposite effect – spreading the stress more uniformly through the target, which reduces extreme deformations in any single spot but can increase the overall damage to the front rubber and ceramics due to more direct transmission of shock. Across the different configurations, a clear pattern emerges: interfaces and boundaries (between materials or between tiles) present both advantages and disadvantages – they can dissipate and redirect stress, thus protecting some areas, but they also can become points of stress concentration or reflection that amplify damage in other ways. The ceramic layer's configuration (mosaic vs. monolithic, one thick tile vs. two thinner) is shown to critically influence how the projectile is stopped. A monolithic ceramic plate spreads out the impact load and can absorb a great deal of energy (often outperforming a multi-layer stack in preventing back-layer stress), but it fails in an extensive manner. Mosaic ceramic tiles, especially with elastic separation, limit failure to the impact zone and prevent total breakage of the ceramic layer but transfer more stress into backing layers.

The simulation's findings highlight that by adjusting the interfaces between the layers and the arrangement of the materials, a required stress distribution can be achieved – avoiding stress concentrations (which cause perforation or excessive back-face deformation) and maximizing the armor's ability to absorb and disperse the projectile's kinetic energy within its layers.

6.6. Validation of the numerical models. Comparison of numerical and experimental results

The depth of back-face deformation and the diameter of the crater on the clay backing material, observed during the experimental tests are detailed in Table 6.4.

Table 6.4 The back face deformation after the ballistic impact

Configuration	Depth of penetration (mm)		Diameter of the crater (mm)	Obs.
	Numerical	Experimental		
P1	12,67	8,9	62	
P1_INT	12,04			
P2	8,8	7	58	
P3	4,05	4,5	45	
P4	7,81			
P4_INT	15,6	10,5	65	longitudinal cracks
P5	6,95			
P5_INT	7,94	7,9	56	
P6	5,71	4,7	59	
P6_INT	22,6			
P7	5,5	5,6	60	
P7_INT	6,84			

When experimental and numerical results are compared, it can be observed that the depth of penetration values in the numerical simulations are higher than in the experimental tests, except for the P3 and P7 configurations where they are slightly lower. This is indicated by the fact that in the numerical analysis the projectile was constrained to a frontal impact, while in reality it is very difficult to achieve a frontal contact and also part of the kinetic energy of the projectile was consumed by its deflection at the interface of the material layers, while in the numerical analysis it penetrated straight and its kinetic energy was absorbed by its erosion.

The experimental results demonstrate a consistent correlation between crater diameter, impact intensity, and the observed deformation of the back face. The diameter of the crater reflects not only the energy transfer at the point of impact but also the material response of the clay backing and the damage mode of the front layers. Notably, configurations such as P1 and P4_INT display larger crater diameters, which correspond with higher depth of penetration values, indicating more extensive energy transmission and localized failure.

The comparative analysis between experimental and numerical results for the rigid armor configurations demonstrates a strong correlation in terms of penetration behavior, stress distribution, projectile erosion, and back-face deformation (BFD). The numerical model successfully reproduces the primary damage mechanisms, including ceramic fracture, stress wave propagation, and energy dissipation through the PUR-85 and SBR-65 rubbers. The formation of circumferential and radial cracks, conoidal failure in the ceramic, and projectile erosion patterns closely align with experimental observations, supporting the consistency of the simulation approach. However, slight discrepancies

exist due to the idealized assumption of a perfect frontal impact, and the absence of slight projectile yaw or ricochet effects. Despite these minor deviations, the overall agreement between experiments and simulations confirms the validity of the numerical approach for analyzing impact resistance and energy dissipation in rigid ballistic plate configurations.

6.7. Conclusions

This chapter has provided an in-depth theoretical and experimental analysis of novel rigid ballistic structures subjected to high-velocity impact, focusing on the effectiveness of composite armor configurations. The study demonstrated that integrating ceramic plates with fiber-reinforced composites and rubber layers improves energy absorption, mitigating the effects of projectile penetration. Through analytical modeling, experimental testing, and numerical simulations, essential information on the damage mechanisms and structural responses of these materials under ballistic impact were obtained.

The presence of rubber materials such as SBR-65 and PUR-85 rubber further improves impact resistance. These materials function as energy-absorbing layers by attenuating stress waves and reducing back-face deformation (BFD), which is crucial for minimizing injuries to personnel wearing the armor. The findings indicate that different configurations of rubber layers influence the overall ballistic performance by altering stress wave transmission and crack propagation behavior. For example, rubber honeycomb structures help limit crack propagation in ceramic layers, preserving the integrity of the armor against multiple impacts. An important aspect is the effectiveness of PUR-85 rubber as a critical energy-absorbing layer in ballistic protection systems. Experimental results show that PUR-85 rubber plays a significant role not only in mitigating the impact force but also in capturing ceramic debris and projectile fragments, reducing the risk of secondary injuries.

Comparative analysis of different armor configurations revealed variations in failure mechanisms and structural integrity. The presence or absence of intermediate rubber layers between stacked ceramic tiles significantly influenced crack propagation and energy dissipation. Configurations with directly stacked ceramic layers displayed more extensive brittle failure, whereas those incorporating rubber interfaces demonstrated improved stress redistribution and improved multi-hit resistance.

The experimental results from ballistic testing using a 5.56 mm M855 projectile confirm the theoretical predictions regarding penetration depth, material deformation, and failure modes. The back-face deformation measurements indicate that the hybrid composite configurations successfully meet ballistic resistance standards, with deformation levels within acceptable limits for personnel protection. The integration of UHMWPE UD and SBR-65 rubber backing layers proved effective in reducing ballistic trauma and improving durability.

7. Final conclusions, original contributions and future research directions

This doctoral thesis consists of comprehensive research on advanced ballistic protection materials and structures. Starting from a comprehensive overview of the literature, the research problem was identified and formulated: to develop an innovative armor solution to improve the ballistic performance of personal protective equipment using lightweight and cost-effective materials. As a first phase, novel multi-layer armor configurations (both flexible "soft" armor and hard "rigid" armor plates) that integrated rubber materials, high-performance fiber composites, and ceramics were developed. Subsequently, theoretical modeling, numerical simulation, and experimental testing of these configurations under ballistic impact were conducted. The findings demonstrate that combining rubber-based composites, fiber-reinforced layers, and ceramic materials can significantly improve energy absorption and ballistic resistance compared to conventional armor designs. There have been obtained essential insights into the deformation and failure mechanisms of each material within these hybrid systems, forming a basis for optimized next-generation armor solutions.

7.1 Final conclusions

The following main conclusions can be drawn from the research conducted within this thesis:

1. **Rubber layers demonstrate critical impact energy absorption capabilities.** The research confirmed that rubber layers (specifically SBR-65 and PUR-85 rubber) play a crucial role in mitigating impact forces. Rubber's hyper-elastic behavior allows it to undergo large deformations and absorb substantial strain energy during impact. Quasi-static, dynamic and ballistic tests showed that SBR-65 and PUR-85 display distinct mechanical responses. Notably, at high strain rates (simulating ballistic impact), the harder PUR-85 rubber experienced a noticeable reduction in ductility – its elongation at break dropped from ~760% under slow loading to roughly 240% under ballistic conditions. PUR-85 showed brittle failure tendencies under extreme loading, with localized cracking instead of uniform stretching. In contrast, the slightly softer SBR-65 rubber maintained greater elasticity and did not exhibit such premature fracture, even though its effective elongation also decreased (from ~140% to ~110% in ballistic loading). These experiments and corresponding Mooney-Rivlin simulations validated the rubber material models, showing close correlation between predicted and observed stress–strain responses. Overall, the rubber layers proved to be effective energy absorbers, attenuating stress waves and reducing the intensity of force transmitted to subsequent layers. This behavior supports their value in ballistic package designs.

2. **PUR-85 rubber effectively reduces secondary injury risk by containing ceramic debris and projectile fragments.** Experimental results show that PUR-85 rubber plays a significant role not only in mitigating the impact force but also in capturing ceramic debris and projectile fragments, reducing the risk of secondary injuries. When a high-velocity projectile penetrates the ceramic layers, the ceramic fractures into small, high-speed fragments, which can represent a serious threat to the wearer. However, the PUR-85 rubber absorbs and retains these fragments, preventing their dispersion and reducing potential injuries caused by secondary projectiles. This behavior significantly improves the

overall safety of the armor, making it particularly suitable for personal protective equipment in military and law enforcement applications.

3. Composite laminates-rubber interaction significantly improves shock absorption and ballistic performance. Fiber-based composite laminates – specifically panels of unidirectional UHMWPE (Dyneema® HB26) – served as the flexible backing in soft armor and as intermediate energy-dissipating layers in rigid armor. Ballistic impact tests on the UHMWPE fabrics exposed multiple energy absorption and failure mechanisms: fiber stretched and ruptured, layers delaminated or shear-plugged, and the back face bulged. The ability of UHMWPE to deform out-of-plane (forming a bulge) while retaining structural integrity is particularly beneficial for absorbing residual kinetic energy and minimizing trauma. The research documented that these fiber layers captured projectile fragments and dissipated energy through tensile fiber failure and friction, preventing complete perforation in all tested configurations. When integrated with rubber (Chapter 5), the fiber and rubber layers spread and absorb the shock, leading to improved back-face signature results. This highlights that the fiber-rubber interaction improves ballistic performance: the fibers withstand most of the penetration resistance (tensile strength), while the rubber retards the projectile and absorbs the shock, resulting in a more efficient overall system.

4. Mosaic ceramic architecture improves crack containment and multi-hit capability. For high-velocity rifle threats, the presence of ceramic tiles as the secondary strike face was shown to be essential. Ceramic materials blunt and erode projectiles, shattering themselves in the process and thus absorbing a large portion of the impact energy. In Chapter 6's tests with 5.56×45 mm NATO rounds (~902 m/s impact), the ceramic front layer effectively fractured into a conoid and pulverized, consuming energy through crack propagation and projectile erosion. A major finding was that ceramics, while very effective at initial energy dissipation, depend on the striking and backing layers to contain fragments and absorb residual forces – by themselves they are too brittle to stop a bullet without shattering. Damage patterns in ceramics varied depending on the tile configuration: a single large monolithic tile exhibited a tendency to produce extensive radial and circumferential cracks on its surface upon impact, while mosaic segmented ceramic tiles localized damage more restricted to the impacted tile and its immediate neighbors. This difference confirmed that breaking the ceramic into smaller pieces (mosaic pattern) can prevent catastrophic spreading of cracks, preserving adjacent areas for potential multi-hit protection – a required characteristic for armor in realistic combat scenarios.

5. Optimal rubber placement in soft armor panels minimizes back-face deformation and ballistic trauma. The true value of the studied materials develops when they are combined into layered hybrid armor systems, and the research delivered several key findings on the performance of different configurations. In the soft armor prototypes (UHMWPE and SBR-65 rubber), three configurations were compared: rubber as the striking face, rubber as an intermediate interlayer, and rubber as a backing layer. Ballistic testing against 9 mm FMJ rounds showed that all three hybrid panels prevented penetration of the projectile. However, the placement of the rubber had a pronounced effect on projectile deceleration and back-face deformation (BFD). Specifically, the configuration with rubber at the back (PE-RCP-B) caused the most rapid projectile deceleration and produced the smallest BFD. Post-impact analysis of the bullets indicated that when the rubber backing was last in the panel, the bullet was captured after perforating the UHMWPE face layers, experiencing catastrophic deformation (mushrooming and flattening into a bowl shape), even separating the copper jacket from the lead core

due to sudden deceleration in the rubber layer. This backing rubber layer absorbed the remaining energy and bulged outward, thus minimizing trauma to a wearer. By contrast, placing the rubber in front or middle still stopped the bullet, but allowed a bit more trauma and left the bullet more intact (a classic mushroom shape). These results highlight that the sequence of layers actually counts: a rubber backing layer is highly effective for blunt trauma reduction, whereas a rubber front layer can dissipate some energy early but may not reduce back-face signature as much. Notably, the hybrid soft armor outperformed a stand-alone fabric, demonstrating how even a thin rubber insertion significantly improves energy absorption.

6. **Rubber honeycomb interlayers improve structural integrity and multi-hit resistance in rigid plates**. For the rigid armor configurations designed for rifle threats, the thesis examined several multi-layer arrangements combining ceramic tiles, rubber layers (both SBR-65 and PUR-85), and UHMWPE UD plies. A total of seven configurations (P1–P7) were developed to explore variables such as: mosaic vs. monolithic ceramic architecture, and the use of a rubber honeycomb interface or direct stacking. Ballistic tests with 5.56 mm M855 rounds demonstrated that integrating these different materials can successfully stop high-velocity projectiles with no through-penetration and acceptable back-face deformation. One notable result was observed in configurations that used two layers of ceramic tiles: when two mosaic ceramic layers were directly stacked without any intermediate cushioning, the damage was more severe. On the other hand, in configurations where a rubber honeycomb interlayer was integrated, the rubber effectively separated the layers and prevented cracks from propagating from one ceramic layer to the next. The presence of this flexible rubber interlayer improves resistance to multiple impacts, as an impact to one tile does not compromise adjacent tiles. Additionally, the rubber interlayer captured many ceramic fragments, preventing them from spreading into the backing, this helping the fiber composite layer behind to remain intact and absorb the residual projectile energy and fragments. In all rigid panel tests, the combination PUR-85 striking layer combined with a hard ceramic layer and energy-absorbing backing layers (UHMWPE and SBR-65 rubber) proved effective: the projectiles were either heavily eroded or fragmented upon hitting the ceramic, and the remaining mass was stopped by the composite backing and rubber, producing back face deformations within safe limits. In addition, the PUR-85 rubber layer helps to capture ceramic debris and projectile fragments, thus reducing the risk of secondary injuries.

7. **Novel ballistic configurations demonstrate superior weight and cost efficiency.** The proposed soft and rigid ballistic structures developed in this research achieved a well-balanced combination of reduced weight, improved ballistic performance, and lower production cost. Soft armor designs incorporating UHMWPE UD and SBR-65 rubber are lighter and more economical than conventional soft armors utilizing Kevlar or UHMWPE bonded with epoxy, without sacrificing protective capabilities. Also, rigid plate configurations, combining mosaic ceramic tiles with rubber layers, UHMWPE UD, and SrPET, demonstrated comparable or superior protection levels at lower weights and costs than traditional ceramic composite plates. These findings confirm the practical applicability of the proposed systems in contexts requiring improved mobility, protection, and cost efficiency, particularly for military and law enforcement use.

8. **Resin-free bonding using SrPET fabric improves structural integrity, reduces interface stress, and contributes to weight reduction in rigid plates**. In contrast to conventional rigid armor systems that depend on epoxy resins for layer adhesion, the configurations developed in this thesis incorporated

SrPET fabric as the bonding agent. This resin-free approach eliminates the added weight and manufacturing complexity associated with epoxy matrices while maintaining effective mechanical connection between layers. Additionally, the use of SrPET contributes to a reduction in stress concentrations at material interfaces, which helps preserve the structural integrity of the armor during high-velocity impacts. The effective integration of SrPET in rigid configurations highlights its potential as a lightweight, high-performance bonding solution for next-generation ballistic protection systems.

Overall, the findings of this research contribute valuable knowledge for optimizing next-generation ballistic protection systems. The study confirms that hybrid armor designs, which combine the properties of ceramics, fiber reinforced-composites and rubber, offer superior protection against high-velocity threats. Future work could explore additional material combinations, alternative geometric configurations, and advanced manufacturing techniques to further refine ballistic performance. Additionally, further computational modeling and experimental testing under varying impact scenarios would improve the predictive accuracy of impact response and armor effectiveness.

By advancing the understanding of energy absorption mechanisms and failure dynamics in ballistic-resistant materials, this research lays the foundation for developing more effective, lightweight, and adaptable armor systems for military and law enforcement applications.

7.2 Original contributions

This doctoral research provides novel insights in the field of ballistic protection materials and armor design, the original contributions of the author being summarized below:

1. **Comprehensive review** of the state-of-the-art of body armor systems, focusing on **materials selection, structural configurations**, and **performance evaluation methodologies**. This review provides a valuable reference for researchers in the field, offering a clear understanding of current challenges and guiding future developments in advanced armor design. **Special attention is given to the emerging role of rubber-based materials** as a significant component in enhancing energy absorption and improving overall ballistic performance.

2. **Development of an innovative armor solution using lightweight and cost-effective materials** with enhanced energy absorption capabilities. The study introduces and validates **novel flexible and rigid armor configurations** that integrate rubber materials, such as UHMWPE-rubber panel and ceramic-rubber composite plate with a honeycomb structure, demonstrating, for the first time, their effectiveness in **reducing back-face deformation, enhancing multi-hit resistance, and improving overall ballistic performance** compared to traditional composite armors.

3. **Experimental characterization of hyper-elastic rubber materials and determination of material constants for numerical modeling**. This research presents **original experimental data** and analysis of the response of hyper-elastic materials, specifically rubber with varying hardness levels (SBR-65 and PUR-85 rubber) under quasi-static, high strain-rate and ballistic loading conditions. The primary goal has been to determine the mechanical response and energy absorption characteristics of rubber materials. Test results were used to extract material constants required for constitutive modeling, particularly for the **Mooney-Rivlin hyper-elastic model**. These constants, calibrated through

high-strain-rate compression tests, enabled accurate simulation of rubber behavior in ballistic applications. The generated data serves as a fundamental reference point for modeling rubber components in armor systems.

4. **Development of experimental methodologies for testing rubber materials and ballistic armor structures.** A significant contribution is the formulation of comprehensive experimental methodologies designed for both **material-level and system-level ballistic evaluation**. Custom test protocols were established for characterizing the response of rubber samples under multiple loading conditions, as well as for evaluating the ballistic performance of soft and rigid armor structures. These methodologies contribute to standardized testing practices for novel protective materials and configurations.

5. **Developing and validation of the numerical model**. This research integrates finite element simulations and experimental data to evaluate the performance of novel soft and rigid armor configurations. A **custom numerical model has been developed using LS-DYNA**, incorporating a Mooney-Rivlin constitutive model calibrated for SBR-65 and PUR-85 rubbers, using the experimental data obtained. For UHMWPE and ceramic materials, the constitutive parameters were selected from relevant literature sources, ensuring realistic representation of their mechanical behavior under ballistic impact. Simulations of ballistic impacts closely matched experimental results in terms of perforation, failure mechanisms, and back-face deformation.

6. **Contribution to the field of ballistic protection through new insights into energy absorption and damage control mechanisms** in body armor and personal protective equipment. This research provides original insights into how ballistic performance can be enhanced through material interaction and structural design. A significant finding is the role of rubber interfaces in attenuating and dispersing stress waves; placing a rubber layer between a ceramic strike face and a fiber-based backing reduces stress wave reflection and promotes energy dispersion, thereby improving multi-hit resistance. Additionally, the study demonstrates that segmenting ceramic layers into a mosaic pattern, confined by rubber, enables controlled tile fracture and prevents crack propagation beyond the impact zone, effectively localizing damage. Another significant contribution is the understanding of material interaction: improved performance results not only from the individual properties of rubber, ceramics, and fibers, but from how they interact. For example, rubber layers have been shown to capture ceramic debris and projectile fragments, acting as an internal buffer that mitigates the risk of secondary injuries. These findings offer valuable guidance for the design of next-generation armor systems, particularly in addressing the real-world challenge of protecting against both primary impacts and secondary fragmentation.

7. **Integration of weight and cost efficiency into ballistic armor design.** The proposed configurations, both soft and rigid, achieve a **superior balance between protection level, mass, and production cost**. Soft armor designs demonstrated significant weight reduction and lower fabrication costs compared to conventional epoxy-based solutions. Also, the rigid ballistic plates achieved **competitive ballistic resistance** while remaining **lighter and more economical** than standard ceramic composite plates.

8. **Integration of resin-free bonding using SrPET fabric as a novel approach to improve mechanical cohesion and reduce system weight**. Unlike conventional composite armor systems that use epoxy resin matrices, this research proposes the use of SrPET fabric as a bonding agent, eliminating

the need for heavy adhesives. The use of SrPET allows resin-free integration of layers, leading to reduced stress concentrations at interfaces, improved mechanical cohesion, and a noticeable decrease in overall plate weight. This approach simplifies manufacturing and contributes to the development of lightweight, durable, and structurally efficient ballistic systems, particularly in rigid plate applications.

7.3 Future research directions

Based on the findings and addressing the limitations identified, several directions for future research can be formulated to further improve ballistic protection technology:

1. **Expanded material exploration**. Future studies could explore a wider spectrum of rubber materials and composites. For example, alternative rubber research may identify materials with even better energy absorption or environmental durability. Varying the hardness and thickness of rubber layers systematically would help determine the optimal range for different threat levels, considering the findings in the present research that rubber materials can become brittle under impact. Also, the use of different fiber reinforcements (aramid fibers like Kevlar®, high-strength glass fibers, or developing nano-fiber fabrics) and hybrid weaves in place of or in addition to UHMWPE could be examined. These materials might offer improved performance against specific threats (for instance, Aramid is more heat-resistant, which could matter for incendiary or tracer rounds). Exploring advanced ceramic materials (e.g. silicon carbide or boron carbide) for the strike face is another logical step – these could reduce weight or improve multi-hit capability but need to be tested with rubber interfaces, since their higher brittleness might interact differently with coatings layers.

2. **Multi-hit and durability testing**. While the current research qualitatively discussed multi-hit resistance (especially with mosaic designs), dedicated multi-hit ballistic tests are needed to quantify how many impacts the new armor configurations can sustain before failure. Future experiments should fire multiple rounds at the same target (at different points and possibly at the same point) to evaluate how rubber-ceramic interfaces hold up to successive strikes. Such testing would validate the assumed improvements in multi-hit resistance due to rubber honeycombs. In addition, long-term durability studies should be conducted. Rubber materials can degrade due to UV exposure, extreme temperatures, or repeated loading. Examining how ballistic performance changes after aging the panels (thermal cycling, humidity exposure, etc.) or after non-ballistic mechanical wear will be important for real-world applications. Ensuring that the bonding between layers (rubber-ceramic, rubber-fabric) remains secure over time is crucial, future work might explore improved adhesives or even vulcanization techniques to bond rubber to ceramics, thus preventing delamination under impact. Monitoring the effects of environmental conditions on the Shore hardness and elasticity of the rubber layers will also guide the design of armor for various climates and scenarios.

3. **Advanced numerical modeling for predictive simulations**. The numerical models developed in this thesis can be expanded and refined. One direction is incorporating even more advanced material modeling for the rubber materials, such as rate-dependent viscoelastic or visco-plastic models that can capture the transition to brittle behavior in rubber materials more accurately. Similarly, improving the fracture modeling for ceramics would allow the simulation of multi-hit scenarios and complex fragment interactions. Furthermore, for UHMWPE, which was simulated using shell elements in this

thesis, future work could benefit from using solid elements to achieve more accurate and detailed representations of its behavior under various loading conditions, especially in relation to the number of damaged layers.

4. **Structural optimization and design of novel armor architectures**. With the resulting insights, it is possible to develop completely new structural concepts for armors. One potential direction is exploring 3D textile architectures and auxetic structures for the fiber component – e.g. three-dimensional woven fabrics or auxetic mesh inserts that could work combined with rubber layers to disperse impact energy even more effectively. Topology optimization tools could be applied to the design of mosaic tiles or the geometry of rubber honeycombs to maximize energy absorption for minimal weight.

5. **Expansion into new application domains**. The innovations from this research have implications beyond personal body armor. Military vehicles and aircraft armor could benefit from the lightweight layered approach. Future work could test rubber-ceramic-fiber armors against higher caliber threats (e.g. 7.62 mm AP or 12.7 mm rounds) to evaluate capability for vehicle shielding. The concept of using a rubber layer to catch spall and fragments can be directly applied to spall liners inside armored vehicles – for instance, bonding a rubber/ fiber composite liner to the inner surface of metallic armor could greatly reduce crew injuries caused by detachment, a hypothesis that deserves investigation. Helmet design is another area: advanced combat helmets could incorporate a thin ceramic application for rifle protection, backed by aramid and a foam or rubber layer to reduce blunt trauma behind the helmet; the results of this thesis provide a basis for selecting the right rubber material for this purpose. In law enforcement, improvements demonstrated against 9 mm bullet and similar bullets suggest that adding rubber layers to bulletproof vests could allow them to meet standards with less material (and therefore less weight), improving comfort and wearability. Future tests could explore rubber-integrated anti-stab armor, since rubber might also help in dissipating energy from stab weapons.

6. **Smart and adaptive armor systems**. Looking further, combining the physical insights from this research with developing technology brings exciting possibilities. One direction is the integration of sensors and health monitoring in the armor, for example, inserting piezoelectric sensors or flexible electronics in the rubber layers to detect impacts or measure the extent of deformation. Given rubber's ability to deform, it could accommodate such inserts. A damaged armor plate could signal to the wearer or maintenance crew that it needs replacement (important for multi-hit situations).

7. **Investigation of the influence of rubber honeycomb interlayers on ballistic limit velocity (V_{bl}).** Building upon the findings of this thesis, future research should examine how rubber honeycomb interlayers affect the V_{bl} of rigid armor configurations. The integration of rubber honeycomb structures between adjacent mosaic ceramic tiles increases the spacing between impact zones and introduces localized flexibility that may influence the onset of tile fracture, crack propagation, and energy transfer dynamics. This structural decoupling could potentially raise or lower the V_{bl}, depending on how the energy is distributed and dissipated across the interface and within the ceramic segments. Detailed experimental and numerical studies should be conducted to quantify the effect of tile separation and honeycomb geometry on V_{bl}, providing deeper insights into damage localization, tile integrity, and multi-hit performance. These findings could inform optimal spacing and interface design strategies to maximize protection while maintaining weight and cost efficiency.

8. Investigation of honeycomb cell size and wall thickness on impact response and energy absorption. Future work should focus on how the cell size and wall thickness of rubber honeycomb structures influence the ballistic performance of rigid armor configurations. These geometric parameters govern the local flexibility, energy dissipation behavior, and stress distribution during impact. Smaller cell sizes may promote greater energy dispersion across the ceramic interface, while thicker walls could offer improved stiffness and resistance to deformation. Systematic experimental and numerical studies are needed to determine the optimal honeycomb design that balances energy absorption, weight efficiency, and fragment confinement, especially under high-velocity multi-hit conditions.

In conclusion, this doctoral thesis has not only answered the initial research questions regarding the roles of rubber, fibers, and ceramics in ballistic armor, but also opened new directions of research and potential improvements in the design, performance, and cost-effectiveness of ballistic protection systems. By achieving a balance of impact resistance, energy absorption, weight and cost efficiency, the study contributes to the advancement of next-generation armor designs. The findings serve as a starting point for researchers directing to develop armors that offer superior protection while remaining lightweight and practical for use in military and civilian applications. The future directions recommended above will contribute to this progress by ensuring that the information on impact mitigation and material interaction obtained here will continue to provide better and more effective protective equipment.

REFERENCES

1. Rosenberg, Z., Dekel, E. *Terminal Ballistics, 3rd ed.*; Springer Nature Switzerland AG: Cham, Switzerland, 2020.
2. Nauman, S., Cristian, I. *Smart textiles for the protection of armoured vehicles*. In: Chapman, R.A., Ed. Smart textiles for protection. Woodhead Publishing Series in Textiles, 2013; pp. 306-337.
3. Naik, N.K. *Ballistic impact behavior of composites: analytical formulation*. In: Silberschmidt, V.V., Ed. Dynamic Deformation, Damage and Fracture in Composite Materials and Structures. Woodhead Publishing Series in Composites Science and Engineering, 2016; 69: 425-470.
4. Yadav, R., Naebe, M., Wang, X., Kandasubramanian, B. *Body armour materials: from steel to contemporary biomimetic systems*. RSC Advances, 2016; 6 (116): 115145-115174.
5. Yunanda, W.W., Gunadi, G.I., Kasim, K. *Metal as a Ballistic-Resistant Lightweight Protective Material in the Military Field*. International Journal of Social Science Research and Review, 2022, 5 (12): 287-296.
6. Ranaweera, P., Bambach, M.R., Weerasinghe, D., Mohotti, D. *Ballistic impact response of monolithic steel and tri-metallic steel–titanium–aluminium armour to nonrigid NATO FMJ M80 projectiles*. Thin-Walled Structures, 2023; 182 (Part A): 110200.
7. **Jitarașu, O.** *Hybrid composite materials for ballistic protection. A numerical analysis*. Review of the Air Force Academy, 2019; 17 (2): 47-56.
8. National Research Council. *Opportunities in Protection Materials Science and Technology for Future Army Applications*. Washington, DC: The National Academies Press, 2011.
9. Fras, T., Colard, R., Reck, B. *Modelling of Ballistic Impact of Fragment Simulating Projectiles against Aluminum Plates*. 10th European LS-DYNA Conference, Würzburg, Germany, 2015.
10. Frueh, P., Heine, A., Riedel, W., Wickert, M. *Protection Capabilities of HHA and UHA Steels against Long-Rod Kinetic Energy Penetrators*. 30th International Symposium on Ballistics, Long Beach, California, United States of America, 2017.
11. Zhang, Z., Li, H., Wang, L., Zhang, G., Zong, Z. *Formation of Shaped Charge Projectile in Air and Water*. Materials (Basel), 2022; 15 (21): 7848.
12. Salkičević, M. *Numerical simulations of the formation behavior of explosively formed projectiles*. Defense and Security Studies, 2022; 3: 1-14.
13. Sharma, M., Kar, S. *Estimation of Trajectory of High-Speed Artillery Shell*. Defence Science Journal, 2023; 73 (3) :313-321.
14. Sutejo, M.F., Ruyat, Y., Marsono, M. *Ballistics Study of Mortar Weapon Technology*. International Journal of Progressive Sciences and Technologies (IJPSAT), 2024; 45 (2): 703-710.

15. Fayed, A.I.H., Abo El Amaim Y.A., Elgohary, D.H. *Investigating the Behavior of Manufactured Rocket Propelled Grenade (RPG) Armour Net Screens from Different Types of High Performance Fibers*. International Journal of Science and Research (IJSR), 2019; 8 (5): 2088.

16. Chauhan, R., Copeland, C.C., Murray, M. *Improvised Explosive Devices: Anesthetic Implications*. Current Anesthesiology Reports, 2018; 8: 71–77.

17. Helliker, A. *Ballistic threats: Bullets and fragments*. In: Bhatnagar, A., Ed. Lightweight Ballistic Composites (Second Edition). Woodhead Publishing Series in Composites Science and Engineering, 2016; pp. 87-114.

18. Petrudi, A.M., Vahedi, K., Rahmani, M., Petrudi, M.M. *Numerical and analytical simulation of ballistic projectile penetration due to high velocity impact on ceramic target*. Frattura ed Integrità Strutturale, 2020; 54: 239-261.

19. Blumenthal, R., Rossouw, S.H. *Full-Metal Jacket Mild Steel Core Ammunition: A Case Report*. American Journal of Forensic Medicine and Pathology, 2023; 44 (4): e109-e116.

20. Watson, K.E., Henwood, B.J., Hewins, K., Roberts, A., Hazael, R. *Ballistic impact of hollow-point ammunition on porcine bone*. Journal of Forensic Sciences, 2023; 68 (4): 1107-1444.

21. Waghmare, N.P., Gupta, K., Naik, J., Anand, V.R. *Characteristics of Fired Bullet on Different Target Materials*. Journal of Forensic Sciences and Criminal Investigation, 2019; 12 (2): 555833.

22. Piasta, K., Kupidura, P. *Perspective Armour-Piercing Intermediate Cartridge* Projectile. Problemy mechatroniki. Uzbrojenie, lotnictwo, inżynieria bezpieczeństwa, 2023; 14 (1) :89-104.

23. Champion, H.R., Holcomb, J.B., Young, L.A. *Injuries from Explosions: Physics, Biophysics, Pathology, and Required Research Focus*. Journal of Trauma and Acute Care Surgery. 2009; 66 (5): 1468-1477.

24. Bhatnagar, A. *Lightweight Fiber-Reinforced Composites for Ballistic Applications*. In: Beaumont, P.W.R., Zweben, C.H., Eds. Comprehensive Composite Materials II. Elsevier Ltd, 2018; pp. 527-544.

25. Kędzierski, P., Morka, A., Stanisławek, S., Surma, Z. *Numerical modeling of the large strain problem in the case of mushrooming projectiles*. International Journal of Impact Engineering. 2020; 135: 103403.

26. Hazell, P.J., Appleby-Thomas, G.J., Philbey, D., Tolman, W. *The effect of gilding jacket material on the penetration mechanics of a 7.62 mm armour-piercing projectile*. International Journal of Impact Engineering. 2013; 54: 11-18.

27. Di Benedetto, G., Matteis, P., Scavino, G. *Impact behavior and ballistic efficiency of armor-piercing projectiles with tool steel cores*. International Journal of Impact Engineering. 2018; 115: 10-18.

28. Dong, K., Jiang, K., Jiang, C., Wang, H., Tao, L. *Study on Mass Erosion and Surface Temperature during High-Speed Penetration of Concrete by Projectile Considering Heat Conduction and Thermal Softening*. Materials. 2023; 16 (9): 3604.

29. Sun, Q., Sun, Y., Li, R., Deng, G., Hu, J. *The failure and fracture modes of 35CrMnSi steel projectile with simulated charge penetrating rock at about 1000 m/s*. Engineering Failure Analysis. 2019; 97: 617-634.

30. Gomes, G.A. *Designing military uniforms with high-tech materials*. In: Wilusz, E., Ed. Military Textiles. Woodhead Publishing Series in Textiles, 2008; pp. 183-203.

31. Natarajan, V.D. *Materials selection for ballistics*. In: Nawab, Y., Sapuan, S.M., Shaker, K., Eds. Composite Solutions for Ballistics. Woodhead Publishing Series in Composites Science and Engineering, 2021; pp. 55-76.

32. Cronin, J., Kinsler, R., Allen, J. *Testing of armor systems*. In: Bhatnagar, A., Ed. Lightweight Ballistic Composites (Second Edition). Woodhead Publishing Series in Composites Science and Engineering, 2016; pp. 311-326.

33. Yahaya, R., Hidayah, N., Norhayaty, Z., Nor Hafizah, M.J., Sapuan, S.M., Iyas R.A. *Levels of ballistic protection and testing*. In: Nawab, Y., Sapuan, S.M., Shaker, K., Eds. Composite Solutions for Ballistics. Woodhead Publishing Series in Composites Science and Engineering, 2021; pp. 77-108.

34. El Messiry, M. *Protective armor engineering design*. Apple Academic Press, 2019.

35. Quéfélec, B., Dartois, M. *Ceramic-faced molded armor*. In: Bhatnagar, A., Ed. Lightweight Ballistic Composites (Second Edition). Woodhead Publishing Series in Composites Science and Engineering, 2016; pp. 369-391.

36. **Jitarașu, O.** *NUMERICAL SIMULATION OF BALLISTIC IMPACT PERFORMANCE OF COMPOSITE ARMOUR PLATE BY TYPICAL PROJECTILE.* In: Cioacă, C., Gherman, L., Eds. Military Applications of Modeling and Simulation. Wydawnictwo ASzWoj, Warsaw, 2021; pp. 157-174.

37. **Jitarașu, O.**, Cășeriu, B. *Numerical Analysis of the Ballistic Impact Behavior of 2D Woven Fabrics*. Open Access Library Journal. 2024; 11: e12108.

38. Arora, S., Majumdar, A., Butola, B.S. *Soft armour design by angular stacking of shear thickening fluid impregnated high-performance fabrics for quasi-isotropic ballistic response*. Composite Structures. 2020; 233: 111720.

39. Ralph, C., Baker, L., Archer, E., McIlhagger, A. *Optimization of soft armor: the response of homogenous and hybrid multi-ply para-aramid and ultra-high molecular weight polyethylene fabrics under ballistic impact*. Textile Research Journan. 2023; 93 (23–24): 5168–5186.

40. Zhou, Y., Ma, M., Nur, A., Zhang, R., Xiong, Z., Lin, Y., Xiang, Y., Zhang, Z. *An overview on the ballistic performance of woven-fabric-based flexible protective systems: Experimental and numerical studies*. Thin-Walled Structures. 2024; 205 (Part A): 112394.

41. Naveen, J., Jayakrishna, K., Sultan, M.T.H., Amir, S.M.M. Ballistic Performance of Natural Fiber Based Soft and Hard Body Armour- A Mini Review. Frontiers in Materials. 2020; 7: 608139.

42. Chang, C-P., Shih, C-H., You, J-L., Youh, M-J., Liu, Y-M., Ger, M-D. *Preparation and Ballistic Performance of a Multi-Layer Armor System Composed of Kevlar/Polyurea Composites and Shear Thickening Fluid (STF)-Filled Paper Honeycomb Panels*. Polymers. 2021; 13 (18): 3080.

43. Ribeiro, M.P., da Silveira P.H.P.M., de Oliveira Braga, F., Monteiro, S.N. *Fabric Impregnation with Shear Thickening Fluid for Ballistic Armor Polymer Composites: An Updated Overview*. Polymers (Basel). 2022; 14 (20): 4357.

44. Sitotaw, D.B., Ahrendt, D., Kyosev, Y., Kabish, A.K. *A Review on the Performance and Comfort of Stab Protection Armor*. Autex Research Journal. 2021; 22 (1): 96-107.

45. Bhatia, D., Jaswal, P., Sinha, S. *Women's body armor: A comprehensive review of design, performance, and ergonomics*. Journal of Engineered Fibers and Fabrics. 2024; 19.

46. Kumar, N. *Bulletproof Vest and Its Improvement – A Review*. International Journal of Scientific Development and Research. 2016; 1 (1): 34-39.

47. da Luz, F.S., Garcia, Filho, F.d.C., Oliveira, M.S., Nascimento, L.F.C., Monteiro, S.N. *Composites with Natural Fibers and Conventional Materials Applied in a Hard Armor: A Comparison*. Polymers. 2020; 12 (9): 1920.

48. Das, S., Prathasana, K., Nitin, P.A., JayaPriya, K.R.L., Mathivanan, V. *Protection from ballistic threats: an exploration of textile materials for bullet-resistant outerwear*. Zastita materijala. 2024.

49. Chen, X. *Introduction*. In: Chen, X., Ed. Advanced Fibrous Composite Materials for Ballistic Protection. Woodhead Publishing Series in Composites Science and Engineering, 2016; pp. 1-10.

50. Mohammed M.N., Al-Zubaidi, S., Bahrain, S.H.K., Sapuan, S.M. *State-of-the-art review on recent advances and perspectives of ballistic composite materials*. In: Nawab, Y., Sapuan, S.M., Shaker, K., Eds. Composite Solutions for Ballistics. Woodhead Publishing Series in Composites Science and Engineering, 2021; pp. 3-54.

51. Fonseca, L.C., Peixoto, F., Nichele, J. *Estimation of Ballistic Limit Velocity Using the Finite Element Method*. XXVI Encontro Nacional de Modelagem Computacional. Nova Friburgo, Rio de Janeiro, Brasil. 2023.

52. Nilakantan, G., Nutt, S. *Effects of fabric target shape and size on the V_{50} ballistic impact response of soft body armor*. Composite Structures. 2014; 116: 661-669.

53. Sun, D. *Ballistic performance evaluation of woven fabrics based on experimental and numerical approaches*. In: Chen, X., Ed. Advanced Fibrous Composite Materials for Ballistic Protection. Woodhead Publishing Series in Composites Science and Engineering, 2016; pp. 409-435.

54. Kim, J-H., Baik, S., Fu, J., Park, J-H. Ballistic limit velocity of small caliber projectiles against SS400 steel plates: Live fire experiments and empirical models. Defence Technology. 2024; 41: 22-34.

55. Carlucci, D.E., Jacobson, S.S. Ballistics: *Theory and Design of Guns and Ammunition, Third Edition*. CRC Press. 2018.

56. National Institute of Justice. *Ballistic Resistanceof Body Armor. NIJ Standard 0101.07*. U.S. Department of Justice, Washington, DC. 2023.

57. National Institute of Justice. *Specification for NIJ Ballistic Protection Levels and Associated Test Threats. NIJ Standard 0123.00*. U.S. Department of Justice, Washington, DC. 2023.

58. Home Office. *Body Armour Standard (2017)*. Centre for Applied Science and Technology. 2017.

59. Mrozek, R., Edwards, T., Bain, E., Cole, S., Napadensky, E., Freeney, R. *Developing an Alternative to Roma Plastilina #1 as a Ballistic Backing Material for the Ballistic Testing of Body Armor*. In: Kimberley, J., Lamberson, L., Mates, S., Eds. Dynamic Behavior of Materials, Volume 1. Conference

Proceedings of the Society for Experimental Mechanics Series. Springer, Cham. 2019; pp. 297–299.

60. Zhang, T.G., Graham, M.J., Satapathy, S.S. *Modeling the Rebound of Ballistic Roma Plastilina No. 1 Clay*. DEVCOM Army Research Laboratory. 2022.

61. Gautam, P.C., Gupta, R., Sharma, A., Singh, M. *Determination of Hugoniot Elastic Limit (HEL) and Equation of State (EOS) of Ceramic Materials in the Pressure Region 20 GPa to 100 GPa*. Procedia Engineering. 2017; 173:198-205.

62. Cheng, Y., Song, C., Tan, Y., Yue, S., Li, G., Qiu, Y., Xu, T., Liu, Y., Gao, F., Yu, Q. *Theoretical Calculation Method for the Hugoniot Elastic Limit of Hard Rock Based on Ideal Elastoplastic Model*. Shock and Vibration. 2021; 4: 1-8.

63. Shevchenko, V.Y., Oryshchenko, A.S., Lepin, V.N. et al. *Measurement of the Hugoniot Elastic Limit in Ideal Ceramics*. Glass Physics and Chemistry. 2023; 49 (Suppl 1): S1–S7.

64. da Silveira, P.H.P.M., da Silva, T.T., Ribeiro, M.P., de Jesus, P.R.R., Gomes, A.V., *A Brief Review of Alumina, Silicon Carbide and Boron Carbide Ceramic Materials for Ballistic Applications*. Academia Letters. 2021; pp. 1-11.

65. Aprilya, S., Aritonang, S. *Comparison of Al_2O_3, SiC, and B_4C as Ballistic-Resistant Body Armor*. International Journal of Progressive Sciences and Technologies (IJPSAT). 2024; 42: 413-418.

66. Boldin, M.S., Berendeev, N.N., Melekhin, N.V., Popov, A.A., Nokhrin, A.V., Chuvildeev, V.N. *Review of ballistic performance of alumina: Comparison of alumina with silicon carbide and boron carbide*. Ceramics International. 2021; 47 (18): 25201-25213.

67. Rashid, M.T., Aleem, A., Akbar, S., Rauf, A., Shuaib, M. *Numerical simulation of armor capability of Al_2O_3 and SiC armor tiles*. IOP Conference Series: Materials Science and Engineering. 2016; 146 (1): 012049.

68. Crouch, I.G., Franks, G.V., Tallon, C., Thomas, S., Naebe, M. *Glasses and ceramics*. In: Crouch, I.G., Ed. The Science of Armour Materials. Woodhead Publishing in Materials. 2017; pp. 331-393.

69. Gallo, L., Boas, M.O.C.V., Rodrigues, A.C.M., Melo, F.C.L., Zanotto, E.D. *Transparent glass–ceramics for ballistic protection: materials and challenges*. Journal of Materials Research and Technology. 2019; 8 (3): 3357-3372.

70. Dresch, A.B., Venturini, J., Arcaro, S., Montedo, O.R.K., Bergmann, C.P. *Ballistic ceramics and analysis of their mechanical properties for armour applications: A review*. Ceramics International. 2021; 47 (7) Part A: 8743-8761.

71. Stupar, S. *Ballistic composites, the present and the future*. In: Mhadhbi, M., Ed. Smart and Advanced Ceramic Materials and Applications. IntechOpen. 2022; pp. 33-50.

72. Andraskar, N.D., Tiwari, G., Goel, M.D. *Impact response of ceramic structures – A review*. Ceramics International. 2022; 48 (19 Part A): 27262-27279.

73. Lv, X., Yin, Z., Yang, Z., Chen, J., Zhang, S., Song, S., Yu, G. *Review on the Development of Titanium Diboride Ceramics*. Recent Progress in Materials. 2024; 06 (02): 1-48.

74. Nadda, J. *Influence of Boundary Conditions on Ceramic/Metal Plates under Ballistic Loads*. Journal of Materials Science and Chemical Engineering, 2015; 7 (3): 97-101.

75. Fejdyś, M., Kośla, K., Kucharska-Jastrząbek, A., Landwijt, M. *Hybride Composite Armour Systems with Advanced Ceramics and Ultra-High Molecular Weight Polyethylene (UHMWPE) Fibres*. Fibres and Textiles in Eastern Europe. 2016; 24(3):79-89.

76. Jiang, A., Li, Y., Li, D., Hou, H. *Study on Anti-Penetration Performance of Semi-Cylindrical Ceramic Composite Armor against 12.7 mm API Projectile*. Crystals, 2022; 12 (10): 1343.

77. Wu, H.L., Miao, C., Mu, X.M., Cui, X.Z., Yang, Z.Z., Lu, R.J., Dang, W., Bai, L.H., Wu, X. *Study on ballistic performance of a spherical cylindrical ceramic armor structure*. Journal of Physics: Conference Series, 2023; 2478: 072010.

78. Acar, E., Çelikbaş, D. *Effect of sphere radius and bullet hitting location on the ballistic performance of alumina ceramic tile*. Procedia Structural Integrity. 2022; 35: 269-278.

79. Hu, P., Zhao, F., Yang, H., Cheng, Y., Liu, J., Zhang, P. *The effect of ceramic column shape on the ballistic performance of the SiC/UHMWPE composite armor-Numerical simulation*. Journal of Physics: Conference Series, 2023; 2478: 112007.

80. Wang, J.H., Shi, X.M., Wang, Q., Xia, X., Fang, X.Z., Zeng, T., Zhang, L.J., Ye, C.J. *Study on ballistic performance of metal matrix ceramic ball composite*. Journal of Physics: Conference Series, 2023; 2478: 112005.

81. **Jitarașu, O.** *Numerical investigation on the impact of various construction designs of ceramic mosaic armour on ballistic resistance*. UPB Scientific Bulletin, Series D: Mechanical Engineering, 2024; 86 (4): 181-196.

82. Zhang, R., Han, B., Lu, T.J. *Confinement effects on compressive and ballistic performance of ceramics: a review*. International Materials Reviews. 2021; 66 (5): 287-312.

83. Zhao, Z-N., Han, B., Li, F-H., Zhang, R., Su, P-B., Yang, M., Zhang, Q., Zhang, Q-C., Lu, T-J. *Enhanced bi-layer mosaic armor: experiments and simulation*. Ceramics International. 2020; 15 (46): 23854-23866.

84. Guodong, G., Shah, A., Larry, D.P. *Numerical Analysis of Ceramic Mosaic Armor Subjected to Ballistic Impact*. International Journal of Composite Materials. 2021; 11 (1): 5–12.

85. Alam, S., Aboagye, P. *Numerical Modeling on Ballistic Impact Analysis of the Segmented Sandwich Composite Armor System*. Applied Mechanics 2024; 5: 340–361.

86. Si, P., Liu, Y., Yan, J., Bai, F., Huang, F. *Ballistic Performance of Polyurea-Reinforced Ceramic/Metal Armor Subjected to Projectile Impact*. Materials. 2022; 15: 3918.

87. **Jitarașu, O.**, Lache, S. *Ballistic performance of monolithic rubber-ceramic composite armor*. Journal of Composite Materials. 2024; 58 (5): 689-706.

88. Usman, J., Othman, M.H.D., Ismail, A.F., Rahman, M.A., Jaafar, J., Raji, Y.O., Gbadamosi, A.O., El Badawy, T.H., Said, K.A.M. *An overview of superhydrophobic ceramic membrane surface modification for oil-water separation*. 2021; 12: 643-667.

89. Pico, D., Steinmann, W. *Synthetic Fibres for Composite Applications*. In: Rana, S., Fangueiro, R., Eds. Fibrous and Textile Materials for Composite Applications. Textile Science and Clothing Technology. Springer, Singapore, 2016; pp. 135–170.

90. Crouch, I.G., Arnold, L., Pierlot, A., Billon, H. *Fibres, textiles and protective apparel*. In: Crouch, I.G., Ed. The Science of Armour Materials. Woodhead Publishing in Materials. 2017; pp. 269-330.

91. Sugimoto, Y., Irisawa, T., Hatori, H., Inagaki, M. *Yarns of carbon nanotubes and reduced graphene oxides*. Carbon; 2020; 165: 358-377.

92. Tam, T., Bhatnagar, A. *High-performance ballistic fibers and tapes*. In: Bhatnagar, A., Ed. Lightweight Ballistic Composites (Second Edition). Woodhead Publishing Series in Composites Science and Engineering, 2016; pp. 1-39.

93. Sun, H., Kong, H., Ding, H., Xu, Q., Zeng, J., Jiang, F., Yu, M., Zhang, Y. Improving UV Resistance of Aramid Fibers by Simultaneously Synthesizing TiO2 on *Their Surfaces and in the Interfaces Between Fibrils/Microfibrils Using Supercritical Carbon Dioxide*. Polymers; 2020, 12 (1): 147.

94. Dixit, D., Pal, R., Kapoor, G., Stabenau, M. *Lightweight composite materials processing*. In: Bhatnagar, A., Ed. Lightweight Ballistic Composites (Second Edition). Woodhead Publishing Series in Composites Science and Engineering, 2016; pp. 157-216.

95. da Silva, L.F., Lavoratti, A., Pereira, I.M., Dias, R.R., Amico, S.C., Zattera, A.J. *Development of multilaminar composites for vehicular ballistic protection using ultra-high molecular weight polyethylene laminates and aramid fabrics*. Journal of Composite Materials. 2018; 53 (14): 1907-1916.

96. Bucur, F., Rotariu, A., Matache, L-C., Baciu, F., Jiga, G., Trană, E. *Experimental and Numerical Study on the Behavior of Dyneema® HB26 Composite in Compression*. Materiale Plastice. 2020; 57 (2): 113-122.

97. Saleem, I.A., Ahmed, P.S., Abed, M. *Experimental and numerical investigation of Kevlar and UHMWPE multi-layered armors against ballistic impact*. Materials Today: Proceedings. 2022; 56 (5): 2516-2524

98. Weerasinghe, D., Breen, S., Wang, H., Mohotti, D., Hazell, P.J., Escobedo-Diaz, J.P. *Impact resistance and yarn pull-out behaviour of polymer spray-coated UHMWPE fabrics*. Materials Today Communications. 2022; 33: 104473.

99. Wu, Y., Lu, W., Yu, Y., Ma, M., Ren, W., Xu, L., Gao, G. *Dynamic response mechanisms of thin UHMWPE under high-speed impact*. Thin-Walled Structures. 2024; 205, Part A: 112391.

100. Crouch, I.G., Sandlin, J., Thomas, S. *Polymers and fibre-reinforced plastics*. In: Crouch, I.G., Ed. The Science of Armour Materials. Woodhead Publishing in Materials. 2017; pp. 203-268.

101. Balasubramanian, M. *Introduction to Composite Materials*. In: Rana, S., Fangueiro, R., Eds. Fibrous and Textile Materials for Composite Applications. Textile Science and Clothing Technology. Springer, Singapore, 2016; pp. 1–38.

102. Bhatnagar, N., Asija, N. *Durability of high-performance ballistic composites*. In: Bhatnagar, A., Ed. Lightweight Ballistic Composites (Second Edition). Woodhead Publishing Series in Composites Science and Engineering, 2016; pp. 231-283.

103. Naik, N.K. *Analysis of woven fabric composites for ballistic protection*. In: Chen, X., Ed. Advanced Fibrous Composite Materials for Ballistic Protection. Woodhead Publishing Series in Composites Science and Engineering, 2016; pp. 217-262.

104. Webster, G.A.T. *Nonwoven and crossplied ballistic materials*. In: Bhatnagar, A., Ed. Lightweight Ballistic Composites (Second Edition). Woodhead Publishing Series in Composites Science and Engineering, 2016; pp. 55-85.

105. Carr, D.J., Crawford, C. *High performance fabrics and 3D materials*. In: Bhatnagar, A., Ed. Lightweight Ballistic Composites (Second Edition). Woodhead Publishing Series in Composites Science and Engineering, 2016; pp. 41-53.

106. Fu, H-D., Feng, X-Y., Liu, J-X., Yang, Z-M., He, C., Li, S-K. *An investigation on anti-impact and penetration performance of basalt fiber composites with different weave and lay-up modes*. Defence Technology. 2020; 16 (4): 787-801.

107. Hu, P., Ge, S., Dou, S., Lv, Z., Li, M., Zhao, Z., Zhang, P., Wang, J., Sun, Z.M. *Ultralight M5 Aerogels with Superior Thermal Stability and Inherent Flame Retardancy*. Chemistry and Sustainability. 2024; 18 (3): e202401062.

108. Sun, B., Yu, J. *High-Performance Composites and Their Applications*. In: Yang, Y., Yu, J., Xu, H., Sun, B., Eds. Porous lightweight composites reinforced with fibrous structures. Springer, Berlin, Heidelberg, 2017; pp. 341–368.

109. Singh, N., Kumar, P. *Polybenzimidazole Fiber (PBI): Synthetic Fibre from Benzimidazole*. International Journal for Research in Applied Science & Engineering Technology. 2020; 8 (1): 742-744.

110. Zhou, H., Jia, B., Huang, H., Mou, Y. *Experimental Study on Basic Mechanical Properties of Basalt Fiber Reinforced Concrete*. Materials. 2020; 13 (6): 1362.

111. Rani, M., Sehrawat, M., Sharma, S., Bharadwaj, S., Chauhan, G.S., Dhakate, S.R., Singh, B.P. *Carbon nanotube-based soft body armor: Advancements, integration strategies, and future prospects*. Diamond and Related Materials. 2024; 148: 111446.

112. Ameer H., Ahmad, S., Nawab, Y., Ali, Z., Ullah, T. *Natural fiber–reinforced composites fo ballistic protection*. In: Nawab, Y., Sapuan, S.M., Shaker, K., Eds. Composite Solutions for Ballistics. Woodhead Publishing Series in Composites Science and Engineering, 2021; pp. 229-248.

113. Braga, F.O., Bolzan, L.T., Ramos, F.J.H.T.V., Monteiro, S.N., Lima, E.P., da Silva, L.C. *Ballistic Efficiency of Multilayered Armor Systems with Sisal Fiber Polyester Composites*. Materials Research. 2017; 20 (Suppl. 2): 767-774.

114. Ribeiro, M.P., Neuba, L.M., da Silveira, P.H.P.M., da Luz, F.S., Figueiredo, A.B-H.S., Monteiro, S.N., Moreira, M.O. *Mechanical, thermal and ballistic performance of epoxy composites reinforced with Cannabis sativa hemp fabric*. Journal of Materials Research and Technology. 2021; 12: 221-233.

115. Reis, R.H.M., Nunes, L.F., da Luz, F.S., Candido, V.S., da Silva, A.C.R., Monteiro, S.N. *Ballistic Performance of Guaruman Fiber Composites in Multilayered Armor System and as Single Target*. Polymers. 2021; 13 (8): 1203.

116. Abhilash, R.M., Venkatesh, G.S., Chauhan, S.S. *Development of bamboo polymer composites with improved impact resistance*. Polymers and Polymer Composites. 2021; 29 (9_suppl): S464-S474.

117. Bharathi, V.S., Vinodhkumar, S., Saravanan, M.M. *Strength characteristics of banana and sisal fiber reinforced composites*. IOP Conference Series: Materials Science and Engineering. 2021; 1055: 012024.

118. Nurazzi, N.M., Asyraf, M.R.M., Khalina, A., Abdullah, N., Aisyah, H.A., Rafiqah, S.A., Sabaruddin, F.A., Kamarudin, S.H., Norrrahim, M.N.F., Ilyas, R.A., Sapuan, S.M. *A Review on Natural Fiber Reinforced Polymer Composite for Bullet Proof and Ballistic Applications*. Polymers. 2021; 13 (4): 646.

119. Azevedo, A.R.G., Lima, T.E.S., Reis, R.H.M., Oliveira, M.S., Candido, V.S., Monteiro, S.N. *Guaruman fiber: A promising reinforcement for cement-based mortars*. Case Studies in Construction Materials. 2022; 16: e01029.

120. Bergmann, F., Stadlmayr, S., Millesi, F., Zeitlinger, M., Naghilou, A., Radtke, C. *The properties of native Trichonephila dragline silk and its biomedical applications*. Biomaterials Advances. 2022; 140: 213089.

121. Gao, X., Zhu, D., Fan, S., Rahman, M.Z., Guo, S., Chen, F. *Structural and mechanical properties of bamboo fiber bundle and fiber/bundle reinforced composites: a review*. Journal of Materials Research and Technology. 2022; 19: 1162-1190.

122. Fei, T. *High-performance fibers for textiles*. In: Miao, M., Xin, J.H., Eds. Engineering of High-Performance Textiles. The Textile Institute Book Series. Woodhead Publishing, 2018; pp. 27-58.

123. Wang, Z., Sangroniz, L., Xu, J., Zhu, C., Müller, A. *Polymer Physics behind the Gel-Spinning of UHMWPE Fibers*. Macromolecular Rapid Communications. 2024; 45 (15): 2400124.

124. Bilisik, K., Karaduman, N.S., Bilisik, N.E. *Fiber Architectures for Composite Applications*. In: Rana, S., Fangueiro, R., Eds. Fibrous and Textile Materials for Composite Applications. Textile Science and Clothing Technology. Springer, Singapore, 2016; pp. 75–134.

125. Bastovansky, R., Smetanka, L., Kohar, R., Mishra, R.K., Petru, M. *Comparison of Mechanical Property Simulations with Results of Limited Flexural Tests of Different Multi-Layer Carbon Fiber-Reinforced Polymer Composites*. Polymers. 2024; 16 (11): 1588.

126. Zhou, Y., Yao, W., Zhang, Z., Lin, Y., Xiong, Z., Zhao, Y., Wang, M. *Ballistic performance of the structure-modified plain weaves with the improved constraint on yarn mobility: Experimental investigation*. Composite Structures. 2022; 280: 114913.

127. Zhang, D., Gu, Y., Zhang, Z., Jia, M., Yue, S., Li, G. *Effect of off-axis angle on low-velocity impact and compression after impact damage mechanisms of 3D woven composites*. Materials & Design. 2020; 192: 108672.

128. Chen, X., Chu, Y. *I Failure mechanisms and engineering of ballistic materials*. In: Chen, X., Ed. Advanced Fibrous Composite Materials for Ballistic Protection. Woodhead Publishing Series in Composites Science and Engineering, 2016; pp. 263-304.

129. Boussu, F., Provost, B., Lefebvre, M., Coutellier, D. *New Textile Composite Solutions for Armouring of Vehicles*. Advances in Materials Science and Engineering. 2019; 2019: 1-14.

130. Wu, Z., Zhang, L., Ying, Z., Ke, J., Hu, X. *Low-velocity impact performance of hybrid 3D carbon/glass woven orthogonal composite: Experiment and simulation*. Composites Part B: Engineering. 2020; 196: 108098.

131. Wei, Q., Yang, D., Gu, B., Sun, B. *Numerical and experimental investigation on 3D angle interlock woven fabric under ballistic impact*. Composite Structures. 2021; 266: 113778.

132. Kazemianfar, B., Nami, M.R. *Influence of oblique low velocity impact on damage behavior of 2D and 3D woven composites: Experimental and numerical methods*. Thin-Walled Structures. 2021; 167: 108253.

133. Kazemianfar, B., Nami, M.R. *Can a 3D woven GFRP composite really provide better impact resistance compared to a 2D woven GFRP composite at all of the thicknesses?* Structures. 2022; 35 (3): 36-45.

134. Zhang, R., Han, B., Zhong, J-Y., Qiang, L-S., Ni, C-Y., Zhang, Q., Zhang, Q-C., Li, B-C., Lu, T.J. *Enhanced ballistic resistance of multilayered cross-ply UHMWPE laminated plates*. International Journal of Impact Engineering. 2022; 159: 104035.

135. Zhang, R., Qiang, L-S., Han, B., Zhao, Z-Y., Zhang, Q-C., Ni, C-Y., Lu, T.J. *Ballistic performance of UHMWPE laminated plates and UHMWPE encapsulated aluminum structures: Numerical simulation*. Composite Structures. 2020; 252: 112686.

136. Zhao, Z-N., Han, B., Zhang, R., Zhang, Q., Zhang, Q-C., Ni, C-Y., Lu, T.J. *Enhancement of UHMWPE encapsulation on the ballistic performance of bi-layer mosaic armors*. Composites Part B: Engineering. 2021; 221: 109023.

137. Wu, Y., Lu, W., Yu, Y., Ma, M., Gao, G. *The energy absorption characteristics and structural optimization of titanium/UHMWPE fiber metal laminates under high-speed impact*. International Journal of Impact Engineering. 2025; 195: 105097.

138. Cao, M., Chen, Li., Xu, R., Fang, Q. *Effect of the temperature on ballistic performance of UHMWPE laminate with limited thickness*. Composite Structures. 2021; 277: 114638.

139. Chen, L., Cao, M., Fang, Q. *Ballistic performance of ultra-high molecular weight polyethylene laminate with different thickness*. International Journal of Impact Engineering. 2021; 156: 103931.

140. Bajya, M., Majumdar, A., Butola, B.S., Arora, S., Bhattacharjee, D. *Ballistic performance and failure modes of woven and unidirectional fabric based soft armour panels*. Composite Structures. 2021; 255: 112941.

141. Patnaik, P.K., Swain, P.T.R., Mishra, S.K., Purohit, A., Biswas, S. *Recent developments on characterization of needle-punched nonwoven fabric reinforced polymer composites – A review*. Materials Today: Proceedings. 2020; 26 (2): 466-470.

142. Martínez-Hergueta, F., Ridruejo, A., González, C., Llorca, J. *Ballistic performance of hybrid nonwoven/woven polyethylene fabric shields*. International Journal of Impact Engineering. 2018; 111: 55-65.

143. Zhou, Y., Ding, S., Zhang, Z., Li, H., Lin, Y., Sun, M., Wang, M. *The Ballistic responses of thread-quilted plain weaves with increased yarn–yarn friction*. Thin-Walled Structures. 2022; 171: 108762.

144. Zhou, Y., Ding, S., Zhang, Z.W., Xiong, Z., Sun, J., Liu, X. *The responses of stitched ultra-high-molecular-weight polyethylene woven fabrics upon ballistic impact*. Journal of Industrial Textiles. 2022; 51 (5_suppl): 8764S-8787S.

145. Khan, M.I., Umair, M., Nawab, Y. *Use of auxetic material for impact/ballistic applications*. In: Nawab, Y., Sapuan, S.M., Shaker, K., Eds. Composite Solutions for Ballistics. Woodhead Publishing Series in Composites Science and Engineering, 2021; pp. 199-228.

146. Nguyễn, H., Fangueiro, R., Ferreira, F., Nguyễn, Q. *Auxetic materials and structures for potential defense applications: An overview and recent developments*. Textile Research Journal. 2023; 93 (23-24): 5268-5306.

147. Shah, I.A., Khan, R., Koloor, S.S.R., Petrů, M., Badshah, S., Ahmad, S., Amjad, M. *Finite Element Analysis of the Ballistic Impact on Auxetic Sandwich Composite Human Body Armor*. Materials. 2022; 15 (6): 2064.

148. Vo, D.M.P., Hoffmann, G., Cherif, C. *Novel Weaving Technology for the Manufacture of 2D Net Shape Fabrics for Cost Effective Textile Reinforced Composites*. Autex Research Journal. 2018; 18 (3): 251-257.

149. Memon, S.I., Peerzada, M.H., Jhatial, R.A., Fahad, R. *Modification of 2D Conventional Weaving Machine for the Fabrication of High Performance Woven Preforms: Part-I: Design and Manufacturing of Warp Creel*. Mehran University Research Journal of Engineering and Technology. 2020; 39 (1): 205-212.

150. Perera, Y.S., Muwanwella, R.M.H.W., Fernando, P.R. Fernando, S.K., Jayawardana, T.S.S. *Evolution of 3D weaving and 3D woven fabric structures*. Fashion and Textiles. 2021; 8:11.

151. Chen, X. *Design and Manufacture of 3D Woven Textiles*. In: Kyosev, Y., Boussu, F., Eds. Advanced Weaving Technology. Springer Nature Switzerland AG. 2022; pp. 449–474.

152. Liu, Y., Pan, Z., Yu, J. Hong, X., Ying, Z., Wu, Z. *Numerical simulation of 3D angle-interlock woven fabric forming and compression processes*. International Journal of Material Forming. 2024; 17: 24.

153. Guo, W., Chang, H., Ni, J., Zhu, K., Gao, B., Yang, D., Gao, Y.T. *Low-velocity impact performance of ultra-high molecular weight polyethylene/aramid-polyester core-spun yarn hybrid composites*. Journal of Industrial Textiles. 2023; 53: 152808372311540.

154. Venkataraman, D., Shabani, E., Park, J.H. *Advancement of Nonwoven Fabrics in Personal Protective Equipment*. Materials. 2023; 16 (11): 3964.

155. Singha, K., Maity, S., Pandit, P., Mondal, M.I.H. *Introduction to protective textiles*. In: Mondal, M.I.H., Ed. The Textile Institute Book Series. Protective Textiles from Natural Resources. Woodhead Publishing. 2022; pp. 3-38.

156. Abtew, M.A., Boussu, F., Bruniaux, P., Loghin, C., Cristian, I. *Ballistic impact mechanisms – A review on textiles and fibre-reinforced composites impact responses*. Composite Structures. 2019; 223: 110966.

157. Cunniff, P. *Dimensionless parameters for optimization of textile-based body armor systems*. Proceedings of the 18th International Symposium on Ballistics, San Antonio, 1999; pp. 1303-1310.

158. Haris, A., Tan, V.B.C. *Effects of spacing and ply blocking on the ballistic resistance of UHMWPE laminates*. International Journal of Impact Engineering. 2021; 151: 103824.

159. May, B., Critchley, R., Carr, D., Peare, A., Dowen, K. *Ballistic protective properties of material representative of English civil war buff-coats and clothing*. International Journal of Legal Medicine. 2020; 134: 1949–1956.

160. Jiang, Y., Peng, K., Wang, Y., Xie, J., Lu, X., Zhang, P., Fu, Y. *Optimizing core yarn twist levels for enhanced mechanical properties of aramid-wrapped yarns and fabrics*. Journal of Industrial Textiles. 2025; 55.

161. Gong, R.H., *Yarn to Fabric: Specialist Fabric Structures*. In: Sinclair, R. Ed. Textiles and Fashion. Materials, Design and Technology. Woodhead Publishing Series in Textiles. 2015; pp. 337-354.

162. Peinado, J., Wang, L.J., Olmedo, A., Santiuste, C. *Influence Of Stacking Sequence On The Impact Behaviour Of Uhmwpe Soft Armor Panels*. Composite Structures. 2022; 286 (10): 115365.

163. Petyukov, A.V., Bobrova, A.I., Grishin, I.R. Ivanov, D.A., Sotskii, M.Y. *PHYSICOMATHEMATICAL MODELING OF PROJECTILE PENETRATION INTO FLEXIBLE FABRIC TARGETS*. Journal of Applied Mechanics and Technical Physics. 2024; 65: 543–553.

164. Ingle, S., Yerramalli, C.S., Guha, A., Mishra, S. *Effect of material properties on ballistic energy absorption of woven fabrics subjected to different levels of inter-yarn friction*. Composite Structures. 2021; 266: 113824.

165. Steinke, K., Sodano, H.A. *Improved inter-yarn friction and ballistic impact performance of zinc oxide nanowire coated ultra-high molecular weight polyethylene (UHMWPE)*. Polymer. 2021; 231: 124125.

166. Hasan-Nezhad, H., Yazdani, M., Jeddi, M. *High- and low-velocity impact experiments on treated STF/3D glass fabrics*. Thin-Walled Structures. 2022; 171: 108720.

167. Mishra, V.D., Mishra, A., Singh, A., Verma, L., Rajesh, G. *Ballistic impact performance of UHMWP fabric impregnated with shear thickening fluid nanocomposite*. Composite Structures. 2022; 281: 114991.

168. Tang, F., Dong, C., Yang, Z., Kang, Y., Huang, X., Li, M., Chen, Y., Cao, W., Huang, C., Guo, Y., Wei, Y. *Protective performance and dynamic behavior of composite body armor with shear stiffening gel as buffer material under ballistic impact*. Composites Science and Technology. 2022; 218: 109190.

169. Xu, Y.J., Zhang, H., Huang, G.Y. *Ballistic performance of B4C/STF/Twaron composite fabric*. Composite Structures. 2022; 279: 114754.

170. Khodadadi, A., Liaghat, G., Taherzadeh-Fard, A., Shahgholian-Ghahfarokhi, D. *Impact characteristics of soft composites using shear thickening fluid and natural rubber–A review of current status*. Composite Structures. 2021; 271: 114092.

171. Bajya, M., Majumdar, A., Butola, B.S. *A review on current status and development possibilities of soft armour panel assembly*. Journal of Materials Science. 2023; 58: 14997–15020.

172. Weerasinghe, D., Bambach, M.R., Mohotti, D., Wang, H., Jiang, S. Hazell, P.J., Escobedo-Diaz, J.P. *Development of a Coated Fabric Armour System of Aramid Fibre and Rubber*. Thin-Walled Structures. 2022; 179: 109679.

173. Yang, Y., Ling, T., Liu, Y., Xue, S. *Synergistic effect of hybrid ballistic soft armour panels*. Composite Structures. 2021; 272: 114211.

174. Chen, X., Zhou, Y., Wells, G. *Numerical and experimental investigations into ballistic performance of hybrid fabric panels*. Composites Part B: Engineering. 2014; 58: 35-42.

175. Wang, C., Su, D., Xie, Z., Zhang, K., Wu, N., Han, M., Zhou, M. *Low-velocity impact response of 3D woven hybrid epoxy composites with carbon and heterocyclic aramid fibres*. Polymer Testing. 2021; 101: 107314.

176. Bao, J-W., Wang, Y-W., An, R., Cheng, H-W., Wang, F-C. *Investigation of the mechanical and ballistic properties of hybrid carbon/ aramid woven laminates*. Defence Technology. 2022; 18 (10): 1822-1833.

177. Wu, S., Xu, Z., Hu, C., Zou, X., He, X. *Numerical simulation study of ballistic performance of Al2O3/aramid-carbon hybrid FRP laminate composite structures subject to impact loading*. Ceramics International. 2022; 48 (5): 6423-6435.

178. Shaker, K. *Mechanical characterization*. In: Nawab, Y., Sapuan, S.M., Shaker, K., Eds. Composite Solutions for Ballistics. Woodhead Publishing Series in Composites Science and Engineering, 2021; pp. 269-298.

179. Demircioglu, T.K., Balikoglu, F., Beyaz, S., Bülbül, B. *Effect of lead metaborate as novel nanofiller on the ballistic impact behavior of Twaron® /epoxy composites*. Composites Communications. 2021; 27: 100832.

180. Sukanya, N.M., *Sundaram, S.K. Ballistic behaviour of nanosilica and rubber reinforced kevlar/epoxy composite targets*. Engineering Failure Analysis. 2022; 142: 106845.

181. Jen, Y-M., Chen, Y-J., Yu, T-H. *Improving the Impact Resistance and Post-Impact Tensile Fatigue Damage Tolerance of Carbon Fiber Reinforced Epoxy Composites by Embedding the Carbon Nanoparticles in Matrix*. Polymers. 2024; 16 (24): 3589.

182. Wang, B., Tian, W., Wang, C., Wang, Q. *Research on Interlayer Toughening and Damage Detection of Laser-Induced Graphene and Short Kevlar Fibers Aramid Fiber/Epoxy Resin Composites*. Polymers. 2024; 16 (23): 3380.

183. Costa, U.O., Filho, F.C.G., Gómez-del Río, T., Rodrigues, J.G.P., Simonassi, N.T., Monteiro, S.N., Nascimento, L.F.C. *Mechanical Properties Optimization of Hybrid Aramid and Jute Fabrics-Reinforced Graphene Nanoplatelets in Functionalized HDPE Matrix Nanocomposites*. Polymers. 2023; 15 (11): 2460.

184. da Cunha, J.S.C., Nascimento, L.F.C., Costa, U.O., Bezerra, W.B.A., Oliveira, M.S., Marques, M.F.V., Soares, A.P.S., Monteiro S.N. *Ballistic Behavior of Epoxy Composites Reinforced with Amazon Titica Vine Fibers (Heteropsis flexuosa) in Multilayered Armor System and as Stand-Alone Target*. Polymers. 2023; 15 (17): 3550.

185. Meliande, N.M., Oliveira, M.S., Lemos, M.F., Pereira, A.C., Figueiredo, A.B.-H.S., Monteiro, S.N., Nascimento, L.F.C. *Thermal Behavior of Curaua-Aramid Hybrid Laminated Composites for Ballistic Helmet*. Polymers. 2023; 15 (15): 3214.

186. Jiao-Wang, L., Charca, S., Valverde, B., Loya, J. A., Santiuste, C. *Experimental Analysis of Hybrid Panels Combining Flax/PLA Composite with UHMWPE and Steel Under Ballistic Impact*. Journal of Natural Fibers. 2024; 22(1): 2445574.

187. Marchi, B.Z., Silveira, P.H.P.M., Bezerra, W.B.A., Nascimento, L.F.C., Lopes, F.P.D., Candido, V.S., Silva, A.C.R., Monteiro, S.N. *Ballistic Performance, Thermal and Chemical Characterization of Ubim Fiber (Geonoma baculifera) Reinforced Epoxy Matrix Composites*. Polymers. 2023; 15 (15): 3220.

188. Chaves, Y.S., Monteiro, S.N., Nascimento, L.F.C., Rio, T.G. *Mechanical and Ballistic Properties of Epoxy Composites Reinforced with Babassu Fibers (Attalea speciosa)*. Polymers. 2024; 16 (7): 913.

189. Ghiaskar, A., Nouri, M.D. *High-velocity impact behavior of lignin/NR/hemp green composite: a comparative study*. Journal of the Brazilian Society of Mechanical Sciences and Engineering. 2022; 44: 413.

190. Ghiaskar, A., Nouri, M.D. *A novel flexible biocomposite with hemp woven fabric and natural rubber based on lignin green filler: investigation numerical and experimental under high-velocity impact*. Physica Scripta. 2023; 98: 105307.

191. Kumar, T.S.M, Joladarashi, S., Kulkarni, S.M. Doddamani, S. *Optimization of process parameters for ballistic impact response of hybrid sandwich composites*. International Journal on Interactive Design and Manufacturing (IJIDeM). 2023; 17: 1099-1111.

192. Mardiyati, Y., Putra, D.A., Fauziah, L., Rachman, O.A., Hariyanto, A., Steven, S. *Development of sansevieria trifasciata/natural rubber composites for a soft body armor application*. Composites Part C: Open Access. 2023; 12: 100407.

193. Gowda, D., Bhat, R.S. *Bio-inspired helicoidal hemp/basalt/polyurethane rubber bio-composites: Experimental, numerical and analytical ballistic impact study with residual velocity prediction using artificial neural network*. Industrial Crops and Products. 2024; 222 (Part 2): 119600.

194. Mahesh, V. *Conceptual design on optimal thickness selection of natural compliant composite for ballistic protection*. International Journal on Interactive Design and Manufacturing (IJIDeM). 2024; 18: 1949–1954.

195. Francesconi, L., Aymerich, F., *Effect of Z-pinning on the impact resistance of composite laminates with different layups*. Composites Part A: Applied Science and Manufacturing. 2018; 114: 136-148.

196. Behroozi, Z., Nosraty, H., Tehrani, M. *High velocity impact properties of composites reinforced by stitched and unstitched glass woven fabrics*. Journal of Industrial Textiles. 2022; 51 (3_suppl): 4540S-4553S.

197. Muñoz, R., Martínez-Hergueta, F., Gálvez, F., González, C., Llorca, J. *Ballistic performance of hybrid 3D woven composites: Experiments and simulations*. Composite Structures. 2015; 127: 141-151.

198. Chen, F., Peng, Y., Chen, X., Wang, K., Liu, Z., Chen, C. *Investigation of the Ballistic Performance of GFRP Laminate under 150 m/s High-Velocity Impact: Simulation and Experiment*. Polymers. 2021; 13 (4): 604.

199. Key, C.T., Alexander, C.S., *Experimental Testing and Numerical Modeling of Ballistic Impact on S-2 Glass/SC15 Composites*. Journal of Dynamic Behavior of Materials. 2018; 4: 373–386.

200. Malikov, A., Golyshev, A. *Investigation of the Resistance to High-Speed Impact Loads of a Heterogeneous Materials Reinforced with Silicon Carbide Fibers and Powder*. Materials. 2023; 16 (2): 783.

201. Peng, L., Tan, M.T., Zhang, X., Han, G., Xiong, W., Al Teneiji, M., Guan, Z.W. *Investigations of the ballistic response of hybrid composite laminated structures*. Composite Structures. 2022; 282: 115019.

202. Scazzosi, R., Souza, S.D.B., Amico, S.C., Giglio, M., Manes, A. *Experimental and numerical evaluation of the perforation resistance of multi-layered alumina/aramid fiber ballistic shield impacted by an armor piercing projectile*. Composites Part B: Engineering. 2022; 230: 109488.

203. Shi, Y., Pinna, C., Soutis, C. *Low-velocity impact of composite laminates: damage evolution*. In: Silberschmidt, V.V. Ed. Woodhead Publishing Series in Composites Science and Engineering, 2016; 69: 117-146.

204. Bhat, A., Naveen, J., Jawaid, M., Norrrahim, M.N.F., Rashedi, A., Khan, A. *Advancement in fiber reinforced polymer, metal alloys and multi-layered armoursystems for ballistic applications – A review*. Journal of Materials Research and Technology. 2021; 15: 1300-1317.

205. Minak, G., Fotouhi, M., Ahmadi, M. *Low-velocity impact on laminates*. In: Silberschmidt, V.V. Ed. Dynamic Deformation, Damage and Fracture in Composite Materials and Structures. Woodhead Publishing Series in Composites Science and Engineering, 2016; 69: 147-165.

206. Pasquali, M., Gaudenzi, P. *Effects of curvature on high-velocity impact resistance of thin woven fabric composite targets*. Composite Structures. 2017; 160: 349-365.

207. Tiwari, G., Khaire, N. *Ballistic performance and energy dissipation characteristics of cylindrical honeycomb sandwich structure*. International Journal of Impact Engineering. 2022; 160: 104065.

208. Wu, C., Zhao, P., Chang, Z., Li, L., Zhang, D. *An experimental and numerical investigation of ballistic penetration behaviors of deployable composite shells*. Acta Astronautica.2024; 224: 533-545.

209. Jabbar, M., Nasreen, A. *Composite fabrication and joining*. In: Nawab, Y., Sapuan, S.M., Shaker, K., Eds. Composite Solutions for Ballistics. Woodhead Publishing Series in Composites Science and Engineering, 2021; pp. 177-197.

210. Shen, Y., Wang, Y., Du, S., Yang, Z., Cheng, H., Wang, F. *Effects of the adhesive layer on the multi-hit ballistic performance of ceramic/metal composite armors*. Journal of Materials Research and Technology. 2021; 13: 1496-1508.

211. Başer, T.T, Karataş, Ç., Karadağlı, E., Toksoy, A.K. *Investigation of the effect of adhesive type for ballistic armor applications*. International Journal of Protective Structures. 2024; 0 (0).

212. Alil, L.C., Barbu, C., *Materials used in ballistic protection - the current stage and trends*. Impact of Socio-economic and Technological Transformations at National, European and International Level (ISETT), Institute for World Economy, Romanian Academy. 2015; 8.

213. Alil, L.C. *Theoretical Study on Adhesives Used in Ballistic Protection Structures and Transparent Armor*. Scientific Bulletin. 2015; 20 (1): 86-91.

214. Thakur, N., Bharj, R.S., Kumar, P. *Effect of Type of Adhesive Material on the Strength of Bullet-Proof Glass: A Parametric Study*. Asian Review of Mechanical Engineering. 2019; 8 (1): 8-10.

215. İbış, M.Ö., Kahraman, Y., Genel, K. *Effect of adhesive on ballistic performance of multi-layered steel*. International Journal of Impact Engineering. 2023; 176: 104559.

216. Jull, E.I.L., Dekker, R., Amaral, L. *Impact of adhesive layer properties on ceramic multi-layered ballistic armour systems: A review*. Defence Technology. 2024;

217. Ozturk, F., Cobanoglu, M., Ece, R.E. *Recent advancements in thermoplastic composite materials in aerospace industry*. Journal of Thermoplastic Composite Materials. 2024; 37 (9): 3084-3116.

218. Shabaridharan, K., Bhattacharyya, A. *Metallic Fibers for Composite Applications*. In: Rana, S., Fangueiro, R., Eds. Fibrous and Textile Materials for Composite Applications. Textile Science and Clothing Technology. Springer, Singapore, 2016; pp. 205–230.

219. Iredale, R.J., Ward, C., Hamerton, I. *Modern advances in bismaleimide resin technology: A 21st century perspective on the chemistry of addition polyimides*. Progress in Polymer Science. 2017; 69: 1-21.

220. Maxineasa, S.G., Taranu, N. *Life cycle analysis of strengthening concrete beams with FRP*. In: Pacheco-Torgal, F., Melchers, R.E., Shi, X., De Belie, N., Van Tittelboom, K., Sáez, A., Eds. Eco-Efficient Repair and Rehabilitation of Concrete Infrastructures, Woodhead Publishing Series in Civil and Structural Engineering. 2018; pp. 673-721.

221. Lee, C.H., Khalina, A., Nurazzi, N.M., Norli, A., Harussani, M.M., Rafiqah, S.A., Aisyah, H.A., Ramli, N. *The Challenges and Future Perspective of Woven Kenaf Reinforcement in Thermoset Polymer Composites in Malaysia: A Review*. Polymers. 2021; 13 (9): 1390.

222. Zhu, X., Yin, S., Liu, L., Yi, W., Luo, G., Zhao, Z., Chen, W. *Effects of temperature on mechanical properties and impact resistance of carbon fiber/bismaleimide resin composites*. Journal of Materials Research and Technology. 2025; 34: 2553-2569.

223. Çuvalci, H., Erbay, K., İpek, H. *Investigation of the Effect of Glass Fiber Content on the Mechanical Properties of Cast Polyamide*. Arabian Journal for Science and Engineering. 2014; 39: 9049–9056.

224. Zhang, X., Hao, H., Shi, Y., Cui, J. *The mechanical properties of Polyvinyl Butyral (PVB) at high strain rates*. Butyral (PVB) at high strain rates. 2015; 93: 404-415.

225. Maddah, H.A. *Polypropylene as a Promising Plastic: A Review*. American Journal of Polymer Science. 2016; 6 (1): 1-11.

226. Jogur, G., Nawaz, A.K., Das, A., Mahajan, P., Alagirusamy, R. *Impact properties of thermoplastic composites. Textile Progress*. 2018; 50 (3): 109–183.

227. Karl, J., Kirsch, F., Faderl, N., Perko, L., Fras, T. *Optimizing Viscoelastic Properties of Rubber Compounds for Ballistic Applications*. Applied Sciences. 2020; 10 (21): 7840.

228. Fras, T. *Experimental and Numerical Study on a Non-Explosive Reactive Armour with the Rubber Interlayer Applied against Kinetic-Energy Penetrators—The 'Bulging Effect' Analysis*. Materials. 2021; 14 (12): 3334.

229. Asemani, S.S., Liaghat, G., Ahmadi, H., Anani, Y., Charandabi, S.C., Khodadadi. *Analysis of Ballistic Impact Performance and Shear Effect on Elastomeric and Thermoset Composites*. International Journal of Applied Mechanics. 2022; 14 (2): 2250013.

230. Ji, Y., Li, X., Zhou, L., Liu, X. *Experimental and Numerical Study on Ballistic Impact Response of Vehicle Tires*. Latin American Journal of Solids and Structures. 2023; 20 (7): e506.

231. Zochowski, P., Cegła, M., Szczurowski, K., Mączak, J., Bajkowski, M., Bednarczyk, E., Grygoruk, R., Magier, M., Pyka, D., Bocian, M., Jamroziak, K., Gieleta, R., Prasuła, P. *Experimental and numerical study on failure mechanisms of the 7.62× 25mm FMJ projectile and hyperelastic target material during ballistic impact*. Continuum Mechanics and Thermodynamics. 2023; 35: 1745–1767.

232. Doddamani, S., Kulkarni, S.M., Joladarashi, S., Kumar, T.S.M., Gurjar, A.K. *Enhancing energy absorption in rubber–sand (Ru–San) composite blocks against ballistic impact: a multi-objective optimisation approach*. Multiscale and Multidisciplinary Modeling, Experiments and Design. 2024; 7: 4039–4055.

233. Li, Z., Zhang, Z., Ren, Z., Gao, S., Liu, Z. *Research on damage behavior of silicone rubber under dynamic impact*. International Journal of Non-Linear Mechanics. 2024; 164 (2): 104775.

234. Asavavisithchai, S., Marlaiwong, T., Nuttayasakul, N. *Developement of Composite Armors Using Natural Rubber Reinforced with Steel Wire Mesh for Ballistic Resistance*. IOP Conference Series: Materials Science and Engineering. 2018; 409: 012001.

235. Khodadadi, A., Liaghat, G., Shahgholian-Ghahfarokhi, D., Chizari, M., Wang, B. *Numerical and experimental investigation of impact on bilayer aluminum-rubber composite plate*. Thin-Walled Structures. 2020; 149: 106673.

236. Kasım, H. *Investigation on the ballistic performance of rubber-aluminum (AA7075-T651) laminated plates reinforced with borosilicate glass balls*. Proceedings of the Institution of Mechanical Engineers, Part L: Journal of Materials: Design and Applications. 2022; 236 (2) :280-298.

237. Klosak, M., Bendarma, A., Jankowiak, T., Bahi, S., Rusinek, A. *Aluminium-Rubber Composite – Experimental and Numerical Analysis of Perforation Process at Ambient and High Temperatures*. Acta Polytechnica Hungarica. 2022; 19 (11): 85-105.

238. Fadly, M.S., Bakri, B., Anwar, K., Chandrabakty, S., Mustafa, M., Naharuddin, N., Fauzan, F. *Evaluation of Projectile Penetration Position on Perforated Plate on Ballistic Resistance of Composite Sandwich Panels*. IOP Conference Series: Earth and Environmental Science. 2023; 1157: 012033.

239. Mosa, M.H., Fahem, A.F., Guthai, A.T. *Experimental investigation of perforated multi-layered composite armor subjected to ballistic impact*. Al-Qadisiyah Journal for Engineering Sciences. 2024; 17: 016–021.

240. Choudhury, S., Yerramalli, C.S., Guha, A., Ingle, S. *Prediction and mitigation of behind armor blunt trauma in composite plate armor using rubber backing or air gaps*. European Journal of Mechanics / A Solids. 2022; 93: 104533.

241. Jassem, A.E., Jawad, A.J., Samarmad, A.O., Hamzah, A.F. *Numerical and Experimental Study of Multi-layer Armors for Personal Protection*. Physics and Chemistry of Solid State. 2022; 23 (3): 550-558.

242. **Jitarașu, O.,** Lache, S., Velea, M.N. *Impact performance analysis of a novel rubber-composite combat helmet*. Proceedings of the Institution of Mechanical Engineers, Part C: Journal of Mechanical Engineering Science. 2023; 237 (7): 1755-1767.

243. Abdelal, N.R. *A shield of defense: Developing ballistic composite panels with effective electromagnetic interference shielding absorption*. Defence Technology. 2024; 35: 123-136.

244. Khodadadi, A., Liaghat, G., Ahmadi, H., Bahramian, A.R., Razmkhah, O. *Impact response of Kevlar/rubber composite*. Composites Science and Technology. 2019; 184: 107880.

245. Liu, Q., Guo, B., Chen, P., Su, J., Arab, A., Ding, G., Yan, G., Jiang, H., Guo, F. *Investigating ballistic resistance of CFRP/polyurea composite plates subjected to ballistic impact*. Thin-Walled Structures. 2021; 166: 108111.

246. Mahesh, V., Joladarashi, S., Kulkarni, S.M. *Comparative study on ballistic impact response of neat fabric, compliant, hybrid compliant and stiff composite*. Thin-Walled Structures. 2021; 165: 107986.

247. Weerasinghe, D., Bambach, M.R., Mohotti, D., Wang, H., Hazell, P.J. *High-velocity projectile impact response of rubber-coated aramid Twaron fabrics*. International Journal of Mechanical Sciences. 2022; 229: 107515.

248. Sidiq, M.F., Wibowo, A., Adewijaya, P. *Composite bulletproof vest reinforced rubberized coir*. AIP Conference Proceedings. 2024; 2952 (1): 090018.

249. Braga, F.O., Milanezi, T.L., Monteiro, S.N., Louro, L.H.L., Gomes, A.V., Lima, E.P. *Ballistic comparison between epoxy-ramie and epoxy-aramid composites in Multilayered Armor Systems*. Journal of Materials Research and Technology. 2018; 7 (4): 541-549.

250. Sangamesh, R., Ravishankar, K.S., Kulkarni, S.M. *Ballistic Impact Study on Jute-Epoxy and Natural Rubber Sandwich Composites*. Materials Today: Proceedings. 2018; 5 (2): 6916-6923.

251. Wang, X., Zhang, J., Bao, L., Yang, W., Zhou, F., Liu, W. *Enhancement of the ballistic performance of aramid fabric with polyurethane and shear thickening fluid*. Materials & Design. 2020; 196: 109015.

252. **Jitarașu, O.,** Lache, S., Velea, M.N. *Mechanical characterization of hyper-elastic rubber materials used as protective layers for structures operating under high dynamic loading conditions*. (submitted to the Proceedings of the Institution of Mechanical Engineers, Part C: Journal of Mechanical Engineering Science).

253. Somarathna, H.M.C.C., Raman, S.N., Badri, K.H., Mutalib, A.A., Mohotti, D., Ravana, S.D. *Quasi-Static Behavior of Palm-Based Elastomeric Polyurethane: For Strengthening Application of Structures under Impulsive Loadings*. Polymers. 2016; 8 (5): 202.

254. Papagiannis, P., Azariadis, P., Papanikos, P. *Evaluation and optimization of footwear comfort parameters using finite element analysis and a discrete optimization algorithm*. IOP Conference Series: Materials Science and Engineering. 2017; 254 (16): 162010.

255. Thomas, S., George, S.C., Thomas, S. *Rigid Amorphous Phase: Mechanical and Transport Properties of Nitrile Rubber/Clay Nanocomposites*. Progress in Rubber, Plastics and Recycling Technology. 2017; 33 (2): 103-126.

256. Tarodiya, R., Levy, A. *Surface erosion due to particle-surface interactions - A review*. Powder Technology. 2021; 387: 527-559.

257. Vinith, K.S.K., Sreenaveen, S., Sarveshnarayanan, G., Muthukumar, S. *Experimental Testing of Rubber Materials for Enhancement of Suspension Bush Performance*. Journal of Physics: Conference Series. 2024; 2837: 012014.

258. Liu, Y., Li, R., Zhou, P. *Interlayer Material Interactions on Shaped Charge Jet Protection Performance of Passive Armor*. Journal of Physics: Conference Series. 2021; 1855: 012026.

259. Ucar, H., Basdogan, I. *Dynamic characterization and modeling of rubber shock absorbers: A comprehensive case study*. Journal of Low Frequency Noise, Vibration and Active Control. 2018; 37(3): 509–518.

260. Lei, J., Xuan, Y., Liu, T., Duan, F., Sun, H., Wei, Z. *Static and dynamic mechanical behavior and constitutive model of polyvinyl chloride elastomers for design processes of soft polymer materials*. Advances in Mechanical Engineering. 2020; 12 (6): 1–12.

261. Jebur, Q.H., Jweeg, M.J., Al-Waily, M., Ahmad, H.Y., Resan, K.K. *Hyperelastic models for the description and simulation of rubber subjected to large tensile loading*. Archives of Materials Science and Engineering. 2021; 108 (2): 75-85.

262. Zhao, Z., Yuan, X., Zhang, W.Z., Niu, D., Zhang, H. *Dynamical modeling and analysis of hyperelastic spherical shells under dynamic loads and structural damping*. Applied Mathematical Modelling. 2021; 95: 468-483.

263. Chen, Y., Guo, H., Sun, M., Lv, X. *Tensile Mechanical Properties and Dynamic Constitutive Model of Polyurea Elastomer under Different Strain Rates*. Polymers. 2022; 14 (17): 3579.

264. Hou, J., Lu, X., Zhang, K., Jing, Y., Zhang, Z., You, J., Li, Q. *Parameters Identification of Rubber-like Hyperelastic Material Based on General Regression Neural Network*. Materials. 2022; 15 (11): 3776.

265. Naik, N., Kumar, S., Ratnaveer, D., Joshi, M., Akella, K. *An energy-based model for ballistic impact analysis of ceramic-composite armors*. International Journal of Damage Mechanics. 2013; 22 (2): 145-187.

266. ISO 815-1:2019(E*). Rubber, vulcanized or thermoplastic - Determination of compression set - Part 1: At ambient or elevated temperatures*.

267. ASTM D 412. *Standard Test Methods for Vulcanized Rubber and Thermoplastic Elastomers – Tension.*

268. ISO 37:2017(E). *Rubber, vulcanized or thermoplastic - Determination of tensile stress-strain properties.*

269. Billon, H.H., Robinson, D.J. *Models for the ballistic impact of fabric armour*. International Journal of Impact Engineering. 2001; 25 (4): 411-422.

270. Duan, Y., Keefe, M., Bogetti, T.A., Powers, B. *Finite element modeling of transverse impact on a ballistic fabric*. International Journal of Mechanical Sciences. 2006; 48: 33-43.

271. Pandya, K.S., Kumar, S., Nair, N., Patil, P., Naik, N. *Analytical and Experimental Studies on Ballistic Impact Behavior of 2D Woven Fabric Composites*. International Journal of Damage Mechanics. 2015; 244: 471–511.

272. Ryan, S. *Analytical techniques and mathematical modelling*. In: Crouch, I.G., Ed. The Science of Armour Materials. Woodhead Publishing in Materials. 2017; pp. 395-481.

273. Sastranegara, A., Putra, K.E., Halawa, E., Sutisna, N.A., Topa, A. *Finite Element Analysis on ballistic impact performance of multi-layered bulletproof vest impacted by 9 mm bullet*. SINERGI. 2023; 27 (1): 15-22.

274. Ma, D., Scazzosi, R., Manes, A. *Modeling approaches for ballistic simulations of composite materials: Analytical model vs. finite element method*. Composites Science and Technology. 2024; 248: 110461.

275. Malciu, A., Puică, C.C., Noja, G.F., Krupenschi, B. *Experimental and numerical investigation regarding the impact behaviour of 7,62 mm bullet steel core with a multilayered armour plate*. Proceedings of the 8th International Scientific Conference SEA-CONF. 2022; pp. 26-38.

276. Zhai, J., Zhao, Y., Hao, L., Shang, B., Song, L., Qi, C. *Numerical investigation of ballistic impact performance about ultra-high molecular weight polyethylene (UHMWPE) under high velocity impact*. Journal of Materials, Processing and Design. 2024; 8 (1): 156-166.

277. Jintao, L., Moubin, L. *An analytical model to predict the impact of a bullet on ultra-high molecular weight polyethylene composite laminates*. Composite Structures. 2022; 202: 115064.

278. Florence, A.L. *Interaction of Projectiles and Composite Armor. Part II*. AMMRC CR 69-15, Stanford Research Institute, Palo Alto, CA, August 1969.

279. Walker, J.D., Anderson, C.E. *An analytical model for ceramic-faced light armors*. 16th International Symposium on Ballistics, San Francisco, CA, September, 1996; pp. 23–28.

280. Zaera, R., Sánchez-Gálvez, V. *Analytical modelling of normal and oblique ballistic impact on ceramic/ metal lightweight armors*. International Journal of Impact Engineering. 1998; 21 (3): 133–148.

281. Bresciani, L.M., Manes, A., Giglio, M. *An analytical model for ballistic impacts against ceramic tiles*. Ceramics International. 2018; 44 (17): 21249-21261.

282. Wang, Z., Li, P. *A model incorporating damage evolution to predict the penetration behavior of a ceramic target subjected to the long projectile impact*. International Journal of Impact Engineering. 2020; 135: 103393.

283. Daniel, I.M., Liber, T. *Wave Propagation in Fiber Composite Laminates*. Part II, NASA CR-135086. 1976.

284. Sierakowski, R.L., Chaturvedi, S.K. *Dynamic loading and characterization of fiber-reinforced composites*. Wiley. 1997.

285. Xue, P., Peng, X., Cao, J. *A non-orthogonal constitutive model for characterizing woven composites*. Composites Part A: Applied Science and Manufacturing. 2003; 34 (2): 183-193.

286. Naik, N.K., Shrirao, P. *Composite structures under ballistic impact*. Composite Structures. 2004; 66 (1-4): 579-590.

287. Naik, N.K., Shrirao, P., Reddy, B.C.K. *Ballistic impact behaviour of woven fabric composites: Formulation*. International Journal of Impact Engineering. 2006; 32: 1521-1552.

288. Paradela, L.S., Sanchez-Galvez, V. *Analytical simulation of high-speed impact onto composite materials targets*. The Journal of Strain Analysis for Engineering Design. 2013; 48 (5): 282-290.

289. Sanchez-Galvez, V., Paradela, L.S., Gálvez, F. *Analytical simulation of high-speed impact onto hybrid glass/carbon epoxy composites targets*. International Symposium on Dynamic Response and Failure of Composite Materials. 2014; 88: 101-108.

290. Bresciani, L.M., Manes, A., Giglio, M. *An analytical model for ballistic impacts against plain-woven fabrics with a polymeric matrix*. International Journal of Impact Engineering. 2015; 78: 138-149.

291. Langston, T. *An analytical model for the ballistic performance of ultra-high molecular weight polyethylene composites*. Composite Structures. 2017; 179: 245-257.

292. Doddamani, S., Kulkarni, S.M., Joladarashi, S., Mohan Kumar, T.S., Gurjar, A.K. *Analysis of light weight natural fiber composites against ballistic impact: A review*. International Journal of Lightweight Materials and Manufacture. 2023; 6 (3): 450-468.

293. Choudhury, S., Yerramalli, C.S., Guha, A. *Analytical modeling of the ballistic impact performance of glass fabric – epoxy composites at low temperatures*. International Journal of Impact Engineering. 2023; 176: 104565.

294. Popa, I-D., Dobrița, F. *Considerations on Dop (Depth Of Penetration) Test for Evaluation of Ceramics Materials Used in Ballistic Protection*. Acta Universitatis Cibiniensis. Technical Series. 2017; 69 (1): 162 – 166.

295. Savio, S.G., Madhu, V. *Ballistic performance evaluation of ceramic tiles with respect to projectile velocity against hard steel projectile using DOP test*. International Journal of Impact Engineering. 2018; 113: 161-167.

296. Crouch, I.G. *Introduction to armour materials*. In: Crouch, I.G., Ed. The Science of Armour Materials. Woodhead Publishing in Materials. 2017; pp. 1-54.

297. Karahan, M., Ahmed, H.I. *Simulation of ballistic composites*. In: Nawab, Y., Sapuan, S.M., Shaker, K., Eds. Composite Solutions for Ballistics. Woodhead Publishing Series in Composites Science and Engineering, 2021; pp. 299-339.

298. Rajan, S.D. *Numerical analysis of ballistic composite materials*. In: Bhatnagar, A., Ed. Lightweight Ballistic Composites (Second Edition). Woodhead Publishing Series in Composites Science and Engineering, 2016; pp. 327-348.

299. Nsiampa, N., Coghe, F., Dyckmans, G. *Numerical investigation of the bodywork effect (K-effect)*. DYMAT-9th International Conference on the Mechanical and Physical Behaviour of Materials under Dynamic Loading. 2009; 2: 1561-1566.

300. Børvik, T., Dey, S., Clausen, A.H. *Perforation resistance of five different high-strength steel plates subjected to small-arms projectiles*. International Journal of Impact Engineering. 2009; 36: 948–964.

301. Kazemahvazi, S., Schneider, C., Deshpande, V.S. *A constitutive model for self-reinforcedductile polymer composites*. Composites Part A: Applied Science and Manufacturing. 2015; 71: 32-39.

302. Nagarajan, Y.R., Farukh, F., Kandan, K. *The Influence of Architecture on the Tensile and Flexural Properties of Single-Polymer Composites*. Journal of Composites Science. 2025; 9 (1): 40.

303. Senthil, K., Iqbal, M.A., Bhargava, P., Gupta, N.K. *Experimental and Numerical Studies on Mild Steel Plates against 7.62 API Projectiles*. In: 11th International Symposium on Plasticity and Impact Mechanics. New Delhi, India, 11-14 December 2016, pp. 369–374.

304. Jørgensen, K.C., Swan, V. *Modeling of Armor-piercing Projectile Perforation of Thick Aluminum Plates*. In: 13th International LS-DYNA Users Conference, Detroit, 2014.

305. Pintilie, D., Puică, C., Pîrvulescu, C., Pupăză, C. *Research on the impact of a projectile with complex kinematics on an armor plate*. UPB Scientific Bulletin, Series D: Mechanical Engineering. 2020; 82 (4): 213 – 224.

306. Khan, M.K., Iqbal, M.A. *Damage and Ballistic Evaluation of Ceramic-Metal Composite Target against Cylindrical Projectile*. Engineering Failure Analysis. 2022; 131 (3): 105903.

307. Shibao, W., Zhonghai, X., Hu, C., Zou, X., He, X. *Numerical simulation study of ballistic performance of Al2O3/aramid-carbon hybrid FRP laminate composite structures subject to impact loading*. Ceramics International. 2022; 48 (5): 6423-6435.

List of publications

The results of the research conducted in this doctoral thesis have been disseminated in seven scientific articles. Three articles were submitted to high reputed scientific journals from which two have already been published and one is currently under review. Throughout the research, the author presented preliminary findings at a national conference. The complete list of publications is presented below.

1. **Jitarașu, O.** *Hybrid composite materials for ballistic protection. A numerical analysis*. Review of the Air Force Academy, 2019; 17 (2): 47-56.
2. **Jitarașu, O.** Numerical Simulation of Ballistic Impact Performance of Composite Armour Plate by Typical Projectile. In: Cioacă, C., Gherman, L., Eds. Military Applications of Modeling and Simulation. Wydawnictwo ASzWoj, Warsaw, 2021; pp. 157-174.
3. **Jitarașu, O.**, Lache, S. Comportarea la impact a țesăturilor 2D utilizate pentru protecția balistică. AFCO 2021 (Absolvenți în Fața Companiilor) conference, 2021; 18 May, Brasov, Romania.
4. Cășeriu, B., **Jitarașu, O.,** Blaga, P. *Aspects regarding the dynamics of a prototype of remote-controlled logistics transport platform*. Acta Technica Napocensis, Series: Applied Mathematics, Mechanics, and Engineering, 2022; 2 (65): 241-250.
5. **Jitarașu, O.**, Lache, S., Velea, M.N. *Impact performance analysis of a novel rubber-composite combat helmet*. Proceedings of the Institution of Mechanical Engineers, Part C: Journal of Mechanical Engineering Science. 2022; 237 (7): 1755-1767. https://journals.sagepub.com/doi/10.1177/09544062221132700, FI=1.758 (2022), SRI=0.703 (2022).
6. **Jitarașu, O.**, Lache, S*. Ballistic performance of monolithic rubber-ceramic composite armor*. Journal of Composite Materials. 2024; 58 (5): 689-706, https://journals.sagepub.com/doi/10.1177/00219983231226412, FI=2.9 (2023), SRI=1.033 (2022).
7. **Jitarașu, O.**, Cășeriu, B. *Numerical Analysis of the Ballistic Impact Behavior of 2D Woven Fabrics*. Open Access Library Journal. 2024; 11: e12108.
8. **Jitarașu, O.** *Numerical investigation on the impact of various construction designs of ceramic mosaic armour on ballistic resistance*. UPB Scientific Bulletin, Series D: Mechanical Engineering, 2024; 86 (4): 181-196.
9. **Jitarașu, O.**, Lache, S., Velea, M.N. *Mechanical characterization of hyper-elastic rubber materials used as protective layers for structures operating under high dynamic loading conditions* (submitted to the Proceedings of the Institution of Mechanical Engineers, Part C: Journal of Mechanical Engineering Science, article under review).